

A Hessian-Aware Stochastic Differential Equation for Modelling SGD

Xiang Li[†] Zebang Shen[†] Liang Zhang[†] Niao He[†]

Abstract

Continuous-time approximation of Stochastic Gradient Descent (SGD) is a crucial tool to study its escaping behaviors from stationary points. However, existing stochastic differential equation (SDE) models fail to fully capture these behaviors, even for simple quadratic objectives. Built on a novel stochastic backward error analysis framework, we derive the Hessian-Aware Stochastic Modified Equation (**HA-SME**), an SDE that incorporates Hessian information of the objective function into both its drift and diffusion terms. Our analysis shows that **HA-SME** achieves the order-best approximation error guarantee among existing SDE models in the literature, while significantly reducing the dependence on the smoothness parameter of the objective. Empirical experiments on neural network-based loss functions further validate this improvement. Further, for quadratic objectives, under mild conditions, **HA-SME** is proved to be the first SDE model that recovers exactly the SGD dynamics in the distributional sense. Consequently, when the local landscape near a stationary point can be approximated by quadratics, **HA-SME** provides a more precise characterization of the local escaping behaviors of SGD. With the enhanced approximation guarantee, we further conduct an escape time analysis using **HA-SME**, showcasing how it can be employed to analytically study the escaping behavior of SGD for general function classes.

1 Introduction

We consider unconstrained stochastic minimization problems of the form

$$\min_x f(x) := \mathbb{E}_\xi [F(x; \xi)], \quad (1)$$

where $f : \mathbb{R}^d \rightarrow \mathbb{R}$ is a smooth function and ξ is a random vector. In this work, we study Stochastic Gradient Descent (SGD) [Robbins and Monro, 1951], the most popular approach for solving such problems, which updates iteratively as follows:

$$x_{k+1} = x_k - \eta_k \nabla F(x_k; \xi_k), \quad (2)$$

where $\eta_k > 0$ is the stepsize and $\nabla F(x_k; \xi_k)$ is an unbiased stochastic gradient at x_k . In the absence of noise, SGD reduces to Gradient Descent (GD). The choice of the stepsize η_k is crucial, affecting aspects such as convergence speed, training stability [Bengio, 2012, Nar and Sastry, 2018], and generalization error [Wilson et al., 2017, Zhou et al., 2022].

Existing non-convex optimization theory have established the non-asymptotic convergence of SGD towards a *stationary point* using a *diminishing* stepsize; see e.g., Drori and Shamir [2020], Fang et al. [2019], Ghadimi and Lan [2013], Khaled and Richtárik [2023], Li and Orabona [2020], Sebbouh et al. [2021] and Yang et al. [2024], to list just a few. Intuitively, the diminishing stepsize reduces the fluctuation caused by SGD’s inherent randomness, ensuring the objective descends in expectation. On the other hand, in practice a *constant* stepsize, i.e. $\eta_k \equiv \eta$, is often preferred and yields better performance. This presents a challenge to classical

[†]Department of Computer Science, ETH Zurich, Switzerland. xiang.li@inf.ethz.ch, zebang.shen@inf.ethz.ch, liang.zhang@inf.ethz.ch, niao.he@inf.ethz.ch.

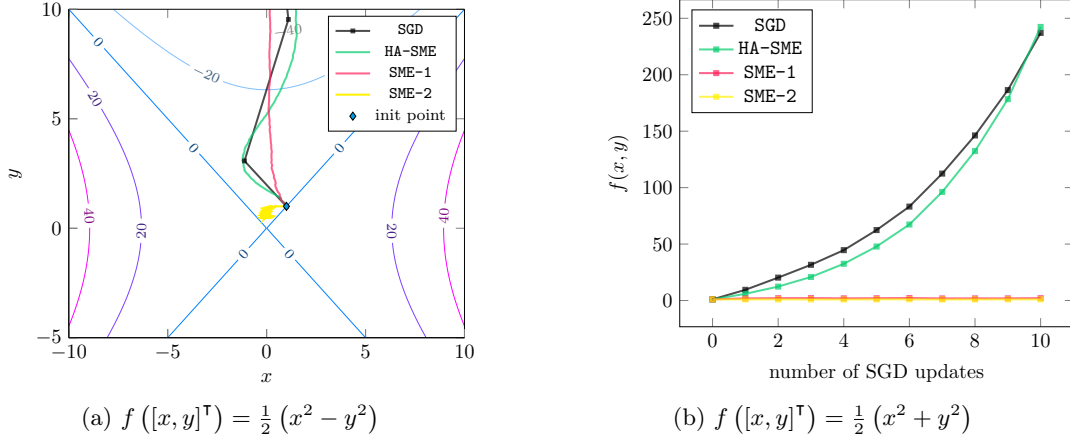


Figure 1: Escaping behaviors of SGD and SDEs on quadratic functions. The left sub-figure demonstrates the trajectories around a saddle point $(0,0)$, while the right sub-figure represents the evolution of the function value around a minimum. We set $\eta = 2.1$, the initial point to $(1,1)$, and the covariance of the additive noise to I for both cases. We conducted the experiments 1000 times to estimate the expectation. For the right sub-figure, we evaluated the SDEs at time stamps corresponding to η times the number of SGD updates. In these two cases, the proposed HA-SME behaves similarly as SGD. However, SME-2 fails to escape the saddle point in case (a), and both SME-1 and SME-2 fail to escape the minimum in case (b). We further provide in Section 6.1 mathematical proofs for the failure cases of these two existing SMEs in approximating SGD.

theory, as it fails to capture the non-diminishing role of noise in SGD dynamics. Additionally, it falls short in differentiating between saddle points and local minima, as well as in identifying favorable stationary points — those that not only are local minima but also exhibit good generalization.

The above limitations underscore the need to understand a critical aspect of SGD in nonconvex optimization: *the transitions between different stationary points*, beyond the traditional focus on convergence towards a stationary point. The selection of stepsize plays a crucial role in SGD’s transition behaviors:

- **Escaping from stationary points.** At a stationary point, either a saddle point or a local minimum, increasing the stepsize raises the likelihood of SGD to escape from it.
- **Minima selection.** Given a constant stepsize, SGD can rapidly exit local minima with a large Hessian norm, also known as sharp minima, but dwell longer at flat minima where the norm is small.

The latter relates to the notable generalization capabilities of SGD, which in prevailing belief, tends to favor flat minima over sharp ones [Keskar et al., 2017, Neyshabur et al., 2017, 2018]. These phenomena have been empirically verified [Zhang et al., 2021] and theoretically investigated [Brandière and Duflo, 1996, Liu and Yuan, 2023, Mertikopoulos et al., 2020, Pemantle, 1990]. Indeed, analyzing the link between stepsize and the escaping dynamics of SGD has emerged as an important topic in non-convex optimization. In particular, there is growing interest in using continuous-time dynamics, specifically Stochastic Differential Equations (SDEs), to understand the mechanisms behind escaping from saddle points and minima selection [Hu et al., 2019, Xie et al., 2022]. This involves quantifying the interplay between escaping speed, stepsizes, and local sharpness [Hu et al., 2019, Ibayashi and Imaizumi, 2023, Nguyen et al., 2019, Xie et al., 2020, Zhu et al., 2019]. A more detailed discussion of these works is provided in Section 1.1.

Existing continuous-time approximations of SGD and their failure modes. Previous study on the escaping behavior of constant-stepsize SGD through its continuous-time approximation typically entails two steps: (1) Proposing a proxy SDE model that approximately tracks the distributional evolution of the SGD dynamics; (2) Analyzing the escaping behavior of the proposed SDE model to predict or interpret the

behavior of SGD. Evidently, whether the behavior of SGD can be precisely captured hinges on the accuracy of the proxy models. Among existing SDE models, the second-order stochastic modified equation (SME-2) [Li et al., 2017] provides the order-best approximation guarantee:

$$dX_t = -\nabla \left(f(X_t) + \frac{\eta}{4} \|\nabla f(X_t)\|^2 \right) dt + \sqrt{\eta \Sigma(X_t)} dW_t, \quad (3)$$

where $\Sigma(X_t)$ denotes the covariance matrix of the stochastic gradient at X_t , W_t represents the standard Wiener process, and η denotes the constant stepsize of SGD.

However, we note that even for simple quadratic objectives, SME-2 and SGD show different behaviors in escaping from saddle points and minima: SME-2 exhibits locally stabilizing behavior while SGD with constant stepsize quickly escapes from the same local region, as illustrated in Figure 1. We further extend this observation to general objectives in Section 7.2. Our study also identifies similar failure modes for other existing SDE models, detailed in Section 6.1. This disparity in behavior suggests the inadequacy of existing SDEs in modeling the escaping dynamics of SGD, even with high-order approximation such as SME-2. Consequently, this brings us to a central question:

How to accurately model SGD in continuous time while preserving its escaping behaviors?

Our contributions. We develop a new Stochastic Backward Error Analysis (SBEA) to approximate the dynamics of constant-stepsize SGD. Our analysis yields an SDE, termed “Hessian-Aware Stochastic Modified Equation” (HA-SME), that integrates Hessian information into both its drift and diffusion terms. By incorporating local curvature information, HA-SME effectively tracks the escape phenomena of SGD. The well-posedness of HA-SME is assured under mild regularity assumptions. Moreover, under similar assumptions, the distribution evolution of HA-SME *exactly* matches that of SGD on quadratic functions.

Our contributions are summarized as follows:

- **Failure modes of existing SDE proxies.** In this study, we identify several shortcomings of current SDE approximations in capturing the escaping behaviors of SGD. We present concrete examples of optimization problems, where SGD exhibits escaping behavior, while existing SDE approximations tend to stabilize around the stationary points. We further pinpoint that this failure mode stems from the negligence of higher-order terms involving Hessians in their derivations.
- **A new Hessian-aware SDE proxy.** We propose the SBEA framework, which enables us to design HA-SME capable of encompassing more error terms involving gradients and Hessians than existing SDEs in the error analysis. Specifically, the drift term and diffusion coefficient of HA-SME are defined by two power series, respectively. Utilizing a generating function approach, we demonstrate that these power series converge when the stepsize is below a certain constant threshold, and their limits possess analytical expressions. We provide sufficient conditions to ensure HA-SME is well-posed.
- **Approximation guarantees on general functions.** We establish that HA-SME adheres to an order-2 weak approximation error guarantee, aligning with the best-known results among existing SDE approximations. To further differentiate HA-SME from existing SMEs, we conduct a fine-grained analysis of the weak approximation error, taking into account of the smoothness parameter of the objective, which we denote as λ . For convex functions, our findings indicate that HA-SME admits an approximation error of order $\mathcal{O}(\eta^2)$. In stark contrast, the error for SME-1 model is $\mathcal{O}(\eta\lambda)$, and for SME-2, it is $\mathcal{O}(\eta^2\lambda^2)$. Our results mark a notable improvement over the dependence on the smoothness parameter compared to existing SDE approximations. To validate these theoretical findings in practical scenarios, we conduct experiments on a classification task using neural networks. The result shows that HA-SME aligns more closely with SGD, outperforming existing SDE models.
- **Exact recovery on quadratic functions.** We further examine quadratic functions, which serve as a crucial benchmark for SDE approximations. We show that accurately mirroring the SGD dynamics

(linear in this setting) with a linear SDE (OU process) is fundamentally impossible, due to a potential mismatch between the ranks of their covariance matrices. Nonetheless, we show that under mild conditions—specifically, when the eigenvectors of the Hessian and noise covariance matrices align or when a small stepsize is used—HA-SME is well-founded and *exactly* replicates constant-stepsize SGD dynamics in a distributional sense. To the best of our knowledge, these findings represent the first instance of exact recovery of the distribution of SGD iterates using continuous-time models.

- **Escape Time Analysis.** To showcase the potential of using HA-SME as an analytical tool for studying SGD, we provide an analysis of the expected hitting time at stationary points. In the small stepsize regime, our analysis recovers classical results about dynamical systems with perturbations. Furthermore, in the large stepsize regime, where the stepsize is inversely proportional to the local Hessian eigenvalues, we demonstrate that SME-2 exhibits exponentially long escape times from saddle points, whereas HA-SME escapes sub-exponentially, better aligning with the behavior of SGD.

1.1 Related Work

Continuous-time approximation of GD and SGD. The connection between differential equations and gradient-based methods has been extensively studied previously, such as in [Attouch et al., 2022, Bloch, 1994, Brown and Bartholomew-Biggs, 1989, Fiori and Bengio, 2005, Helmke and Moore, 2012, Krichene et al., 2015, Muehlebach and Jordan, 2019, 2021, Schropp and Singer, 2000, Shi et al., 2022, Su et al., 2016]. For GD, the most straightforward continuous-time approximation is the gradient flow

$$dX_t = -\nabla f(X_t)dt. \quad (4)$$

While this flow approximates GD accurately as the stepsize approaches zero, the approximation error becomes critical when the stepsize is large. Barrett and Dherin [2021] took a step further by employing backward error analysis (detailed in Section 2.2) to derive a second-order continuous-time approximation for GD:

$$dX_t = -\nabla \left(f(X_t) + \frac{\eta}{4} \|\nabla f(X_t)\|^2 \right) dt. \quad (5)$$

However, this second-order model still has limitations, particularly in capturing certain critical behaviors of GD in discrete-time, such as overshooting, i.e., the iterates oscillate around the minimum or even diverge because of large stepsize. To tackle this issue, Rosca et al. [2022] introduced the Principal Flow (PF), a continuous-time approximation for GD that operates in complex space and can exactly match the discrete-time dynamics of GD on quadratics. This work is closely related to ours, and we will dive deeper in Section 2.3.

When taking noises into account, Mandt et al. [2015, 2016] introduced the following SDE dynamics for approximating SGD (SME-1):

$$dX_t = -\nabla f(X_t)dt + \sqrt{\eta \Sigma(X_t)}dW_t. \quad (6)$$

Later, Li et al. [2017] introduced SME-2 (described in Equation (3)) and established rigorous weak approximation for these SDEs. These SDEs are named according to the order of their weak approximation accuracy (see precise definition in Definition 1). In validating the accuracy of SME-1 with non-infinitesimal stepsize, Li et al. [2021] proposed SVAG, which has been empirically demonstrated to closely resemble SGD and theoretically proven to approximate SME-1. Besides the two SMEs, Orvieto and Lucchi [2019] and Fontaine et al. [2021] examined SDEs where the drift and diffusion terms are scaled by varying stepsizes. Their SDEs reduce to SMEs when adopting constant stepsizes. Another line of work has considered Homogenized SGD, which replaces the diffusion term in SME-1 with $\sqrt{\eta f(X_t) \nabla^2 f(X_t) / B}$ [Paquette and Paquette, 2021, Paquette et al., 2022] or $\sqrt{\eta f(X_t) \nabla^2 f(X^*) / B}$ [Mori et al., 2022], where B denotes the batch size and X^* the local minimum. However, their analyses are limited to the least square loss, lacking approximation guarantees for general non-convex objectives.

Continuous-time tools have also been used to study SGD with adaptive stepsizes. Barakat and Bianchi [2021] modeled Adam with a non-autonomous ODE, proving convergence. Zhou et al. [2020] and Xie et al.

[2022] used SDEs to explain Adam’s poor generalization due to sharp minima preference. Ma et al. [2022] linked Adam’s continuous-time limit to sign gradient flow, explaining fast early convergence and instabilities. Malladi et al. [2022] further used SDEs to propose a scaling rule for stepsize and batchsize tuning. Additionally, Compagnoni et al. [2025] provided theoretical insights into the role of noise in optimization dynamics of SDEs for adaptive stepsizes.

Escaping Behaviors Analysis Back in the 90s, Pemantle [1990] and Brandière and Duflo [1996] showed that SGD with a small stepsize can avoid hyperbolic saddle points, i.e., $\lambda_{\min}(\nabla^2 f(x)) < 0$ and $\det(\nabla^2 f(x)) \neq 0$. Recent studies [Liu and Yuan, 2023, Mertikopoulos et al., 2020] extended this understanding by showing SGD can escape strict saddle points ($\lambda_{\min}(\nabla^2 f(x)) < 0$). Additionally, with slight modifications to the algorithm, such as adding artificial noises, Ge et al. [2015] and Jin et al. [2017] established convergence of noisy SGD to approximate local minima. These discrete-time studies primarily focus on convergence analysis to local minima and show the escape from saddle points through function value descent analysis. However, these analyses, compared to continuous-time approaches: (1) fail to address escaping from local minima or minima selection, (2) lack a systematic characterization of the escape trajectory, including the escaping direction, and (3) are often case-specific, requiring modifications to SGD.

In terms of minima escaping, leveraging continuous-time frameworks, Jastrzebski et al. [2017] highlighted three crucial factors that influence the minima found by SGD: step-size, batchsize, and gradient covariance. Zhu et al. [2019] focused on the role of anisotropic noise and concluded that such noise enables SGD to evade sharp minima more effectively. Quantitatively, the time required for escaping has been theoretically shown to exponentially depend on the inverse of the stepsize, using theory for random perturbations of dynamical systems [Hu et al., 2019]. Subsequent work expanded on these ideas, considering heavy-tail noise and utilizing Lévy-driven SDEs to examine SGD’s stability around minima [Nguyen et al., 2019]. While the aforementioned research largely focused on parameter-independent gradient noise, Xie et al. [2020] analyzed parameter-dependent anisotropic noise. Using the analysis for the classic Kramers’ escape problem, they showed that compared to Stochastic Gradient Langevin Dynamics, SGD can quickly escape sharp minima, with escape speed exponentially depending on the determinant of the Hessian. Their analysis assumes that the system first forms a stationary distribution around a basin before escaping. However, SGD typically selects minima dynamically. New insights into the exponential escape time have been developed by employing Large Deviation Theory in non-stationary settings [Ibayashi and Imaizumi, 2023].

1.2 Paper Structure

The paper is structured as follows. Section 1 introduces the problem of modelling SGD with continuous-time tools, highlighting challenges and limitations of existing SDEs. Section 2 provides preliminaries, including notation, an overview of continuous-time approximations of GD and SGD, and a discussion on BEA and the PF approach. Section 3 develops SBEA as a framework for deriving our improved SDE models, and identifying challenges in exact matching at higher orders. Section 4 derives our HA-SME, demonstrating how Hessian information is integrated into its drift and diffusion terms, ensuring better tracking of SGD’s escaping behaviors, and establishing conditions for its well-posedness. Section 5 analyzes the approximation error of HA-SME, proving that it achieves an order-2 weak approximation guarantee and showing its advantages over existing models in terms of smoothness dependence. These theoretical results are then validated through experiments on neural networks. Section 6 evaluates the exact recovery of SGD dynamics by HA-SME on quadratic objectives, demonstrating failure cases of existing SDE proxies and proving that HA-SME can match SGD distributions under mild conditions. In Section 7, we analyze the expected hitting time of HA-SME near stationary points, demonstrating its utility as an analytical tool. Furthermore, we compare HA-SME with SME-2 in the large stepsize regime, showing that HA-SME more accurately reflects the behavior of SGD. In the end, Section 8 concludes with a summary of contributions and potential directions for future research.

2 Preliminaries

In this section, we first introduce the notations used throughout our analysis, and then review the Backward Error Analysis (BEA), a technique instrumental to the development of our stochastic backward error analysis. Additionally, we discuss the Principal Flow (PF) introduced by [Rosca et al. \[2022\]](#), which inspires the derivation of our HA-SME model.

2.1 Notations

Uppercase variables, such as X , denote continuous-time variables, while lowercase variables like x represent discrete-time variables. The function $X(x_0, t)$ indicates the solution of a continuous-time process starting from the initial point x_0 after a time duration t . For matrix notation, we use $[A]_{i,j}$ to specify the element at the (i, j) -th position in matrix A . For two matrices, A and B , of the same size, we denote $A:B = \text{tr}(A^\top B)$. Applying the logarithmic function to a matrix and dividing between two matrices are by default element-wise. We use the notation I to represent the identity matrix and \odot to denote the Hadamard product between matrices. The square root of a matrix, i.e., \sqrt{A} , is the matrix B such that $BB^\top = A$. In the context of functions, $\|f\|_{C^m}$ is defined as $\sum_{|\alpha| \leq m} |D^\alpha f|_\infty$, and we define the set $C_b^m(\mathbb{R}^d) = \{f \in C^m(\mathbb{R}^d) \mid \|f\|_{C^m} < \infty\}$, where $C^m(\mathbb{R}^d)$ is the set of all m -th differentiable functions on \mathbb{R}^d . For complex number x , $\text{Re}(x)$ and $\text{Im}(x)$ extract the real and imaginary parts, respectively, and \bar{x} denotes the complex conjugate of x . For random variables x and y , the covariance is represented as $\text{Cov}[x, y] = \mathbb{E}[(x - \mathbb{E}(x))(y - \mathbb{E}(y))^\top]$. Lastly, we use W_t to represent the standard Wiener process.

2.2 Backward Error Analysis (BEA)

Consider the GD dynamics¹

$$x_{k+1} = x_k - \eta \nabla f(x_k), \quad (7)$$

with constant stepsize η . Let $\tilde{X} : [0, \infty) \rightarrow \mathbb{R}^d$ be a continuous trajectory. The idea of BEA is to identify a series of functions, denoted as $g_i : \mathbb{R}^d \rightarrow \mathbb{R}^d$ for $i \in \{0, 1, \dots\}$, which constitute a modified equation as:

$$\frac{d}{dt} \tilde{X} = \tilde{G}_\eta(\tilde{X}) := \sum_{p=0}^{\infty} \eta^p g_p(\tilde{X}), \quad (8)$$

such that $\tilde{X}((k+1)\eta)$ closely approximates x_{k+1} , given $\tilde{X}(k\eta) = x_k$. To achieve this goal, we consider the Taylor expansion of the above continuous-time process at time $k\eta$,

$$\tilde{X}((k+1)\eta) = \sum_{j=0}^{\infty} \frac{\eta^j}{j!} \left. \frac{d^j \tilde{X}}{(dt)^j} \right|_{\tilde{X}=x_k} = x_k + \eta \sum_{p=0}^{\infty} \eta^p g_p(x_k) + \frac{\eta^2}{2} \sum_{p=0}^{\infty} \eta^p \nabla g_p(x_k) \sum_{p=0}^{\infty} \eta^p g_p(x_k) + \dots \quad (9)$$

By matching the powers of η in Equation (7) and Equation (9) up to the $(p+1)$ -order, we solve for g_i for $i = 0, \dots, p$. This procedure ensures that the leading error term between the continuous-time variable $\tilde{X}((k+1)\eta)$ and the discrete-time variable x_{k+1} , given $\tilde{X}(k\eta) = x_k$, is of the order $\mathcal{O}(\eta^{p+2})$. For a more comprehensive exploration of BEA, please refer to [Hairer et al. \[2006, Section IX\]](#).

When $p = 0$, the system reduces to gradient flow (Equation (4)) and then $p = 1$, we recover Equation (5). Increasing the order p in the above BEA procedure improves the accuracy of the approximation. The higher order modified flows generated by BEA involve higher-order gradients of the objective function f . For example, for $p = 2$, we obtain the third-order Gradient Flow [\[Rosca et al., 2022\]](#):

$$dX_t/dt = -\nabla f(X_t) - \frac{\eta}{2} \nabla^2 f(X_t) \nabla f(X_t) - \eta^2 \left(\frac{1}{3} \nabla^2 f(X_t) \nabla f(X_t) + \frac{1}{12} \nabla f(X_t)^\top \nabla^3 f(X_t) \nabla f(X_t) \right).$$

¹Similar arguments can be made for other discrete-time dynamics.

2.3 Principal Flow

While theoretically, one could solve for all component function g_i 's to achieve an arbitrary target error order, the resulting modified flow quickly becomes cumbersome due to the involvement of higher-order gradients. Moreover, the resulting power series (w.r.t. the exponent of η) may not even be convergent [Hairer et al., 2006]. In light of this limitation of BEA, Rosca et al. [2022] suggested the following term selection strategy:

Principle 1 (Term selection of PF, BEA). *In BEA, when solving g_i 's in Equation (8), derivatives of $f(x)$ up to the second order, i.e., terms containing $\nabla^p f(x)$ for $p \geq 3$, are omitted.*

With this term selection scheme, the resulting power series not only converges (with convergence radius $\eta\|\nabla^2 f(x)\| = 1$) but admits a concise form. The corresponding modified equation is:

$$dX_t = U(X_t) \frac{\log(I - \eta\Lambda(X_t))}{\eta\Lambda(X_t)} U(X_t)^\top \nabla f(X_t) dt, \quad (10)$$

where for any fixed x , we denote $\nabla^2 f(x) = U(x)\Lambda(x)U(x)^\top$ the eigen-decomposition of $\nabla^2 f(x)$. When the stepsize is large, the logarithmic function could result in complex numbers, as elements of $I - \eta\Lambda$ might be negative. Operating in the complex space is beneficial for modeling the divergent and oscillatory behaviors of gradient descent Rosca et al. [2022]. As only higher-order gradients are omitted in Principle 1, PF provides an *exact* characterization of the discrete GD dynamics on quadratic objectives.

3 Stochastic Backward Error Analysis

We extend BEA to the stochastic domain, termed Stochastic Backward Error Analysis (SBEA), providing a systematic approach for constructing SDEs that approximate stochastic discrete-time processes. While we focus on the analysis for SGD, similar argument can be generalized to other dynamics.

3.1 Differences between BEA and SBEA

Compared with BEA, there are two major modifications in SBEA. First, SBEA includes an additional Brownian motion term in its ansatz, compared to the one in Equation (8), with the diffusion coefficients to be determined; Second, to evaluate the quality of the approximation, SBEA adopts the weak approximation error (see Definition 1) as a metric in the distributional sense.

(1) Ansatz with Brownian motion. In BEA, we define the modified equation with a series of functions $\{g_i\}_{i \in \mathbb{N}}$. To further model the randomness in SGD, we introduce another series $\{h_i\}_{i \in \mathbb{N}_{>0}}$, $h_i : \mathbb{R}^d \rightarrow \mathbb{R}^{d \times d}$, to represent the diffusion coefficients of the Brownian motion. Specifically, we consider a hypothesis continuous-time dynamics as follows:

$$dX = (g_0(X) + \eta g_1(X) + \eta^2 g_2(X) + \dots) dt + \sqrt{\eta h_1(X) + \eta^2 h_2(X) + \dots} dW_t. \quad (11)$$

The rationale stems from the observation that the noise introduced in the ansatz undergoes continuous modification by the drift term. Consequently, it is natural to employ a similar power series representation for the diffusion coefficient². While one can truncate the series $\{h_i\}_{i \in \mathbb{N}}$ to simplify the analysis, as we illustrate in Figure 2 and theoretically justify in Section 6.1, such truncation can compromise the approximation quality and lead to misaligned escaping behaviors.

(2) Weak approximation error as quality metric. Our goal is to solve for the functions g_i 's and h_i 's so that the ansatz in Equation (11) approximates the SGD dynamics accurately. Instead of seeking a path-wise alignment like BEA, we focus on aligning the continuous-time and discrete-time dynamics in a distributional sense, characterized by the following weak approximation error.

²We do not include h_0 in the ansatz as SGD degenerates to gradient flow when $\eta \rightarrow 0$, which implies $h_0 \equiv 0$.

Definition 1 (Weak Approximation Error). Fixing $T > 0$, we say a continuous-time process $X(t)_{t \in [0, T]}$ is an order p weak approximation to the sequence $\{x_k\}$ if for any $u \in C_b^{2(p+1)}(\mathbb{R}^d)$, there exists $C > 0$ and $\eta_0 > 0$ that are independent of η (but may depend on T , u and its derivatives) such that for all $x \in \mathbb{R}^d$,

$$\left| \mathbb{E}[u(x_k) | x_0 = x] - \mathbb{E}[u(X(k\eta)) | X(0) = x] \right| \leq C\eta^p, \quad (12)$$

for all $k = 1, \dots, \lfloor T/\eta \rfloor$ and all $0 < \eta < \eta_0$.

This metric is commonly used for analyzing discretization errors of SDE, as referenced in textbooks [Kloeden and Platen, 2011, Milstein, 2013] and various studies on modeling SGD behavior with SDEs [Feng et al., 2019, Hu et al., 2019, Li and Wang, 2022, Li et al., 2017]. Specifically, we note that the error bound is uniform across all SGD iterations within $\lfloor T/\eta \rfloor$ steps, rather than merely bounding the last iterate. A small weak approximation error means that SGD and HA-SME are indistinguishable when evaluated with a broad class of test functions along the entire trajectory.

Remark 1. We highlight the difference between SBEA and the weak backward error analysis introduced by Debussche and Faou [2012]. The latter provides a framework for constructing a sequence of modified Kolmogorov generators with increasing orders to approximate discrete-time processes. However, since the high-order Kolmogorov generators involve high-order gradients, it *does not* yield an equivalent SDE representation (recall that the Kolmogorov generator corresponding to an Itô SDE contains only second-order gradients). Consequently, their framework is fundamentally different from our approach in terms of the final outcome.

3.2 Procedures in SBEA

We determine the components $\{h_i\}_{i \in \mathbb{N}}$ and $\{g_i\}_{i \in \mathbb{N}}$ by first calculating the semi-group expansions of the two conditional expectations involved in Equation (12) after one step, i.e. $k = 1$, and then match the resulting terms according to the power of η . Such a one-step approximation analysis can be translated to the weak approximation error guarantee via a martingale argument, as we will elaborate in Section 5.

Semi-group expansions. We expand the conditional expectation of the test function u after one SGD step as:

$$\mathbb{E}[u(x - \eta \nabla F(x; \xi)) | x] = u(x) + \eta \sum_{p=0}^{\infty} \eta^p \Phi_p(x), \quad (13)$$

where we use Φ_p to denote the aggregation of terms with η^{p+1} in the expansion. Simple calculation shows

$$\Phi_0(x) = -\nabla f(x)^\top \nabla u(x), \quad \Phi_1(x) = \frac{1}{2} \nabla^2 u(x) : (\nabla f(x) \nabla f(x)^\top + \Sigma(x)), \quad \dots, \quad (14)$$

where $\Sigma(x)$ denotes the covariance matrix of the stochastic gradient at x :

$$\Sigma(x) = \mathbb{E} \left[(\nabla F(x; \xi) - \mathbb{E}[\nabla F(x; \xi)]) (\nabla F(x; \xi) - \mathbb{E}[\nabla F(x; \xi)])^\top \right]. \quad (15)$$

For the continuous-time system, by the semi-group expansion [Hille and Phillips, 1996], the conditional expectation of a test function u under the SDE model yields:

$$\mathbb{E}[u(X(\eta)) | X(0) = x] = (e^{\eta \mathcal{L}} u)(x) = u(x) + \eta \mathcal{L} u(x) + \frac{1}{2} \eta^2 \mathcal{L}^2 u(x) + \frac{1}{6} \eta^3 \mathcal{L}^3 u(x) + \dots, \quad (16)$$

where \mathcal{L} is corresponding the infinitesimal generator [Särkkä and Solin, 2019]. For the SDE described in Equation (11), the generator is given explicitly by

$$\mathcal{L} = (g_0 + \eta g_1 + \dots) \cdot \nabla + \frac{1}{2} (\eta h_1 + \dots) : \nabla^2 = g_0 \cdot \nabla + \sum_{i=1}^{+\infty} \eta^i \left(g_i \cdot \nabla + \frac{1}{2} h_i : \nabla^2 \right) = \sum_{i=0}^{+\infty} \eta^i \mathcal{L}_i,$$

where for the ease of notation, we denote

$$\mathcal{L}_0 := g_0 \cdot \nabla \text{ and } \mathcal{L}_i := g_i \cdot \nabla + \frac{1}{2} h_i : \nabla^2 \text{ for } i \geq 1.$$

Gathering terms with power η^p in Equation (16) leads to the following lemma:

Lemma 1. *Define the function*

$$\Psi_p(x) = \sum_{n=1}^{p+1} \frac{1}{n!} \sum_{\{l_i^n \geq 0\}_{i=1}^n : \sum_{i=1}^n l_i^n = p+1-n} \mathcal{L}_{l_1^n} \mathcal{L}_{l_2^n} \cdots \mathcal{L}_{l_n^n} u(x), \quad (17)$$

where $\mathcal{L}_{l_j^n} \mathcal{L}_{l_{j+1}^n}$ denotes the composition of the operators $\mathcal{L}_{l_j^n}$ and $\mathcal{L}_{l_{j+1}^n}$. We have that

$$(e^{\eta \mathcal{L}} u)(x) = u(x) + \eta \sum_{p=0}^{\infty} \eta^p \Psi_p(x). \quad (18)$$

Next, we determine the components g_p 's and h_p 's in an iterative manner.

Identify components by iteratively matching terms. Our aim is to determine g_i 's and h_i 's by aligning the terms from the discrete-time expansion (Equation (13)) with those from continuous time (Equation (18)), according to the order of η . Note that every application of the generator \mathcal{L} on a function generates terms with all orders of η . Consequently, p -th order terms in the continuous-time expansion become complicated as p grows, as evident in Lemma 1. Fortunately, we can identify g_p 's and h_p 's in an iterative manner. In the following discussion, g_i and h_i for $i = 0, 1, \dots, p-1$ are treated as *known* from our iterative construction, and we solve the *unknowns* g_p and h_p by matching Φ_p and Ψ_p . We make the following two observations:

- $\Psi_p(x)$ (Equation (17)) is linear on g_p and h_p . Recall that g_p and h_p are only contained linearly in $\mathcal{L}_p u$, which appears only once in $\Psi_p(x)$ by choosing $n = 1$ and $l_1^1 = p$.
- Terms in $\Psi_p(x)$ with $n > 1$ contains only known terms. For $n > 1$, the terms in Equation (17) will only include g_i and h_i for $i \leq p-1$, since for any choice of the indices $\{l_j^{n+1}\}_{j=1}^n$, we must have $l_j^n \leq p-1$ if $n > 1$. These terms are already determined by our iterative strategy.

Following Rosca et al. [2022], we also explore various term selection strategies, starting with the exact matching case.

Principle 2 (Term selection of exact-matching, SBEA). *When determining the component functions g_p and h_p , all terms in Φ_p from Equation (13) must match the ones in Ψ_p from Equation (18). In particular, given the arbitrariness of the test function, the coefficients of $\nabla^p u$ ($p \geq 1$) should all be matched.*

With the above principle, we identify the unknowns, g_p and h_p , for $p \leq 1$.

Remark 2 (Recovering SME-2 by SBEA). By matching Ψ_0 and Φ_0 , we deduce that $g_0(x) = -\nabla f(x)$. By matching Ψ_1 with Φ_1 , we solve that $g_1(x) = -\frac{1}{2} \nabla^2 f(x) \nabla f(x)$ and $h_1(x) = \Sigma(x)$. This leads to the formulation of the SME-2 (Equation (3)).

3.3 Exact Matching Fails for Order η^3 in SBEA

We have shown that for $p = 0, 1$, it is possible to exactly solve g_p and h_p . However, for $p \geq 2$, adhering to Principle 2 can be infeasible. Specifically, following Principle 2 leads to an over-determined system when determining the unknown component functions g_p and h_p for $p \geq 2$. Recall that the test function u is chosen arbitrarily and let us consider all the possible occurrence of $\nabla^q u(x)$, $q = 1, 2, \dots$, in Φ_p and Ψ_p .

- For the continuous-time dynamics, the term Ψ_p in Equation (17) can contain terms with factors $\nabla^q u(x)$ for q ranging from 1 to $p+1$. For example, the term $\nabla^{p+1} u(x)$ can be generated from Equation (17) with the choice of $n = p+1$ and $l_j^n = 0$ for all $j \in \{1, \dots, n\}$; the term $\nabla u(x)$ can be generated with the choice $n = 1$ and $l_1^1 = 0$.
- For discrete-time expansion as per Equation (13), the term Φ_p involves only $\nabla^p u(x)$.

For exact matching, the coefficient of $\nabla^p u$ in Ψ_p must match that in Φ_p ; besides, for any $q \neq p$, the coefficient of $\nabla^q u$ in Ψ_p must be zero. This leads to an over-determined system comprising $p+1$ conditions for 2 free variables (g_p and h_p) when $p \geq 2$. In other words, the above iterative construction of the components g_p and h_p fails for $p \geq 2$. The infeasibility result highlights a drastic difference between SBEA and BEA. [Shardlow \[2006\]](#) also noted such infeasibility when attempting to find stochastic modified flows to achieve higher orders of weak approximation guarantees.

Inspired by PF, we introduce a relaxed term selection scheme, compared to Principle 2, so that only a subset of terms in Ψ_p (the continuous-time dynamics) and Φ_p (the discrete-time dynamics) match. Importantly, this term selection scheme should ensure that the resulting continuous-time dynamics still preserve the favorable escaping behaviors of the discrete-time dynamics of interest. This will be the focus of the following section.

4 Hessian-Aware Stochastic Modified Equation

In this section, we first derive the proposed SDE, HA-SME, to model SGD using the idea of SBEA. Then we discuss sufficient conditions for its well-posedness.

Due to the lack of degree of freedom, exactly matching all terms in Φ_p and Ψ_p for $p \geq 2$ is in general infeasible. Instead, we adopt the following term selection principle.

Principle 3 (Term selection in HA-SME, SBEA). *When determining the components g_p and h_p in SBEA, ignore the terms that involve $\nabla^{(r)} f(x)$, $\nabla^{(s)} u(x)$ and $\nabla^{(m)} \Sigma(x)$ for $r, s \geq 3$ and $m \geq 1$.*

Under this principle of term selection, we obtain the following result.

Lemma 2. *Under Principle 3, when applying SBEA on SGD, we have the following results:*

1. The component functions g_p and h_p in Equation (11) are uniquely determined;
2. The component functions g_p and h_p in Equation (11) admit the form

$$g_p(x) = c_p \cdot (\nabla^2 f(x))^p \nabla f(x), \quad (19)$$

$$h_p(x) = \sum_{k=0}^{p-1} a_{k,p-1-k} \cdot (\nabla^2 f(x))^k \Sigma(x) (\nabla^2 f(x))^{p-1-k}; \quad (20)$$

3. The coefficients $\{a_{s,m}\}$ and $\{c_s\}$ in $\{g_p\}$ and $\{h_p\}$ satisfy

$$\frac{\log(1-x)}{x} = \sum_{s=0}^{+\infty} c_s x^s \text{ and } \frac{\log(1-x)(1-y)}{xy - (x+y)} = \sum_{s,m \geq 0}^{+\infty} a_{s,m} x^s y^m.$$

We now derive the limit of the power series defined in Equation (11).

Theorem 1. *Let the components $\{g_p\}$ and $\{h_p\}$ be determined by the SBEA framework applied on SGD under Principle 3. Denote the limits*

$$b(x) = \sum_{p \geq 0} \eta^p g_p(x) \text{ and } \mathcal{D}(x) = \sum_{p \geq 1} \eta^p h_p(x). \quad (21)$$

Under the assumption that $\eta < 1/\|\nabla^2 f(x)\|$, we have that the limits $b(x)$ and $\mathcal{D}(x)$ exist with

$$b(x) = U(x) \frac{\log(I - \eta \Lambda(x))}{\eta \Lambda(x)} U(x)^\top \nabla f(x), \quad (22)$$

$$\mathcal{D}(x) = U(x) S(x) U(x)^\top, \text{ such that } [S(x)]_{i,j} = \frac{[U^\top \Sigma U]_{i,j} \log(1 - \eta \lambda_i)(1 - \eta \lambda_j)}{\eta \lambda_i \lambda_j - (\lambda_i + \lambda_j)}, \quad (23)$$

where $U(x)$ and $\Lambda(x)$ are defined through the eigen-decomposition $\nabla^2 f(x) = U(x) \Lambda(x) U(x)^\top$. The diagonal elements of $\Lambda(x)$ are denoted by $\lambda_i(x)$. For conciseness, we omit the dependence of λ_i , U and Σ on x .

The derivation of the above theorem is highly nontrivial, and represents one of the major contributions of our paper. Its proof includes several critical steps: (1) Identifying the structure of the components g_p and h_p in the SBEA ansatz; (2) Determining the coefficient of the components g_p and h_p ; (3) Computing the limit of the resulting power series, which we defer to Appendix A.

The following lemma provides sufficient conditions for the existence of the diffusion coefficient $\sqrt{\mathcal{D}(x)}$.

Lemma 3. $\mathcal{D}(x)$ is positive semi-definite at point x if either of the following two conditions holds:

1. The Hessian $\nabla^2 f(x)$ and covariance matrix $\Sigma(x)$ commute, and $\eta < 1/\|\nabla^2 f(x)\|$.
2. The covariance matrix $\Sigma(x)$ is positive definite, and η satisfies

$$\eta \leq \frac{1}{\|\nabla^2 f(x)\|} \min \left\{ 1 - \sqrt{1 - \frac{\lambda_{\min}(\Sigma(x))}{\sqrt{d} \lambda_{\max}(\Sigma(x))}}, 1 - \frac{\sqrt{2}}{2} \right\}, \quad (24)$$

where $\lambda_{\max}(\cdot)$ and $\lambda_{\min}(\cdot)$ denote the maximum and minimum eigenvalues of a matrix.

The validity of the above two conditions is discussed at the end of this subsection. With Theorem 1 and Lemma 3, we now present the proposed SDE model.

Definition 2. Let the assumptions in Theorem 1 and Lemma 3 hold for any x , then the drift term $b(x)$ and diffusion coefficient $D(x) := \sqrt{\mathcal{D}(x)}$ in Equation (21) are well-defined. We denote the SDE as the Hessian-Aware Stochastic Modified Equation (HA-SME):

$$dX_t = b(X_t)dt + D(X_t)dW_t. \quad (25)$$

Comparing with SME-1 in Equation (6) and SME-2 in Equation (3), both the drift term and the diffusion coefficient of HA-SME incorporate the Hessian information, hence the name.

Notice that the drift term $b(x)$ of HA-SME exactly corresponds to PF defined in Equation (10). A naive idea would be to combine PF with the conventional diffusion coefficient $\sqrt{\eta \Sigma}$ as in SME-1 and SME-2. The following remark comments on the drawback of such a construction.

Remark 3 (A naive SDE derived from PF). Adding the diffusion coefficient $\sqrt{\eta \Sigma}$ to the PF in Equation (10) gives rise to the following SDE:

$$dX_t = U(X_t) \frac{\log(I - \eta \Lambda(X_t))}{\eta \Lambda(X_t)} U(X_t)^\top \nabla f(X_t) dt + \sqrt{\eta \Sigma(X_t)} dW_t, \quad (26)$$

which we refer to as Stochastic Principal Flow (SPF). Such a straightforward combination could lead to escaping behaviors different from SGD. For example, when considering a multi-mode function, as illustrated in Figure 2, SGD and our proposed HA-SME can easily escape the local minimum and find the global one, whereas SPF remains trapped in the valley of the initial local minimum. A theoretical comparison of HA-SME and SPF on general objective functions is provided in Section 5.2.

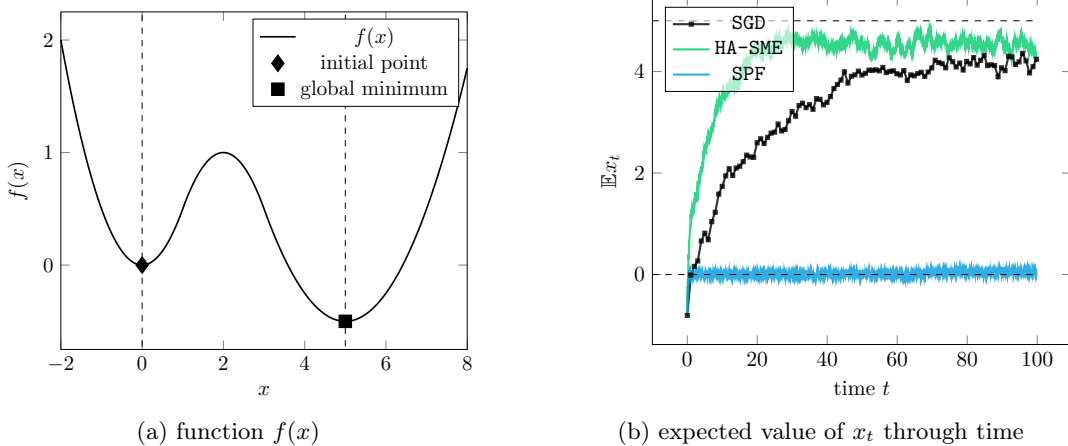


Figure 2: The illustration depicts the failure case for SPF, a naive stochastic extension of PF. The objective function is defined as $f(x) = \frac{1}{2}x^2$ for $x < 1$; $-\frac{1}{2}(x-2)^2 + 1$ for $1 \leq x < 3$; and $\frac{1}{4}(x-5)^2 - \frac{1}{2}$ for $x \geq 3$. We use dashed lines to indicate the two minima. The initial point is set to 0, and we set $\eta = 0.999$ and the noise variance to 1 for all methods. We run the simulation 100 times to estimate the expectation. SGD and HA-SME escape the initial minimum and arrive near the global minimum, while SPF stays around the initial one. A theoretical justification for the failure of SPF is presented in Section 6.1.

Remark 4 (Comparison with existing SMEs). By integrating Hessian into its diffusion coefficient, HA-SME provides a nuanced correction to the SDE noise. This adjustment is crucial for capturing the true dynamics of SGD, even when considering additive, state-independent noise models, such as $\nabla F(x, \xi) = \nabla f(x) + \xi$, where $\xi \sim \mathcal{N}(0, \Sigma)$. While discrete-time models treat noise as state-independent, in continuous time, noise is introduced at infinitesimal time intervals subject to immediate transformation by the drift term, which includes Hessian information. The necessity of incorporating the Hessian matrix into the diffusion term for corrections is also underscored by the failure cases of existing SDE models discussed in Section 6.1.

Remark 5 (Discussion on conditions of Lemma 3). The first condition states that the eigenvectors of $\nabla^2 f(x)$ and $\Sigma(x)$ are aligned. In the vicinity of minima, this condition finds support from both theoretical analysis and empirical evidence, even in deep learning. Theoretically, Jastrzebski et al. [2017] showed that $\Sigma(x^*) \approx \nabla^2 f(x^*)$ when the model fits all the data at x^* , which is further empirically verified by Xie et al. [2020]. For mean-square loss, Mori et al. [2022] and Paquette et al. [2022] derived $\Sigma(x) \approx \frac{2f(x)}{B} \nabla^2 f(x^*)$ near local minima x^* , where B is the mini-batch size. Wang and Wu [2024] further theoretically justified the approximation for nonlinear networks. In addition, the approximation $\Sigma(x) \approx \nabla^2 f(x^*)$ is commonly used in local escaping analysis of SGD [Ibayashi and Imaizumi, 2023, Xie et al., 2020, 2022, Zhu et al., 2019]. Our requirement here is more relaxed, as we only need the eigenvectors to be the same, regardless of eigenvalues.

To guarantee the existence and uniqueness of a solution for an SDE, it is often sufficient to impose regularity conditions on both the drift and diffusion terms. In this context, we show that, when Σ is positive definite, conditions in Lemma 3 lead to the well-posedness of the proposed HA-SME model.

Theorem 2. Assume $f \in C_b^3(\mathbb{R}^d)$, $\Sigma \in C_b^1(\mathbb{R}^{d \times d})$ being positive definite, and that at least one of the two conditions in Lemma 3 is satisfied everywhere. HA-SME has a unique strong solution.

Remark 6. While for general smooth objectives, Lemma 3 requires a small stepsize, in the particular case of quadratic functions with a constant noise covariance, the requirement of small stepsize is not necessary, as will be discussed in Section 6. In this case, the diffusion coefficient is constant, and the drift term depends linearly on X_t , naturally fulfilling the Lipschitz criterion. This is sufficient for proving the well-posedness of SDEs, independent of the stepsize.

5 Approximation Error Analysis of HA-SME

In this section, we analyze the approximation errors of HA-SME in approximating SGD on general smooth functions. Our first result establishes the order 2 weak approximation for HA-SME, as defined in Definition 1, matching the order-best guarantee in the literature. Subsequently, we conduct a more fine-grained analysis, elucidating the explicit dependence of the approximation error on the smoothness parameter of the objective function. We observe a significant improvement of HA-SME over the existing SME models. In particular, for convex objectives, the leading error term of HA-SME is independent of the smoothness parameter. To validate our theoretical findings, we conduct experiments on neural networks, showing that HA-SME more accurately approximates SGD dynamics compared to existing SDE models.

In addition to directly establishing weak approximation error guarantees, we also demonstrate the accuracy of HA-SME through an escape time analysis in Section 7.2, showing that HA-SME more reliably captures the escape time near saddle points compared to SME-2.

5.1 Weak Approximation Error Guarantee

Below, we show a weak approximation error guarantee on sufficiently smooth functions.

Theorem 3. *Assuming for any ξ , $F(\cdot; \xi) \in C_b^7(\mathbb{R}^d)$, HA-SME is an order 2 weak approximation of SGD.*

Remark 7. For all approximation error guarantees developed in this section, we assume that the (high-order) gradients of F are uniformly bounded. This assumption is common in the analysis of weak approximation errors for SDEs that approximate SGD [Feng et al., 2017, 2019, Hu et al., 2019]. Another common assumption is to consider polynomially bounded (high-order) gradients [Li et al., 2017, 2019]. However, this leads to weaker, point-wise approximation guarantees with respect to the initial point; specifically, the constant C in Equation (12) depends on the initial point x . In contrast, our guarantees are uniform over all initial points.

To relax the global boundedness assumption, one could restrict the approximation analysis to a compact set, where the (high-order) gradient bounds can be replaced with their local versions. To be more specific about how such results can be achieved, we outline two possible approaches: 1) modifying HA-SME so that it remains confined within a bounded domain, or 2) studying the approximation error up to the hitting time of the boundary of a compact set. The first approach has been employed in Li and Wang [2022], where, under mild assumptions on the objective function, SGD itself remains within a compact set. Consequently, it can be shown that the modified SDE retains the same approximation guarantees as the original SDE, but with respect to local problem parameters.

An order 2 weak approximation is the order-best approximation guarantee known for SGD in existing literature. Typically, achieving weak approximation results requires bounding the (high-order) derivatives of the drift and diffusion terms of the SDE. While this condition is readily met for existing SMEs, ensuring boundedness for HA-SME presents a challenge, as the drift and diffusion terms in HA-SME are defined as limits of power series and involve logarithmic components. Our proof builds upon the following lemma.

Lemma 4 (Regularity of the drift term and diffusion coefficient). *Consider a fixed $n \geq 0$. Assume for that any ξ , we have $F(\cdot; \xi) \in C_b^{n+2}(\mathbb{R}^d)$. Then, there exists a constant $\eta_0 > 0$ such that, for any $\eta < \eta_0$, $\max_{0 \leq i \leq d} \|b(x)\|_{C^n} < \infty$ and $\max_{0 \leq i, j \leq d} \left\| [D(x)D(x)^\top]_{i,j} \right\|_{C^n} < \infty$.*

Remark 8. A similar proof shows that SPF also admits the order 2 weak approximation error. Although SME-2, SPF, and HA-SME share the same order of weak approximation error, as demonstrated in Section 6, these models can have drastically different behaviors near critical points. This discrepancy between the practice and the above theory arises because the classical analysis solely emphasizes the dependence on the stepsize, while neglecting other crucial factors, such as the norm of the Hessian matrix. To better differentiate these models, a more fine-grained analysis is necessary, where the dependence on the problem-dependent parameters is explicitly accounted for.

5.2 Fine-Grained Error Analysis with Hessian Dependence

The preceding weak approximation results primarily focus on the dependence on the stepsize η , consistent with earlier research on SDEs in the context of SME-1 and SME-2 [Feng et al., 2017, 2019, Hu et al., 2019, Li et al., 2017]. This suggests that SDEs provide accurate approximations when the stepsize is small. However, a more relevant scenario in practice involves larger stepsizes, which are inversely proportional to $\lambda := \sup_{x \in \mathbb{R}^d} \|\nabla^2 f(x)\|$. This regime is supported by the “edge of stability” phenomenon observed in empirical studies of deep neural networks [Cohen et al., 2020, 2022]. These studies have shown that GD tends to converge to solutions where the maximum eigenvalue of the Hessian matrix approaches $2/\eta$. A similar behavior has been noted in SGD, albeit with a smaller final eigenvalue. This phenomenon underscores the significant practical and theoretical importance of considering stepsizes on the order of $\Theta(1/\lambda)$. Consequently, prior approximation error estimates may be imprecise if they consider only the dependence on η while ignoring the role of λ .

Our subsequent analysis explicitly examines the dependence of the error on problem-dependent parameters, the smoothness parameter λ and Lipschitz parameter $s := \sup_{x \in \mathbb{R}^d} \|\nabla f(x)\|$. Through this detailed analysis, we differentiate the approximation guarantees of HA-SME from SME-2 and SPF, highlighting its advantage in modeling SGD.

Theorem 4. *Assume for any ξ , we have $F(\cdot; \xi) \in C_b^8(\mathbb{R}^d)$, and for any $0 \leq i, j \leq d$, we have $[\Sigma(\cdot)]_{i,j} \in C_b^6(\mathbb{R}^d)$. Let $X(t)$ be the stochastic process described by HA-SME and $\{x_k\}$ be the sequence generated by SGD. There exists $\eta_0 > 0$ such that for any $\eta < \eta_0$ and $T > 0$, it holds that for all $x \in \mathbb{R}^d$,*

$$\sup_{k=1, \dots, \lfloor T/\eta \rfloor} |\mathbb{E}[u(x_k) | x_0 = x] - \mathbb{E}[u(X(k\eta)) | X(0) = x]| \leq \mathcal{O}((\eta^2 s^3 + \eta^3 s^4 \lambda^3) M(T)), \quad (27)$$

where for any $p \geq 1$, $M(T) := \eta \sum_{k=0}^{\lfloor T/\eta \rfloor - 1} \sum_{1 \leq |J| \leq 8} |D^J u^k(x)|_\infty$ with $u^k(x) = \mathbb{E}[u(x_k) | x_0 = x]$.

Note that $M(T)$ characterizes how the regularity of the test function u deteriorates along the SGD trajectory. By definition, this quantity is solely determined by the SGD dynamics, thus independent of the SDE models.

Similarly, we derive the following results for SME-2 and SPF.

Theorem 5. *Under the same settings as Theorem 4,*

1. *when $X(t)$ is described by SME-2, it holds that for all $x \in \mathbb{R}^d$,*

$$\sup_{k=1, \dots, \lfloor T/\eta \rfloor} |\mathbb{E}[u(x_k) | x_0 = x] - \mathbb{E}[u(X(k\eta)) | X(0) = x]| \leq \mathcal{O}((\eta^2 (s^3 + s\lambda^2) + \eta^3 s^4 \lambda^3) M(T)),$$

2. *when $X(t)$ is described by SPF, it holds that for all $x \in \mathbb{R}^d$,*

$$\sup_{k=1, \dots, \lfloor T/\eta \rfloor} |\mathbb{E}[u(x_k) | x_0 = x] - \mathbb{E}[u(X(k\eta)) | X(0) = x]| \leq \mathcal{O}((\eta^2 (s^3 + \lambda) + \eta^3 s^4 \lambda^3) M(T)).$$

The above theorems implies that HA-SME demonstrates a clear improvement in terms of dependency on λ . In particular, it eliminates the dependence on λ in the leading error term involving η^2 .

As is common in the finite-time approximation error analysis of SDE [Feng et al., 2017, Hu et al., 2019, Li et al., 2017], we point out that $M(T)$ could exhibit exponential growth in terms of T and λ in general. However, in cases when the function is convex, the following result shows that these constants remain independent of λ .

Lemma 5. *Assuming that for any ξ , $F(\cdot; \xi) \in C_b^9(\mathbb{R}^d)$ is convex, i.e., $F(y; \xi) - F(x; \xi) \geq \nabla F(x; \xi)^\top (y - x)$ for any $x, y \in \mathbb{R}^d$. There exists a constant η_0 such that, for any $\eta < \eta_0$, it holds that*

$$M(T) \leq \mathcal{O}(\|u\|_{C^8}),$$

where $M(T)$ is defined in Theorem 4, and $\mathcal{O}(\cdot)$ hides terms that do not depend on η , λ or s .

The above lemma allows us to develop the following approximation guarantee.

Theorem 6. *Fixing $T > 0$, assume that the test function satisfies $u \in C_b^8(\mathbb{R}^d)$, $F(\cdot; \xi) \in C_b^9(\mathbb{R}^d)$ is convex for any ξ , and for any $0 \leq i, j \leq d$, $[\Sigma(\cdot)]_{i,j} \in C_b^6(\mathbb{R}^d)$. Let $X(t)$ be the stochastic process described by HA-SME and $\{x_k\}$ be the sequence generated by SGD. There exists a constant $\eta_0 > 0$ such that for any $\eta < \eta_0$, it holds that for all $x \in \mathbb{R}^d$,*

$$\sup_{k=1, \dots, \lfloor T/\eta \rfloor} |\mathbb{E}[u(x_k) | x_0 = x] - \mathbb{E}[u(X(k\eta)) | X(0) = x]| \leq \mathcal{O}(\eta^2 s^3).$$

Following a similar proof together with Theorem 5, we can establish that the upper bounds for SME-2 and SPF are $\mathcal{O}(\eta^2(s^3 + s\lambda^2))$ and $\mathcal{O}(\eta^2(s^3 + \lambda))$, respectively. This difference partially explains the limitations of existing SDE models in capturing the escape dynamics as illustrated in Figures 1 and 2.

Intuitively, the advantage of HA-SME is inherent in its construction by SBEA. Even under Principle 3 of term selection, HA-SME incorporates infinite sequences of terms associated with λ , $\{(\nabla^2 f(x))^p\}_{p=0}^\infty$, in both its drift and diffusion terms. This is in stark contrast to SME-1, SME-2, and SPF, all of which truncate the error series at a certain point. All three of these models can be recovered by SBEA with a proper truncated series of $\{g_p\}$ and $\{h_p\}$: SME-1 includes g_0 , h_0 , and h_1 ; SME-2 includes g_0 , g_1 , h_0 , and h_1 ; and SPF includes $\{g_i\}_{i=0}^\infty$, h_0 , and h_1 . We conjecture that the λ -dependence in the error analysis for SME-2 and SPF cannot be improved. This limitation arises because error terms that exhibit such λ -dependence are inherently truncated during their construction within the SBEA framework.

Remark 9. Since Theorem 6 addresses the global point-wise approximation, the dependence on the global gradient norm of f appears unavoidable and cannot be neglected. However, to study the escaping behavior of SGD near a critical point, we believe that the global gradient norm s can be relaxed to its local version. This would be an interesting result because, in the vicinity of a critical point of a smooth function, the local gradient norm can be regarded as a negligible constant. Consequently, the leading term in Theorem 6 would be independent of both s and λ (whereas errors of existing SDE proxies always depend on λ).

Remark 10. If we further assume that $f(\cdot, \xi)$ is strongly-convex for any ξ , then $M(T)$ can be shown to be uniformly bounded w.r.t. T (the proof is provided in Appendix B.1), leading to a uniform-in-time approximation guarantee. A similar guarantee for SME-2 was established in the literature under the strong-convexity assumption [Li and Wang, 2022], but without considering the explicit dependence on the problem parameters s and λ .

5.3 Numerical Experiments

To validate the theoretical results and demonstrate the potential of HA-SME for modeling SGD on practical applications, we conduct numerical experiments comparing SMEs and HA-SME in terms of their alignment with SGD dynamics. Specifically, we run both SGD and the SDE models on a two-hidden-layer neural network with a sigmoid activation function and cross-entropy loss. The network consists of 10 nodes per hidden layer, and we use the Iris dataset [Fisher, 1936] for classification. Since computing the full covariance for the typical mini-batch noise is computationally expensive, particularly for SDEs where each SGD iteration is subdivided into multiple numerical discretization steps, we instead choose Gaussian noise with a covariance of $\Sigma(x) \equiv \sigma^2 I$ as the gradient noise.

The training starts with the same random initialization for all models, and we compute the objective function value at the first 10 SGD iteration and the corresponding continuous timestamp ηk . After averaging over 100 runs, we plot the maximum absolute difference between the objective function values of SGD and the SDE across all iterations, given by $\max_k |\mathbb{E}f(x_k) - \mathbb{E}f(X(k\eta))|$. This measure corresponds exactly to the weak approximation error, with the test function being the training objective. As shown in Table 1, HA-SME consistently outperforms existing SDE models across all stepsize and noise level setups. SME-1 exhibits the worst performance, as it is only a order-1 weak approximation. For SME-2, HA-SME can achieve up to an order of magnitude improvement when the stepsize is large, which aligns with our theoretical findings.

Table 1: Weak approximation error of SDE models approximating SGD

SDE Models	SME-1	SME-2	HA-SME
Fixing σ to be 10^{-3} and changing η			
$\eta = 0.1$	1.4×10^{-3}	5.8×10^{-5}	4.6×10^{-5}
$\eta = 0.2$	3.0×10^{-3}	3.1×10^{-4}	1.1×10^{-4}
$\eta = 0.5$	8.5×10^{-3}	2.4×10^{-3}	5.3×10^{-4}
Fixing η to be 0.5 and changing σ			
$\sigma = 10^{-2}$	8.5×10^{-3}	2.5×10^{-3}	4.9×10^{-4}
$\sigma = 10^{-1}$	4.1×10^{-3}	3.9×10^{-3}	1.8×10^{-3}

6 Exact Recovery of SGD by HA-SME on Quadratics

The quadratic objective, despite its simplicity, holds significance in studying the behaviors of SGD. Its relevance comes from not only its application in linear regression but also its use in modeling the local curvature of complex models through second-order Taylor expansions. Moreover, insights from Neural Tangent Kernel [Arora et al., 2019, Jacot et al., 2018] suggests that in regression tasks, the objectives of sufficiently wide neural networks closely resemble quadratic functions. The convergence of SGD on quadratic models has been extensively studied, for example, for constant stepsizes [Dieuleveut et al., 2020] and stepsize schedulers [Ge et al., 2019, Pan et al., 2021]. Additionally, the exploration of locally escaping behaviors of SGD often relies on a local quadratic assumption [Hu et al., 2019, Ibayashi and Imaizumi, 2023, Xie et al., 2020, 2022, Zhu et al., 2019].

In this section, we aim to compare different SDEs in terms of their ability to approximate SGD on quadratic functions. We believe that accurately capturing the behavior of SGD on simple quadratic functions serves as a touchstone for any SDE model, as local quadratic approximations frequently arise in optimization. In this context, We first discuss the failure cases of existing SDE proxies (including SPF in Equation (26)) and then illustrate how HA-SME can accurately match SGD under certain conditions.

6.1 Failure Cases for Existing SDEs

We now offer a theoretical justification for the phenomena observed in Figures 1 and 2 — specifically, why SME-1, SME-2, and SPF fail in modeling SGD on quadratic functions. We restrict the noise in this analysis to be additive and state-independent.

Assumption 1 (quadratic objective). *The objective function f is defined as $f(x) = \frac{1}{2}x^\top Ax$, where $A \in \mathbb{R}^{d \times d}$ is a symmetric real matrix³. We denote its eigen-decomposition by $A = U\Lambda U^\top$, where $U \in \mathbb{R}^{d \times d}$ satisfies $U^\top U = I_d$ and $\Lambda \in \mathbb{R}^{d \times d}$ is diagonal.*

Assumption 2 (Gaussian noise). *The stochastic gradient satisfies*

$$\nabla F(x, \xi) = \nabla f(x) + \xi, \quad \xi \sim \mathcal{N}(0, \Sigma),$$

where Σ is a constant positive semi-definite matrix.

With state-independent noise, the aforementioned SDEs applied to quadratics can be represented as Ornstein–Uhlenbeck (OU) processes. For simplicity, this subsection considers isotropic noise, i.e. $\Sigma = \sigma^2 I$ for some scalar σ . We show that even within this highly simplified noise setting, existing SDEs may struggle to accurately capture the escaping behaviors exhibited by SGD. The following proposition computes the distributions of the iterates of SGD and the SDE proxies.

³We focus on the simply quadratic $\frac{1}{2}x^\top Ax$, while noting that all results in this section can easily generalize to any quadratic function of the form $\frac{1}{2}x^\top Ax + bx + c$.

Proposition 1. Under Assumptions 1 and 2 with $\Sigma = \sigma^2 I$ for some scalar σ , it holds that

1. The iterates of SGD (Equation (2)) with stepsize $\eta_k \equiv \eta$ satisfy

$$x_k \sim \mathcal{N} \left(U (I - \eta \Lambda)^k U^\top x_0, \eta^2 \sigma^2 \sum_{m=0}^{k-1} U (I - \eta \Lambda)^{2m} U^\top \right).$$

2. The solution of SME-1 (Equation (6)) satisfies

$$X(x_0, t) \sim \mathcal{N} \left(\exp(-At) x_0, \eta \sigma^2 U \frac{I - \exp(-2\Lambda t)}{2\Lambda} U^\top \right).$$

3. The solution of SME-2 (Equation (3)) satisfies

$$X(x_0, t) \sim \mathcal{N} \left(\exp \left(- \left(A + \frac{\eta}{2} A^2 \right) t \right) x_0, \eta \sigma^2 U \frac{I - \exp \left(- (2\Lambda + \eta \Lambda^2) t \right)}{2\Lambda + \eta \Lambda^2} U^\top \right).$$

4. The solution of SPF (Equation (26)), if $\eta < 1/\|A\|$, satisfies

$$X(x_0, t) \sim \mathcal{N} \left(U (1 - \eta \Lambda)^{t/\eta} U^\top x_0, \eta^2 \sigma^2 U \frac{1 - (1 - \eta \Lambda)^{2t/\eta}}{-2 \log(1 - \eta \Lambda)} U^\top \right).$$

Now we delve into the analysis of different escaping scenarios.

Escaping Saddle Points in Figure 1a Consider the function defined in Figure 1a, i.e., $f([x, y]^\top) = \frac{1}{2}(x^2 - y^2)$, where the saddle point is at $(0, 0)$. According to Proposition 1, along the direction of y , the iterate x_k generated by SGD has a mean of $(1 + \eta \lambda_2)^k y_0$ and a variance of $\eta^2 \sigma^2 \sum_{m=0}^{k-1} (1 + \eta \lambda_2)^{2m}$, which drifts away from 0 for any $\eta > 0$. Thus, SGD can successfully escape for any stepsize $\eta > 0$. However, for SME-2, when $\eta \geq 2$, as $t \rightarrow \infty$, its stationary distribution is a Gaussian distribution with mean 0 and covariance $\eta \sigma^2 (2\Lambda + \eta \Lambda^2)^{-1}$. In such a regime of constant stepsize, the dynamics of SME-2 converges to a stationary distribution around 0, while SGD escapes exponentially fast. This observation confirms the numerical simulation presented in Figure 1a.

Escaping Minimum in Figure 1b Consider the objective $f([x, y]^\top) = \frac{1}{2}(x^2 + y^2)$ where all eigenvalues of the Hessian are positive. From Proposition 1, SGD will escape from $(0, 0)$ if $\eta > 2$ — both the mean and covariance of the iterates grow exponentially. However, for SME-1 and SME-2, their stationary distributions are zero-mean Gaussians with covariance $\eta \sigma^2 U (2\Lambda)^{-1} U^\top$ and $\eta \sigma^2 (2\Lambda + \eta \Lambda^2)^{-1}$, respectively. This elucidates why, in Figure 1b, their dynamics oscillate around the minimum.

Escaping Behavior on Bimodal Function in Figure 2 Consider the one-dimensional piece-wise quadratic function depicted in Figure 2a. When we initialize the point within the range $[-1, 1]$, the local function is quadratic. At least for the first step, the behaviors of SGD and SPF should be accurately predicted by Proposition 1. We consider small stepsize close to $1/\|\nabla^2 f(x)\|$ (which is 1 in this case). Due to the additive noise, the iterates of SGD always have a variance no smaller than $\eta^2 \sigma^2$. Such a variance allows the iterates to escape from the local basin and reach the basin around the global minimum at $x = 5$. However, after the first step, SPF would have a mean around 0 and variance also near 0 after time η . It can be shown by substituting $t = \eta$, setting $\eta \Lambda$ close to 1 in Proposition 1 and by noting that $\lim_{z \rightarrow 1} \frac{1 - (1 - z)^2}{\log(1 - z)} = 0$. This explains why SPF tends to stay closely around the initial minimum in our simulation, as shown in Figure 2. This phenomenon underscores the need for a more nuanced correction of the diffusion term to accurately model the escaping behaviors of SGD in such settings.

6.2 Hardness of Approximating SGD with OU Process on Quadratics

Ideally, we would like to approximate SGD on quadratics exactly using SDEs, i.e., the iterates of SGD share the same distribution as its continuous-time counterpart at time stamps $k\eta$ for any natural number k . However, this is not possible for general quadratic objective with arbitrary gradient noises, even if they are additive and state-independent Gaussian noises. We provide a hard instance, demonstrating that no OU process (even extended to complex domain as elaborated below) can achieve this. We focus on the class of OU process because the corresponding transition kernel is Gaussian, which matches the transition kernel of SGD (when viewed as a Markov chain) under Assumptions 1 and 2.

Complex OU Process We note that the iterates of SGD in this context is always *real-valued* and follows a Gaussian distribution, as outlined in Proposition 1⁴. However, to allow the continuous-time proxy to have the maximum capability of approximating SGD, we allow it to be *complex-valued*. The benefit of extending to complex space has been observed by Rosca et al. [2022] when matching the dynamics of GD by PF.

A random vector, denoted by $z = x + iy$, is a complex Gaussian random vector if x and y are two (possibly correlated) real Gaussian random vectors. In the real-valued case, a Gaussian random vector can be characterized by its mean and covariance, while in the complex-valued case, one additional parameter called *pseudo-covariance* is involved. Formally, the covariance is defined as $\Gamma(z) = \mathbb{E}[(z - \mathbb{E}[z])(z - \mathbb{E}[z])^H]$ and pseudo-covariance is defined as $C(z) = \mathbb{E}[(z - \mathbb{E}[z])(z - \mathbb{E}[z])^T]$. We refer to Appendix C.1 for a detailed discussion of properties of complex Gaussian random vectors.

We now state the desideratum when matching the distribution of a real normal variable, denoted as \tilde{z} , and a complex normal variable z .

Desideratum 1. *The distribution of a complex Gaussian random vector z is said to match the distribution of real normal variable \tilde{z} if the following conditions hold:*

$$\mathbb{E}[\operatorname{Re}(z)] = \mathbb{E}[\tilde{z}], \quad \mathbb{E}[\operatorname{Im}(z)] = 0, \quad \Gamma(z) = C(z) = \operatorname{Cov}[\tilde{z}, \tilde{z}].$$

The above result is equivalent to the statement: \tilde{z} and $\operatorname{Re}(z)$ have the same distribution, and $\operatorname{Im}(z)$ have 0 mean and 0 variance. Moreover, consider the setting described by Assumptions 1 and 2 so that the SGD iterates are all real Gaussian random vectors. A complex OU process

$$dX_t = BX_t dt + DdW_t,$$

is said to match the iterates of the SGD if the marginal distributions of X_t matches those of the SGD iterates at all corresponding time stamps, i.e. $t = k\eta$ where k is the iteration index of SGD. Here $B \in \mathbb{C}^{d \times d}$, $D \in \mathbb{C}^{d \times m}$ and W_t represents an m -dimensional standard Wiener process.

Proposition 2. *Consider the setting described by Assumptions 1 and 2. One can construct real matrices A and Σ such that, for any given stepsize $\eta > 0$, there exists no complex OU process⁵ that matches the iterates of SGD, in the sense of Desideratum 1.*

The hard instance is constructed by choosing a *full-rank* matrix A and a *degenerate* covariance matrix Σ such that the eigenvectors of Σ are not aligned with those of A . The distributional mismatch of the SDE and SGD can be intuitively understood through the following argument: Starting from a deterministic initialization, after one SGD step, the covariance of the iterates is $\eta^2 \Sigma$, which is rank-deficient; In contrast, in continuous-time dynamics, the noise injected is rotated by the misaligned linear transformations from the drift term and the covariance matrix quickly becomes full-rank. Please find the rigorous proof in Appendix C.2.

⁴This proposition, while initially framed for isotropic noises, can be easily generalized to anisotropic noises.

⁵In our formulation of complex OU process, we use real Brownian motion W_t . It should be noted, however, that the framework can also include complex Brownian motion [Perret, 2010]. Consider a complex Brownian motion defined by $\tilde{W}_t = W_t^r + iW_t^i$, where W_t^r and W_t^i are two independent real Brownian motions. Consequently, any SDE of the form $dX_t = BX_t dt + Dd\tilde{W}_t$ can be equivalently expressed as $dX_t = BX_t dt + D \begin{bmatrix} I & -iI \end{bmatrix} \begin{bmatrix} dW_t^r & dW_t^i \end{bmatrix}^T$.

6.3 Exact Approximation From HA-SME

While in general, complex OU process cannot exactly model SGD on quadratic functions, HA-SME when extended to complex-valued, achieves an exact match when the matrices A and Σ commute or when the stepsize is small enough. These conditions are slightly weaker than the sufficient conditions for the existence of our HA-SME (Lemma 3).

The following lemma outline conditions for a complex OU process to match SGD on quadratics.

Lemma 6. *Consider the same setting as Proposition 2, and denote the diagonal elements of Λ as $\lambda_1, \lambda_2, \dots, \lambda_d$. After time $k\eta$ for $k \geq 0$, the mean of $X(k\eta)$ equals the mean of x_k , i.e., $\mathbb{E}[X(k\eta)] = \mathbb{E}[x_k]$, if and only if $B = U \frac{\log(1-\eta\Lambda)}{\eta} U^\top$. In addition,*

1. *the covariance of $X(k\eta)$ equals the covariance of x_k if and only if for all $0 \leq i, j \leq d$,*

$$\left[(U^\top D) (U^\top D)^H \right]_{i,j} = \frac{[U^\top \Sigma U]_{i,j} \left(\log(1 - \eta\lambda_i) + \overline{\log(1 - \eta\lambda_j)} \right)}{\eta\lambda_i\lambda_j - (\lambda_i + \lambda_j)}. \quad (28)$$

2. *pseudo-covariance of $X(k\eta)$ equals the covariance of x_k if and only if for all $0 \leq i, j \leq d$,*

$$\left[(U^\top D) (U^\top D)^\top \right]_{i,j} = \frac{[U^\top \Sigma U]_{i,j} (\log(1 - \eta\lambda_i) + \log(1 - \eta\lambda_j))}{\eta\lambda_i\lambda_j - (\lambda_i + \lambda_j)}. \quad (29)$$

Satisfying any of the existence conditions for HA-SME in Lemma 3 ensures the existence of matrix D that adheres to the two required conditions in Lemma 6. Under these existence conditions, the matrices, whose elements are defined in the RHS of Equation (28) and Equation (29), become the same real positive semi-definite matrix. By taking the square roots of this matrix's eigenvalues, we can construct D that satisfies both Equations (28) and (29), thereby achieving an exact match for SGD on quadratic functions.

Theorem 7. *Under Assumptions 1 and 2, the solution of HA-SME exactly matches the iterates of SGD if either of the following two conditions holds:*

1. *A and Σ commute, and $\eta\lambda_i \neq 1$ for all eigenvalues λ_i of A .*
2. *Σ is positive definite, and $\eta \leq \frac{1}{\|A\|} \min \left\{ 1 - \sqrt{1 - \frac{\lambda_{\min}(\Sigma)}{\sqrt{d}\lambda_{\max}(\Sigma)}}, 1 - \frac{\sqrt{2}}{2} \right\}$.*

To the best of our knowledge, this marks the first instance of an SDE that precisely mirrors the distribution of SGD, albeit restricted to quadratic functions.

Remark 11. The first condition in this theorem relaxes the constraints from Lemma 3 to allow larger stepsizes. As noted in Rosca et al. [2022], complex flow is helpful for capturing the instabilities caused by large stepsizes in GD on quadratics. This is also the case for HA-SME. When $\eta < 1/\|A\|$, HA-SME operates in real space. However, when $\eta > 1/\|A\|$, imaginary components emerge due to the logarithmic function.

7 Escape Analysis Beyond Quadratics

Our proposed HA-SME serves as an analytical tool that can be seamlessly integrated into standard SDE analysis to better understand the escaping behavior of SGD. A particularly relevant line of work is the expected hitting time analysis, which focuses on the following expectation:

$$\mathbb{E}[\tau_S] = \mathbb{E}[\inf\{t > 0 \mid X(t) \in \partial S, X(0) = x_0 \in S\}],$$

where S is a compact set and ∂S denotes its boundary. The expected hitting time characterizes how quickly a stochastic process escapes from a given region. This quantity has been extensively studied in the context of randomly perturbed dynamical systems [Day, 1995, Freidlin and Wentzell, 2012, Kifer, 1981, Pavliotis, 2014,

Vent-Tsel' and Freidlin, 1973]. In deep learning, expected hitting time has been used to compare the escape rates from saddle points under different optimization algorithms [Xie et al., 2022], as well as to study minima selection [Ibayashi and Imaizumi, 2023, Xie et al., 2020, 2022, Zhou et al., 2020].

In this section, we conduct such analysis beyond quadratic functions and consider general function classes. We first start with a one-dimensional local minimum/maximum setting under **HA-SME**, illustrating its potential to be used as an analytical tool for capturing the escaping behavior of SGD. We then turn our focus to the regime of larger stepsizes, where existing SDEs begin to fail, as discussed in Section 6.1. Motivated by the insights from that section, we analyze the behavior near multi-dimensional saddle points. In this setting, we show that **SME-2** requires exponentially long escape times, whereas **HA-SME** escapes sub-exponentially fast—closely aligning with the empirical behavior observed in SGD.

7.1 Escaping of HA-SME Near One-Dimensional Local Minimum/Maximum

To illustrate how **HA-SME** can be leveraged to analyze escape times, we begin with a simple one-dimensional setting involving a local minimum or maximum.

Theorem 8. *Assume that there exists a compact domain $S_0 \subset \mathbb{R}$, and let $f : \mathbb{R} \rightarrow \mathbb{R}$ be a $C^4(S_0)$ function. Further, assume the following conditions hold for all $x \in S_0$:*

1. *There exists $x_0 \in S_0$ such that $f'(x_0) = 0$, i.e., x_0 is a stationary point.*
2. *The condition in Theorem 2 holds, ensuring that **HA-SME** is well-posed.*
3. *The function $f(x)$ is symmetric around x_0 ⁶.*

*Let **HA-SME** be initialized at x_0 . Then there exists a compact set $S_1 \subseteq S_0$ with $x_0 \in S_1$ such that:*

1. (Local minimum) *If $f''(x_0) > 0$, then there exists $c > 0$ such that*

$$\lim_{\eta \rightarrow 0} \eta \log \mathbb{E} [\tau_{S_1}] = c. \quad (30)$$

2. (Local maximum) *If $f''(x_0) < 0$, then there exist $c_1, c_2 > 0$ such that*

$$c_1 \leq \lim_{\eta \rightarrow 0} \frac{\mathbb{E} [\tau_{S_1}]}{\log(1/\eta)} \leq c_2. \quad (31)$$

It is known that for the one-dimensional SDE

$$dX_t = b(X_t) dt + \sqrt{\mathcal{D}(X_t)} dW_t,$$

the expected hitting time admits an analytical expression [Pavliotis, 2014]:

$$\mathbb{E} [\tau_{S_1}] = 2 \int_0^a \frac{\exp(-\psi(z))}{\mathcal{D}(z)} dz \int_z^a \exp(\psi(y)) dy,$$

where $\psi'(x) = -2b(x)/\mathcal{D}(x)$ and $S_1 = [-a, a]$. Our results are obtained by analyzing the double integral and characterizing its dependence on the stepsize η . The analysis shows that the expected hitting time at a local minimum scales exponentially with η , and the constant c in Equation (30) corresponds to the Freidlin–Wentzell quasi-potential [Freidlin and Wentzell, 2012], which represents the minimal “energy cost” or action required for the SDE to reach the boundary. In contrast, the expected hitting time at a local maximum scales logarithmically with η , indicating fast escape dynamics consistent with that of SGD.

One can obtain for **SME-1** and **SME-2** the same asymptotic result as stated in Theorem 8. This outcome is expected as the analysis assumes the stepsize is small compared to the local curvature. We will demonstrate in the next section that **SME-2** can fail to capture the correct escape behavior when the stepsize becomes large.

⁶ The symmetry assumption for f was introduced for analytical convenience and can be relaxed. If f is not symmetric, the expected hitting time will be dominated by the less challenging half of the domain.

Remark 12. While the above result is stated for one-dimensional functions, it can potentially be extended to multi-dimensional settings. There is a rich body of classical work on the expected hitting time in the multi-dimensional case, particularly when the drift b is independent of η and the diffusion \mathcal{D} is linear in η [Day, 1995, Freidlin and Wentzell, 2012, Kifer, 1981, Vent-Tsel’ and Freidlin, 1973]. For HA-SME, the dependence of both the drift and diffusion on η is more intricate. However, recent studies have begun to address settings with general η -dependence in both terms [Aleksian and Villeneuve, 2025, Chiarini and Fischer, 2014]. In particular, we can directly apply the result from Aleksian and Villeneuve [2025, Corollary 1.9] to derive multi-dimensional escape time estimates for local minima under HA-SME.

7.2 Escaping Near Multi-Dimensional Saddle Points

In this subsection, we consider the case where the stepsize is inversely proportional to the Hessian eigenvalues, a situation that can naturally arise locally in practice during deep learning training, as motivated in Section 5.2. To model this scenario, we assume that, locally, the Hessian can be approximated as $\nabla^2 f(x) \approx g(x)/\eta$, where $g(x) : \mathbb{R}^d \rightarrow \mathbb{R}^{d \times d}$ is a symmetric matrix-valued function independent of η . Under this assumption, the rescaled quantity $\eta \nabla^2 f(x)$ remains non-negligible, i.e., η is relatively large compared to the local curvature. For analytical tractability, we neglect contributions from terms that are asymptotically smaller than $1/\eta$ in the expansion of $\nabla^2 f(x)$.

Theorem 9. *Assume there exists a compact domain $S_0 \subset \mathbb{R}^d$, and let $f : \mathbb{R}^d \rightarrow \mathbb{R}$ be a $C^4(S_0)$ function. For all $x \in S_0$, suppose the following conditions hold:*

1. *There exists $x_0 \in S_0$ such that $\nabla f(x_0) = 0$, and $\nabla^2 f(x_0)$ has both positive and negative eigenvalues; that is, x_0 is a saddle point.*
2. *The Hessian satisfies $\nabla^2 f(x) = g(x)/\eta$, where $g(x)$ is independent of η . Furthermore, there exists an absolute constant $c_0 > 0$ such that all negative eigenvalues λ_i of $\nabla f(x_0)$ satisfy $\eta \lambda_i \leq -2 - c_0$, i.e., the stepsize is large enough compared to the Hessian eigenvalues.*
3. *The condition in Theorem 2 is satisfied so that HA-SME is well-posed.⁷*
4. *The gradient noise covariance $\Sigma(x)$ satisfies $\|\Sigma(x)\| = \Theta(1)$ uniformly, and the derivatives $|\partial[\Sigma(x)]_{i,j}/\partial[x]_k|$ are uniformly $\mathcal{O}(1)$ for $i, j, k \in [d]$.*

Then, there exists a compact set $S_1 \subseteq S_0$ with $x_0 \in S_1$, independent of η , and constants $\eta_0, c_1, c_2 > 0$ such that for all $\eta < \eta_0$ ⁸:

1. *For SME-2:*

$$\mathbb{E}[\tau_{S_1}] \geq \exp\left(\frac{c_1}{\eta^2}\right).$$

2. *For HA-SME:*

$$\mathbb{E}[\tau_{S_1}] \leq c_2 \eta \log\left(\frac{1}{\eta}\right).$$

⁷To ensure HA-SME is well-posed, we require $|\eta \lambda_i(x)| < 1$ for all $1 \leq i \leq d$ and x , where $\lambda_i(x)$ denotes the i -th eigenvalue of $\nabla^2 f(x)$, as noted in Lemma 3. However, this can be relaxed to an upper bound condition $\eta \lambda_i(x) < 1$ along with a mild lower bound ensuring that $\eta \lambda_i(x) > m$ for some constant $m < 0$. Thus, the second condition required here in this theorem does not contradict well-posedness.

⁸The assumption that η is smaller than some constant η_0 does not contradict the large stepsize assumption. The notion of a “large” stepsize is relative to the local Hessian eigenvalues, whereas η_0 is an absolute constant. In fact, in practice, even with a fixed stepsize η , there exist local regions where the Hessian eigenvalues can grow as large as $2/\eta$ [Cohen et al., 2020].

Since we assume that locally $\eta \nabla^2 f$ is independent of η , the dependence on η in the drift and diffusion terms of both **SME-2** and **HA-SME** is simply linear. As a result, classical results on exit times [Kifer, 1981, Vent-Tsel’ and Freidlin, 1973] apply directly. If we instead consider a broader class of functions where f and η exhibit more intricate local dependencies, additional care is needed. As mentioned in Remark 12, recent works have studied settings where the drift and diffusion terms can depend on η in arbitrary ways [Aleksian and Villeneuve, 2025, Chiarini and Fischer, 2014]. These advances suggest that our result can potentially be extended to a much wider class of functions.

The above theorem demonstrates that **SME-2** requires exponentially long time to escape a saddle point, whereas **HA-SME** escapes in sub-exponential time. For SGD, even a small amount of noise is sufficient to perturb the iterates away from a stationary saddle point. Once perturbed, the iterates quickly escape along the direction of negative curvature, as the gradient naturally points away from the saddle. **HA-SME** accurately captures this rapid escape behavior, aligning closely with that of SGD, while **SME-2** fails to reflect this dynamic.

Remark 13. Near a local saddle point, we note that the drift in **SME-2** is the negative gradient of the function $f + \frac{\eta}{4} \|\nabla f\|^2$. The regularizer $\frac{\eta}{4} \|\nabla f\|^2$ can transform a negative curvature direction—where the second-order gradient is negative, causing SGD to escape—into a positive one. Consequently, the process may stabilize at the saddle point rather than escape, causing an exponentially long escape time as indicated in the theorem. According to our SBEA framework, we observe that while **SME-2** attempts to capture more $\Theta(\eta^2)$ terms compared to **SME-1**, it still truncates many higher-order terms related to the stepsize and Hessian, thus, the local curvature information is not well captured—even wrongly captured in this case. In contrast, **HA-SME** incorporates as many Hessian-related terms as possible, providing a more accurate curvature estimation.

8 Conclusion and Future Work

In this work, we present **HA-SME**, an advancement over existing SDEs for approximating the dynamics of SGD. Specifically, **HA-SME** offers improved theoretical approximation guarantees for general smooth objectives over current SDEs in terms of the dependence on the smoothness parameter of the objective. For quadratic objectives, **HA-SME** exactly recovers the dynamics of SGD under mild conditions. The primary innovation lies in integrating Hessian information into both the drift and diffusion terms of the SDE, achieved by extending backward error analysis to the stochastic setting. This integration preserves the interplay of noise and local curvature in approximating SGD, allowing to better capture its escaping behaviors.

We anticipate that the current results will deepen our understanding of SGD’s escape dynamics and minima selection, enhance hyperparameter tuning, and inspire the development of more effective optimization algorithms. Furthermore, applying our SBEA framework to other optimization algorithms, such as momentum methods and adaptive gradient methods, would be an intriguing direction for future research. It would also be interesting to explore SDEs driven by alternative noise processes, such as Lévy noise. In deriving the weak approximation error, we established a uniform-in-time guarantee for strongly convex objectives. A natural question for future work is whether similar guarantees can be obtained for broader function classes, such as those satisfying the Polyak–Łojasiewicz (PL) condition.

References

- Ashot Aleksian and Stéphane Villeneuve. Freidlin-wentzell type exit-time estimates for time-inhomogeneous diffusions and their applications. *arXiv*, page 2501.11797, 2025. (Cited on pages 21, 22, and 69.)
- Sanjeev Arora, Simon S Du, Wei Hu, Zhiyuan Li, Russ R Salakhutdinov, and Ruosong Wang. On exact computation with an infinitely wide neural net. In *Advances in Neural Information Processing Systems*, 2019. (Cited on page 16.)
- Hedy Attouch, Zaki Chbani, Jalal Fadili, and Hassan Riahi. First-order optimization algorithms via inertial systems with Hessian driven damping. *Mathematical Programming*, 193:113–155, 2022. (Cited on page 4.)

- Anas Barakat and Pascal Bianchi. Convergence and dynamical behavior of the Adam algorithm for nonconvex stochastic optimization. *SIAM Journal on Optimization*, 31(1):244–274, 2021. (Cited on page 4.)
- David GT Barrett and Benoit Dherin. Implicit gradient regularization. In *International Conference on Machine Learning*, 2021. (Cited on page 4.)
- Yoshua Bengio. Practical recommendations for gradient-based training of deep architectures. In *Neural Networks: Tricks of the Trade: Second Edition*, pages 437–478. Springer, 2012. (Cited on page 1.)
- Anthony Bloch. *Hamiltonian and gradient flows, algorithms and control*, volume 3. American Mathematical Soc., 1994. (Cited on page 4.)
- Odile Brandière and Marie Duflo. Les algorithmes stochastiques contournent-ils les pièges ? *Annales de l’I.H.P. Probabilités et statistiques*, 32(3):395–427, 1996. (Cited on pages 2 and 5.)
- Andrew A Brown and Michael C Bartholomew-Biggs. Some effective methods for unconstrained optimization based on the solution of systems of ordinary differential equations. *Journal of Optimization Theory and Applications*, 62:211–224, 1989. (Cited on page 4.)
- Augustin Louis Baron Cauchy. *Analyse algébrique*, volume 1. Debure, 1821. (Cited on page 49.)
- Alberto Chiarini and Markus Fischer. On large deviations for small noise itô processes. *Advances in Applied Probability*, 46(4):1126–1147, 2014. (Cited on pages 21 and 22.)
- Jeremy Cohen, Simran Kaur, Yuezhi Li, J Zico Kolter, and Ameet Talwalkar. Gradient descent on neural networks typically occurs at the edge of stability. In *International Conference on Learning Representations*, 2020. (Cited on pages 14 and 21.)
- Jeremy M Cohen, Behrooz Ghorbani, Shankar Krishnan, Naman Agarwal, Sourabh Medapati, Michal Badura, Daniel Suo, David Cardoze, Zachary Nado, George E Dahl, and Justin Gilmer. Adaptive gradient methods at the edge of stability. *arXiv*, page 2207.14484, 2022. (Cited on page 14.)
- Enea Monzio Compagnoni, Tianlin Liu, Rustem Islamov, Frank Norbert Proske, Antonio Orvieto, and Aurelien Lucchi. Adaptive methods through the lens of SDEs: Theoretical insights on the role of noise. In *International Conference on Learning Representations*, 2025. (Cited on page 5.)
- Martin V Day. On the exit law from saddle points. *Stochastic processes and their applications*, 60(2):287–311, 1995. (Cited on pages 19 and 21.)
- Arnaud Debussche and Erwan Faou. Weak backward error analysis for SDEs. *SIAM Journal on Numerical Analysis*, 50(3):1735–1752, 2012. (Cited on page 8.)
- Aymeric Dieuleveut, Alain Durmus, and Francis Bach. Bridging the gap between constant step size stochastic gradient descent and Markov chains. *The Annals of Statistics*, 48(3):1348 – 1382, 2020. (Cited on page 16.)
- Yoel Drori and Ohad Shamir. The complexity of finding stationary points with stochastic gradient descent. In *International Conference on Machine Learning*, 2020. (Cited on page 1.)
- Cong Fang, Zhouchen Lin, and Tong Zhang. Sharp analysis for nonconvex sgd escaping from saddle points. In *Conference on Learning Theory*, 2019. (Cited on page 1.)
- Yuanfeng Feng, Lei Li, and Jian-Guo Liu. Semi-groups of stochastic gradient descent and online principal component analysis: properties and diffusion approximations. *arXiv*, page 1712.06509, 2017. (Cited on pages 13, 14, 42, 43, 44, 45, and 53.)
- Yuanfeng Feng, Tingran Gao, Lei Li, Jian-Guo Liu, and Yulong Lu. Uniform-in-time weak error analysis for stochastic gradient descent algorithms via diffusion approximation. *arXiv*, page 1902.00635, 2019. (Cited on pages 8, 13, and 14.)

- Simone Fiori and Yoshua Bengio. Quasi-geodesic neural learning algorithms over the orthogonal group: A tutorial. *Journal of Machine Learning Research*, 6(5), 2005. (Cited on page 4.)
- Ronald A Fisher. The use of multiple measurements in taxonomic problems. *Annals of eugenics*, 7(2):179–188, 1936. (Cited on page 15.)
- Xavier Fontaine, Valentin De Bortoli, and Alain Durmus. Convergence rates and approximation results for SGD and its continuous-time counterpart. In *Conference on Learning Theory*, 2021. (Cited on page 4.)
- Mark I. Freidlin and Alexander D. Wentzell. *Random Perturbations of Dynamical Systems*. Springer, 2012. (Cited on pages 19, 20, 21, and 69.)
- Rong Ge, Furong Huang, Chi Jin, and Yang Yuan. Escaping from saddle points—online stochastic gradient for tensor decomposition. In *Conference on Learning Theory*, 2015. (Cited on page 5.)
- Rong Ge, Sham M Kakade, Rahul Kidambi, and Praneeth Netrapalli. The step decay schedule: A near optimal, geometrically decaying learning rate procedure for least squares. In *Advances in Neural Information Processing Systems*, 2019. (Cited on page 16.)
- Saeed Ghadimi and Guanghui Lan. Stochastic first-and zeroth-order methods for nonconvex stochastic programming. *SIAM Journal on Optimization*, 23(4):2341–2368, 2013. (Cited on page 1.)
- Ernst Hairer, Marlis Hochbruck, Arieh Iserles, and Christian Lubich. Geometric numerical integration. *Oberwolfach Reports*, 3(1):805–882, 2006. (Cited on pages 6 and 7.)
- Uwe Helmke and John B Moore. *Optimization and dynamical systems*. Springer Science & Business Media, 2012. (Cited on page 4.)
- Einar Hille and Ralph Saul Phillips. *Functional analysis and semi-groups*, volume 31. American Mathematical Society, 1996. (Cited on page 8.)
- Wenqing Hu, Chris Junchi Li, Lei Li, and Jian-Guo Liu. On the diffusion approximation of nonconvex stochastic gradient descent. *Annals of Mathematical Sciences and Applications*, 4(1):3–32, 2019. (Cited on pages 2, 5, 8, 13, 14, and 16.)
- Hikaru Ibayashi and Masaaki Imaizumi. Why does SGD prefer flat minima?: Through the lens of dynamical systems. In *When Machine Learning meets Dynamical Systems: Theory and Applications*, 2023. (Cited on pages 2, 5, 12, 16, and 20.)
- Arthur Jacot, Franck Gabriel, and Clément Hongler. Neural tangent kernel: Convergence and generalization in neural networks. In *Advances in Neural Information Processing Systems*, 2018. (Cited on page 16.)
- Stanisław Jastrzebski, Zachary Kenton, Devansh Arpit, Nicolas Ballas, Asja Fischer, Yoshua Bengio, and Amos Storkey. Three factors influencing minima in SGD. *arXiv*, page 1711.04623, 2017. (Cited on pages 5 and 12.)
- Chi Jin, Rong Ge, Praneeth Netrapalli, Sham M Kakade, and Michael I Jordan. How to escape saddle points efficiently. In *International Conference on Machine Learning*, 2017. (Cited on page 5.)
- Nitish Shirish Keskar, Dheevatsa Mudigere, Jorge Nocedal, Mikhail Smelyanskiy, and Ping Tak Peter Tang. On large-batch training for deep learning: Generalization gap and sharp minima. In *International Conference on Learning Representations*, 2017. (Cited on page 2.)
- Ahmed Khaled and Peter Richtárik. Better theory for SGD in the nonconvex world. *Transactions on Machine Learning Research*, 2023. (Cited on page 1.)
- Yuri Kifer. The exit problem for small random perturbations of dynamical systems with a hyperbolic fixed point. *Israel Journal of Mathematics*, 40:74–96, 1981. (Cited on pages 19, 21, 22, and 70.)

- P.E. Kloeden and E. Platen. *Numerical Solution of Stochastic Differential Equations*. Stochastic Modelling and Applied Probability. Springer Berlin Heidelberg, 2011. (Cited on page 8.)
- Walid Krichene, Alexandre Bayen, and Peter L Bartlett. Accelerated mirror descent in continuous and discrete time. In *Advances in Neural Information Processing Systems*, 2015. (Cited on page 4.)
- Lei Li and Yuliang Wang. On uniform-in-time diffusion approximation for stochastic gradient descent. *arXiv*, page 2207.04922, 2022. (Cited on pages 8, 13, and 15.)
- Qianxiao Li, Cheng Tai, and Weinan E. Stochastic modified equations and adaptive stochastic gradient algorithms. In *International Conference on Machine Learning*, 2017. (Cited on pages 3, 4, 8, 13, and 14.)
- Qianxiao Li, Cheng Tai, and Weinan E. Stochastic modified equations and dynamics of stochastic gradient algorithms i: Mathematical foundations. *Journal of Machine Learning Research*, 20(40):1–47, 2019. (Cited on page 13.)
- Xiaoyu Li and Francesco Orabona. A high probability analysis of adaptive sgd with momentum. *arXiv*, page 2007.14294, 2020. (Cited on page 1.)
- Zhiyuan Li, Sathika Malladi, and Sanjeev Arora. On the validity of modeling sgd with stochastic differential equations (sdes). In *Advances in Neural Information Processing Systems*, 2021. (Cited on page 4.)
- Tsung-Yu Lin and Subhansu Maji. Improved bilinear pooling with CNNs. *arXiv*, page 1707.06772, 2017. (Cited on page 40.)
- Jun Liu and Ye Yuan. Almost sure saddle avoidance of stochastic gradient methods without the bounded gradient assumption. *arXiv*, page 2302.07862, 2023. (Cited on pages 2 and 5.)
- Chao Ma, Lei Wu, and Weinan E. A qualitative study of the dynamic behavior for adaptive gradient algorithms. In *Mathematical and Scientific Machine Learning*. PMLR, 2022. (Cited on page 5.)
- Sathika Malladi, Kaifeng Lyu, Abhishek Panigrahi, and Sanjeev Arora. On the sdes and scaling rules for adaptive gradient algorithms. In *Advances in Neural Information Processing Systems*, 2022. (Cited on page 5.)
- Stephan Mandt, Matthew D Hoffman, and David M Blei. Continuous-time limit of stochastic gradient descent revisited. In *OPT workshop, NIPS*, 2015. (Cited on page 4.)
- Stephan Mandt, Matthew Hoffman, and David Blei. A variational analysis of stochastic gradient algorithms. In *International Conference on Machine Learning*, 2016. (Cited on page 4.)
- Panayotis Mertikopoulos, Nadav Hallak, Ali Kavis, and Volkan Cevher. On the almost sure convergence of stochastic gradient descent in non-convex problems. In *Advances in Neural Information Processing Systems*, 2020. (Cited on pages 2 and 5.)
- Grigori Noikhovich Milstein. *Numerical integration of stochastic differential equations*, volume 313. Springer Science & Business Media, 2013. (Cited on page 8.)
- Takashi Mori, Liu Ziyin, Kangqiao Liu, and Masahito Ueda. Power-law escape rate of SGD. In *International Conference on Machine Learning*, 2022. (Cited on pages 4 and 12.)
- Michael Muehlebach and Michael I Jordan. A dynamical systems perspective on Nesterov acceleration. In *International Conference on Machine Learning*, 2019. (Cited on page 4.)
- Michael Muehlebach and Michael I Jordan. Optimization with momentum: Dynamical, control-theoretic, and symplectic perspectives. *Journal of Machine Learning Research*, 22(73):1–50, 2021. (Cited on page 4.)

- Kamil Nar and Shankar Sastry. Step size matters in deep learning. In *Advances in Neural Information Processing Systems*, 2018. (Cited on page 1.)
- Behnam Neyshabur, Srinadh Bhojanapalli, David Mcallester, and Nati Srebro. Exploring generalization in deep learning. In *Advances in Neural Information Processing Systems*, 2017. (Cited on page 2.)
- Behnam Neyshabur, Srinadh Bhojanapalli, and Nathan Srebro. A PAC-bayesian approach to spectrally-normalized margin bounds for neural networks. In *International Conference on Learning Representations*, 2018. (Cited on page 2.)
- Thanh Huy Nguyen, Umut Simsekli, Mert Gurbuzbalaban, and Gaël Richard. First exit time analysis of stochastic gradient descent under heavy-tailed gradient noise. In *Advances in Neural Information Processing Systems*, 2019. (Cited on pages 2 and 5.)
- Antonio Orvieto and Aurelien Lucchi. Continuous-time models for stochastic optimization algorithms. In *Advances in Neural Information Processing Systems*, 2019. (Cited on page 4.)
- Rui Pan, Haishan Ye, and Tong Zhang. Eigencurve: Optimal learning rate schedule for SGD on quadratic objectives with skewed hessian spectrums. *arXiv*, page 2110.14109, 2021. (Cited on page 16.)
- Courtney Paquette and Elliot Paquette. Dynamics of stochastic momentum methods on large-scale, quadratic models. In *Advances in Neural Information Processing Systems*, 2021. (Cited on page 4.)
- Courtney Paquette, Elliot Paquette, Ben Adlam, and Jeffrey Pennington. Homogenization of SGD in high-dimensions: Exact dynamics and generalization properties. *arXiv*, page 2205.07069, 2022. (Cited on pages 4 and 12.)
- Grigorios A Pavliotis. Stochastic processes and applications. *Texts in applied mathematics*, 60, 2014. (Cited on pages 19, 20, and 66.)
- Robin Pemantle. Nonconvergence to unstable points in urn models and stochastic approximations. *The Annals of Probability*, 18(2):698–712, 1990. (Cited on pages 2 and 5.)
- Christian Perret. *The stability of numerical simulations of complex stochastic differential equations*. PhD thesis, ETH Zurich, 2010. (Cited on page 18.)
- Herbert Robbins and Sutton Monro. A Stochastic Approximation Method. *The Annals of Mathematical Statistics*, 22(3):400 – 407, 1951. (Cited on page 1.)
- Mihaela Rosca, Yan Wu, Chongli Qin, and Benoit Dherin. On a continuous time model of gradient descent dynamics and instability in deep learning. *Transactions on Machine Learning Research*, 2022. (Cited on pages 4, 6, 7, 9, 18, 19, 32, 38, and 59.)
- Peter Ross. Generalized hockey stick identities and n -dimensional blockwalking. *The College Mathematics Journal*, 28(4):325, 1997. (Cited on page 35.)
- Simo Särkkä and Arno Solin. *Applied stochastic differential equations*, volume 10. Cambridge University Press, 2019. (Cited on pages 8, 54, and 62.)
- Johannes Schropp and I Singer. A dynamical systems approach to constrained minimization. *Numerical functional analysis and optimization*, 21(3-4):537–551, 2000. (Cited on page 4.)
- Othmane Sebbouh, Robert M Gower, and Aaron Defazio. Almost sure convergence rates for stochastic gradient descent and stochastic heavy ball. In *Conference on Learning Theory*, 2021. (Cited on page 1.)
- Boris V Shabat. *Introduction to complex analysis Part II. Functions of Several Variables*, volume 110 of *Translations of Mathematical Monographs*. American Mathematical Society, 1992. (Cited on page 50.)

- Tony Shardlow. Modified equations for stochastic differential equations. *BIT Numerical Mathematics*, 46: 111–125, 2006. (Cited on page 10.)
- Bin Shi, Simon S Du, Michael I Jordan, and Weijie J Su. Understanding the acceleration phenomenon via high-resolution differential equations. *Mathematical Programming*, 195:79–148, 2022. (Cited on page 4.)
- Willi-Hans Steeb and Yorick Hardy. *Matrix calculus and Kronecker product: a practical approach to linear and multilinear algebra*. World Scientific Publishing Company, 2011. (Cited on page 40.)
- Weijie Su, Stephen Boyd, and Emmanuel J Candes. A differential equation for modeling Nesterov’s accelerated gradient method: Theory and insights. *Journal of Machine Learning Research*, 17(153):1–43, 2016. (Cited on page 4.)
- Flemming Topsøe. Some bounds for the logarithmic function. *Inequality theory and applications*, 4:137, 2007. (Cited on page 60.)
- AD Vent-Tsel’ and MI Freidlin. Some problems concerning stability under small random perturbations. *Theory of Probability & Its Applications*, 17(2):269–283, 1973. (Cited on pages 20, 21, 22, and 69.)
- Mingze Wang and Lei Wu. A theoretical analysis of noise geometry in stochastic gradient descent. *arXiv*, page 2310.00692, 2024. (Cited on page 12.)
- Ashia C Wilson, Rebecca Roelofs, Mitchell Stern, Nati Srebro, and Benjamin Recht. The marginal value of adaptive gradient methods in machine learning. In *Advances in Neural Information Processing Systems*, 2017. (Cited on page 1.)
- Zeke Xie, Issei Sato, and Masashi Sugiyama. A diffusion theory for deep learning dynamics: Stochastic gradient descent exponentially favors flat minima. In *International Conference on Learning Representations*, 2020. (Cited on pages 2, 5, 12, 16, and 20.)
- Zeke Xie, Xinrui Wang, Huishuai Zhang, Issei Sato, and Masashi Sugiyama. Adaptive inertia: Disentangling the effects of adaptive learning rate and momentum. In *International Conference on Machine Learning*, 2022. (Cited on pages 2, 4, 12, 16, and 20.)
- Junchi Yang, Xiang Li, Ilyas Fatkhullin, and Niao He. Two sides of one coin: the limits of untuned SGD and the power of adaptive methods. In *Advances in Neural Information Processing Systems*, 2024. (Cited on page 1.)
- Chiyuan Zhang, Samy Bengio, Moritz Hardt, Benjamin Recht, and Oriol Vinyals. Understanding deep learning (still) requires rethinking generalization. *Commun. ACM*, 64(3):107–115, 2021. (Cited on page 2.)
- Pan Zhou, Jiashi Feng, Chao Ma, Caiming Xiong, Steven Chu Hong Hoi, and Weinan E. Towards theoretically understanding why SGD generalizes better than Adam in deep learning. In *Advances in Neural Information Processing Systems*, 2020. (Cited on pages 4 and 20.)
- Yi Zhou, Yingbin Liang, and Huishuai Zhang. Understanding generalization error of SGD in nonconvex optimization. *Machine Learning*, 111(1):345–375, 2022. (Cited on page 1.)
- Zhanxing Zhu, Jingfeng Wu, Bing Yu, Lei Wu, and Jinwen Ma. The anisotropic noise in stochastic gradient descent: Its behavior of escaping from sharp minima and regularization effects. In *International Conference on Machine Learning*, 2019. (Cited on pages 2, 5, 12, and 16.)

Contents

1	Introduction	1
1.1	Related Work	4
1.2	Paper Structure	5
2	Preliminaries	6
2.1	Notations	6
2.2	Backward Error Analysis (BEA)	6
2.3	Principal Flow	7
3	Stochastic Backward Error Analysis	7
3.1	Differences between BEA and SBEA	7
3.2	Procedures in SBEA	8
3.3	Exact Matching Fails for Order η^3 in SBEA	9
4	Hessian-Aware Stochastic Modified Equation	10
5	Approximation Error Analysis of HA-SME	13
5.1	Weak Approximation Error Guarantee	13
5.2	Fine-Grained Error Analysis with Hessian Dependence	14
5.3	Numerical Experiments	15
6	Exact Recovery of SGD by HA-SME on Quadratics	16
6.1	Failure Cases for Existing SDEs	16
6.2	Hardness of Approximating SGD with OU Process on Quadratics	18
6.3	Exact Approximation From HA-SME	19
7	Escape Analysis Beyond Quadratics	19
7.1	Escaping of HA-SME Near One-Dimensional Local Minimum/Maximum	20
7.2	Escaping Near Multi-Dimensional Saddle Points	21
8	Conclusion and Future Work	22
A	Construction of HA-SME	29
A.1	Proof of Lemma 1	29
A.2	Proof of Lemma 2	29
A.2.1	Proof of Lemma 7	31
A.2.2	Proof of Lemma 8	31
A.2.3	Proof of the Functional Structures in Equations (35) and (36)	31
A.2.4	Proof of Lemma 9 and the Recursive Expressions of $\{c_i\}$ and $\{a_{i,j}\}$	35
A.3	Proof of Theorem 1	38
A.4	Proof of Lemma 3	38
A.5	Proof of Theorem 2	39
A.6	Helper Lemmas	40
B	Approximation Error Analysis	42
B.1	Proofs for Section 5	42
B.2	Helper Lemmas	48

C Exact Match of SGD on Quadratics	53
C.1 Complex Normal Distribution	53
C.2 Proofs for Section 6	54
C.3 Helper Lemmas	60
D Escape Analysis	66

A Construction of HA-SME

A.1 Proof of Lemma 1

Proof. In the semi-group expansion of Equation (16), consider the term $\frac{1}{n!}\eta^n \mathcal{L}^n u(x)$ for $1 \leq n \leq p+1$. Since we already have η^n , to get η^{p+1} , $\mathcal{L}^n u(x)$ must contribute η^{p+1-n} . As \mathcal{L}_i contains η^i , we obtain the conclusion. \square

A.2 Proof of Lemma 2

We start with a sketch of the proof for Lemma 2, where we first determine the functional structure of the components g_i 's and h_i 's in the SBEA ansatz in Equation (11) and then determine their exact expression using a generating function based approach. We prove via induction. The complexity in our analysis emerges from identifying all possible terms generated by the expansion of $\mathcal{L}_{l_1} \mathcal{L}_{l_2} \cdots \mathcal{L}_{l_n}$ in Equation (17). The collective expansion of these operators unfolds as a multinomial series. This sets our work apart from the PF, as in the latter, in the absence of diffusion terms, the expansion generates only a monomial. The rigorous proofs of the statements made in the induction are provided afterwards.

Before providing the inductive proof, statement (1) in Lemma 2, i.e. the uniqueness of g_p and h_p , can be easily obtained from the following argument.

Proof of point (1) in Lemma 2. We first give examples for solving the first few g_i and h_i , then we use an argument of induction to finish the proof. For the terms associated with η^0 , Equation (13) and Equation (16) already match, i.e., $u(x)$. For terms associated with η , we can solve that $g_0(x) = -\nabla f(x)$ and $h_0(x) = 0$. Considering terms with η^2 , we have for discrete-time (Equation (13))

$$\eta^2 \cdot \frac{1}{2} \nabla^2 u(x) : (\nabla f(x) \nabla f(x)^\top + \Sigma(x)),$$

and for continuous-time (Equation (16))

$$\eta^2 \cdot \left(\underbrace{g_1(x)^\top \nabla u(x) + \frac{1}{2} h_1(x) : \nabla^2 u(x)}_{\text{from } \eta \mathcal{L} u(x)} + \underbrace{\frac{1}{2} (-\nabla f \cdot \nabla (-\nabla f \cdot \nabla u))(x)}_{\text{from } \frac{1}{2} \eta^2 \mathcal{L}^2 u(x)} \right).$$

Note that this holds for any proper u , so we group terms associated with ∇u and $\nabla^2 u$ and match the terms in discrete-time and continuous-time. In this way, we obtain 2 equations, which gives us the following g_1 and h_1 :

$$g_1(x) = -\frac{1}{2} \nabla^2 f(x) \nabla f(x) \quad \text{and} \quad h_1(x) = \Sigma(x). \quad (32)$$

Now assume we already know $\{g_i\}_{1 \leq i < p}$ and $\{h_i\}_{1 \leq i < p}$. We will proceed to solve g_p and h_p . This is done by solving terms with η of order $p+1$. The terms associated with η^{p+1} are shown in Lemma 1. When $n = 1$, we will have linear terms with g_p and h_p , respectively. When $n \geq 2$, since $l_1 + l_2 + \cdots + l_n$ could only sum to $p-1$, we only have g_i and h_i for $i < p$. Given that we assume $\{g_i\}_{1 \leq i < p}$ and $\{h_i\}_{1 \leq i < p}$ are already solved, by grouping terms with ∇u and $\nabla^2 u$, we obtain two linear equations and can solve for g_p and h_p . Note that the coefficients for g_p and h_p in these two linear equations are non-zero, therefore, the solution exists and is unique. \square

We now give a sketch of the inductive proof of the second statement in Lemma 2, on the functional structure of the components h_p 's and g_p 's. Recall point (2) in Lemma 2: The components g_p and h_p admit the form

$$g_p(x) = c_p \cdot (\nabla^2 f(x))^p \nabla f(x), \quad (33)$$

$$h_p(x) = \sum_{k=0}^{p-1} a_{k,p-1-k} \cdot (\nabla^2 f(x))^k \Sigma(x) (\nabla^2 f(x))^{p-1-k}, \quad (34)$$

where $\{c_k\}$ and $\{a_{k,p-1-k}\}$ are constants to be determined. Let q be the induction index and let Equations (19) and (20) be the induction hypothesis for $q = p \geq 1$. Such a hypothesis clearly holds for $q = 1$ (recall the calculation in Remark 2). The following lemma shows that the nice functional structures in Equations (19) and (20) are preserved for $q = p + 1$.

Lemma 7. *Under Principle 3, suppose that Equations (19) and (20) hold in step $q = p$. They also hold for $q = p + 1$.*

Proof sketch. To establish the induction, we need to enumerate all possible terms generated by the expansion in Equation (17). Viewing the application of each \mathcal{L}_{l_i} as a layer, this process entails a dual-stage selection mechanism:

1. Within each layer we consider the terms generated from either $\eta^{l_i} g_{l_i} \cdot \nabla$ or $\frac{\eta^{l_i}}{2} h_{l_i} : \nabla^2$ in \mathcal{L}_{l_i} .
2. For a fixed layer, we consider how the operators ∇ and ∇^2 are applied on the subsequent layer. For example, for the operator ∇ , it could be acting on $g_{l_{i+1}}$ to yield a concrete function $\nabla g_{l_{i+1}}$, or it can engage with the operator ∇^2 from the subsequent layer to form the operator ∇^3 .

Finally, for every possible **sequence-of-selections** made in the above mechanism, any remaining differential operators ∇^j will be applied on the test function u . Hereafter, we use the typewriter font to emphasize that the **sequence-of-selections** is with respect to the above selection mechanism.

Unraveling all potential selection in Equation (17) is inherently difficult. However, Principle 3 allows us to ensure the particular structures of g_p and h_p . For the following discussion, we introduce the concept of **free-nabla-j**: During unraveling of the operator compositions in Equation (17), a **free-nabla-j** is generated if we obtain an operator ∇^j during any stage of the above selection mechanism.

We have the following result.

Lemma 8. *Once **free-nabla-j**, for $j \geq 3$, is generated, one can terminate the subsequent operator expansion as all the resulting terms will be excluded by Principle 3.*

See an elaborated discussion in Appendix A.2.1. From this observation, the expansion of Equation (17) can be significantly simplified and one can show that if the induction in Equations (19) and (20) holds for $q = p$, g_{p+1} and h_{p+1} admit the following form:

$$g_{p+1}(x) = c_{p+1} \cdot (\nabla^2 f(x))^{p+1} \nabla f(x) \quad (35)$$

$$h_{p+1}(x) = \sum_{k=0}^p (a_{k,p-k} + b_{k,p-k} \cdot \|\nabla f(x)\|^2) \cdot (\nabla^2 f(x))^k \Sigma(x) (\nabla^2 f(x))^{p-k}. \quad (36)$$

Further, a detailed examination of the combinations reveals the following result.

Lemma 9. $b_{k,p-k} \equiv 0$.

The above results together establish the induction step of $q = p + 1$. □

Once we have determined the functional structure of g_p and h_p , the next step is to determine the coefficients $a_{i,j}$ and c_p . As we obtain the structures of g_p and h_p by induction, the coefficients admit recursion forms. To resolve these coefficients, we utilize an argument based on the generating functions. As a result, we obtain point (3) in Lemma 2.

A.2.1 Proof of Lemma 7

To establish the inductive step in Lemma 7, we prove the following points in this section.

- (a) We first prove Lemma 8, which allows us to significantly simplify the expansion of the compositions of the generators \mathcal{L}_i 's.
- (b) We analyze all possible terms generated without incurring **free-nabla**- j , for $j \geq 3$, and find that there are only three possibilities. This leads to the functional structure described in Equations (35) and (36).
- (c) We further provide the recursive definitions of the coefficients $\{c_i\}$, $\{a_{i,j}\}$, and $\{b_{i,j}\}$. This allows us to conclude that $b_{k,p-k} \equiv 0$ (Lemma 9) and also it allows us to calculate the limit of the power series $\{g_p\}$ and $\{h_p\}$, i.e. point (3) in Lemma 2.

A.2.2 Proof of Lemma 8

Let us recall the concept of **free-nabla**- j : During unraveling of the operator compositions in Equation (17), a **free-nabla**- j is generated if we obtain an operator ∇^j during any stage of the selection mechanism mentioned in the proof sketch of Lemma 7.

In the following, we will show that once **free-nabla**- j for $j \geq 3$ is generated in a **sequence-of-selections** mentioned in the proof sketch of Lemma 7, the term resulting from this sequence is excluded by Principle 3, i.e. it contains at least one of the terms $\nabla^{(r)}f(x)$, $\nabla^{(s)}u(x)$ and $\nabla^{(m)}\Sigma(x)$ for $r, s \geq 3$ and $m \geq 1$. To establish this result, there are two possibilities once **free-nabla**- j for $j \geq 3$ is generated:

1. The **free-nabla**- j operator is to be directly applied on the test function u . In this case, all the resulting term from this **sequence-of-selections** contains $\nabla^{(j)}u(x)$, $j \geq 3$, which is excluded by Principle 3.
2. The **free-nabla**- j operator is to be applied on a generator \mathcal{L}_i , i.e. we encounter the term

$$\nabla^{(j)}(\eta^i g_i \cdot \nabla + \frac{1}{2} \eta^i h_i : \nabla^2). \quad (37)$$

One can prove that (see the discussion below) all terms in the expansion of the above expression either is excluded by Principle 3 or it contains **free-nabla**- q for $q \geq j$ ⁹. Consequently, the order j does not decrease after the operator **free-nabla**- j being applied on a generator \mathcal{L}_i .

One can repeat the case 2 until the **free-nabla**- j operator is directly applied on the test function u , which reduces to case 1. From the above argument, all terms generated are to be excluded by Principle 3.

A.2.3 Proof of the Functional Structures in Equations (35) and (36)

According to Lemma 8, we only need to consider the **sequence-of-selections** mentioned in the proof sketch of Lemma 7 such that no **free-nabla**- j operator is generated, for $j \geq 3$. It turns out that there are only three possible **sequence-of-selections**, as depicted in Figure 3.

In this section, we elaborate on these three possible sequences, based on which we then establish the functional structures in Equations (35) and (36). In the meantime, we also derive the recursive definitions of the coefficients $\{c_i\}$, $\{a_{i,j}\}$, and $\{b_{i,j}\}$.

⁹For simplicity, we take $j = 3$ as example. For $j > 3$, the logic is similar. One has for the first term in Equation (37)

$$\nabla^{(3)}(g_i \cdot \nabla) = \underbrace{g_i \cdot \nabla^{(4)}}_{\text{free-nabla-4}} + \underbrace{\nabla g_i \cdot \nabla^{(3)}}_{\text{free-nabla-3}} + \underbrace{\nabla^2 g_i \cdot \nabla^{(2)} + \nabla^3 g_i \cdot \nabla}_{\text{every term contains } \nabla^r f, r \geq 3}.$$

By the product rule of the differential and based on the induction in Equation (35), one can check that in the expansions of $\nabla^2 g_i$ and $\nabla^3 g_i$, all terms contain $\nabla^r f$, for $r \geq 3$. Hence, the last two terms in the above expression are excluded by Principle 3. The second term in Equation (37) can be excluded with a similar argument.

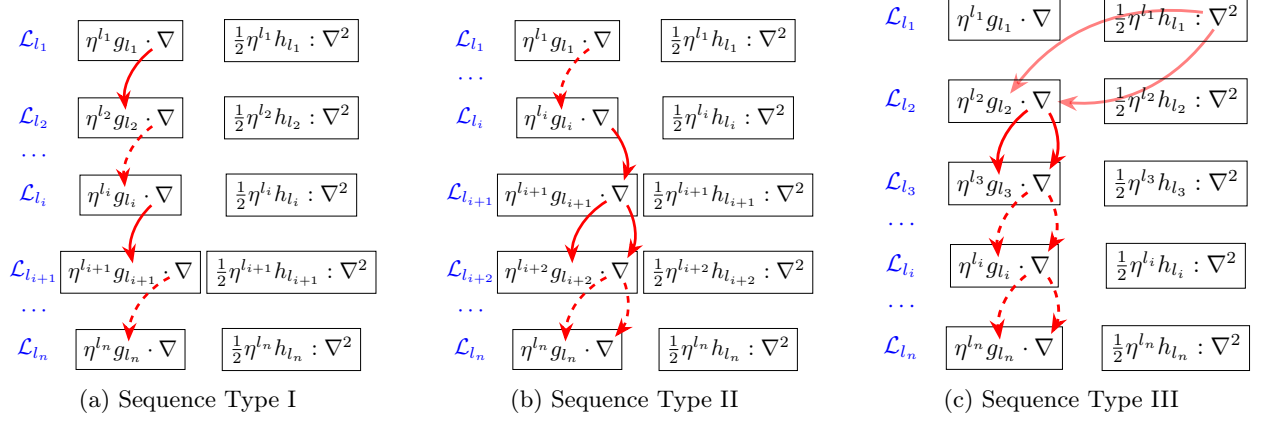


Figure 3: Illustrations of possible combinations in the construction of HA-SME. In constructing HA-SME, we examine the product of $\mathcal{L}_{l_1} \mathcal{L}_{l_2} \cdots \mathcal{L}_{l_n}$, where each \mathcal{L}_{l_i} contains two terms. The red arrows indicate the remaining Sequences after filtering out those with higher-order derivatives of f , u , or Σ , which are excluded in the construction rules of HA-SME. These arrows originate from ∇ or ∇^2 and lead to g_{l_i} or ∇ , demonstrating how the ∇ from the previous operator is applied in the subsequent operator. The dashed arrows represent the exclusion of repeated operations.

Notation For the ease of the proof, we define for $n \geq 1$, $m \geq 0$ and sequence $\{c_i\}_{i=0}^{+\infty}$,

$$\rho(n, m, \{c_i\}_{i=0}^{+\infty}) = \sum_{l_1 + l_2 + \dots + l_n = m} c_{l_1} c_{l_2} \cdots c_{l_n},$$

i.e., sum of all possible combinations of n items from sequence $\{c_i\}_{i=0}^{+\infty}$ such that the sum of indices is m . A way to look at this is through generating functions. Let $c(x) = \sum_{i=0}^{+\infty} c_i x^i$, then $\rho(n, m, \{c_i\}_{i=0}^{+\infty})$ is equivalent to the coefficient of x^m in $c(x)^n$.

Solve for g_p We claim that we can solve g_p by matching terms with ∇u . To show the claim, we observe that ∇u terms could only be achieved by choosing g_{l_i} and never selecting h_{l_i} for all $1 \leq i \leq n$. This is the case of our Sequence Type I illustrated in Figure 3a. To see why this is the case, we start with \mathcal{L}_{l_n} , since we want terms with $\nabla u(x)$, we must select g_{l_n} instead of h_{l_n} . Next, when selecting from $\mathcal{L}_{l_{n-1}}$, we could also only select $g_{l_{n-1}}$, since if $h_{l_{n-1}}$ is chosen, we would have $h_{l_{n-1}} : \nabla^2 (g_{l_n} \cdot \nabla u)$. The ∇^2 operation must be applied to g_{l_n} otherwise we will have $\nabla^2 u$ instead of ∇u . However, when we apply the gradient operator twice in g_{l_n} , there must be a third-order gradient factor, which we choose to exclude, popping up as we have g_{l_n} of form Equation (19). Following this logic recursively, we have that ∇u terms contain only g_i (with $0 \leq i \leq p-1$). Also note that the gradient operator in $g_{l_i} \cdot \nabla$ must be applied to $g_{l_{i+1}}$ except when $i = n$ where the gradient operator is applied to u , otherwise we will have ∇^2 operator and face the same issue as when we selecting h_{l_i} .

Since now in the ∇u terms only contains g_p (with non-zero coefficient) without h_p , we can solve for g_p . Again, since the gradient operator from g_{l_i} (except $i = n$) could only be used for the next $g_{l_{i+1}}$, specifically applied on the $\nabla f(x)$ factor of $g_{l_{i+1}}$ otherwise we would have third-order gradient of $f(x)$, we have $n-1$ factors of $\nabla f(x)$ changed to $\nabla^2 f(x)$ and only one remains. Therefore, g_p is of form Equation (19).

The remaining proof for finding c_p is almost the same as the proof for Theorem A.2 of Rosca et al. [2022]. The resulting c_i is the coefficients of the Taylor expansion of $c(x) = \frac{\log(1-x)}{x}$, i.e., $c(x) = \sum_{i=0}^{+\infty} c_i x^i$.

Solve for h_p In the proof g_p , we have shown that the ∇u terms allow us to solve g_p , and now we proceed to solve the form of h_p by considering $\nabla^2 u$ terms. Again, to solve h_p , we need terms with the order of η

summing up to $p + 1$ and consider Lemma 1. Let us discuss what are the valid possibilities of selections from such an expansion.

Let us call the selection between g_{l_i} and h_{l_i} the i -th step of selection. Assume we have the gradient operator ∇^q after the i -th step. If in the next step, we select $g_{l_{i+1}} \cdot \nabla$, since $g_{l_{i+1}}$ has only one factor of ∇f , which means we can only apply the gradient operator once on this $g_{l_{i+1}}$, the order of the remaining gradient operator passed to the next step is still at least q . If in the $i + 1$ -th step, we select $h_{l_{i+1}} : \nabla^2$ instead, all the gradient operators should go to the next step (otherwise, if applied on $h_{l_{i+1}}$, factors we exclude will emerge), resulting in a ∇^{q+2} . Note that by our construction, in the end, the operator applied on u should not exceed 2. Therefore no matter what we select from the first step, which produces at least ∇ , we should only select g_{l_i} instead h_{l_i} for $i > 1$. Because otherwise we would have at least ∇^3 passing to u . According to the above reasoning, we have only two cases left:

1. **If we select g_{l_1} in the first step**, which corresponds to Figure 3b, then in order to get $\nabla^2 u$ at the end, we will need at a step i with $2 \leq i \leq n$, the gradient operator is not applied to g_{l_i} but passed to the next step. For other steps, the operator is applied to g . This is the only way to have $\nabla^2 u$. Plugging in the solution of g_i , we know that the resulting term in Equation (16) is of form

$$\eta^{p+1} \sum_{s=0}^{p-1} b_{s,p-1-s} \text{Tr} \left\{ \nabla f(x) (\nabla^2 f(x))^s \nabla^2 u(x) (\nabla^2 f(x))^{p-1-s} \nabla f(x)^\top \right\},$$

where $b_{s,p-1-s}$ can be written as

$$b_{s,p-1-s} = \sum_{n=2}^{p+1} \frac{1}{n!} \sum_{i=2}^n \sum_{q=0}^{n-i} \binom{n-i}{q} \rho(q+1, p-1-s-q, \{c_k\}_{k=0}^{+\infty}) \rho(n-1-q, s+q-n+2, \{c_k\}_{k=0}^{+\infty}), \quad (38)$$

where $c_k = -\frac{1}{1+k}$, the coefficient associated with g_i . Note that the coefficient is for terms with $\nabla^2 f(x)$ to the power of s on the left of $\nabla^2 u$ and $p-1-s$ on the right. To see why this is the case, we have the following selection procedure:

- (a) Such terms can be found in $\frac{\eta^n}{n!} \mathcal{L}^n u$ for $n = 2$ to $p+1$.
- (b) As mentioned before, we have at step $2 \leq i \leq n$, the gradient operator is not applied to g_{l_i} . Note that in this case the $\nabla^2 f(x)$ coming from g_{l_i} will contribute to the RHS of $\nabla^2 u$. Then we will have for the remaining steps of selection,

$$\nabla^2 (g_{l_{i+1}} \cdot \nabla (g_{l_{i+2}} \cdot \nabla (\cdots g_{l_n} \cdot \nabla u))).$$

- (c) According to Lemma 13, there are $\binom{n-i}{q}$ combinations such that the number of ∇g resulting in the RHS of $\nabla^2 u$ is q .
- (d) For the RHS of $\nabla^2 u$, we have g_{l_i} and q of ∇g selected from the last step. Note that g_k would contains $(\nabla^2 f(x))^k$ for $k \geq 0$, and for the q of ∇g , we obtain additional $(\nabla^2 f(x))^q$ because of the ∇ operator. Therefore, the total number of $\nabla^2 f(x)$ on the RHS of $\nabla^2 u$ comes from g_{l_i} and q of ∇g and an additional q . Therefore, we select from $q+1$ of g , whose indices sum up to $p-1-s-q$ (so that the total order of $\nabla f(x)$ is $p-1-s-q+q=p-1-s$).
- (e) For the LHS of $\nabla^2 u$, we have g_1 , $\{\nabla g_{l_k}\}_{k=2}^{i-1}$ and $n-i-q$ of ∇g selected according to Step 1c. Following similar logic as the last step, in total we select $1+i-2+n-i-q=n-1-q$ of g , whose indices sum up to $s+q-n+2$.

We note that for any matrix A , $\text{Tr}\{A\} = \text{Tr}\{A^\top\}$, so the traces associated with $b_{s,m}$ and $b_{m,s}$ are the same for $s, m \geq 0$. According to Lemma 10, $b_{s,m} + b_{m,s} = 0$ for $m+s \geq 1$. Therefore, the coefficients cancel each other. For the case of $b_{s,s}$ with $s \geq 1$, Lemma 10 also implies $b_{s,s} + b_{s,s} = 0 \implies b_{s,s} = 0$.

Therefore, in summary, in this whole case, there is no term generated.

2. **If we select h_{l_1} in the first step**, which corresponds to Figure 3c, then in order to get $\nabla^2 u$ at the end, we will in the following steps apply the gradient at g_{l_k} for $k \geq 2$ at once and pass to the next step the other gradient operator. In this way, all terms of Equation (16) with order of η summing to $p+1$ and coming from $\frac{1}{n!}\mathcal{L}^n u$, has the following form:

$$\frac{1}{2}\eta^{p+1}\tilde{a}_{i,j,k} \text{Tr}\left\{(\nabla^2 f(x))^i \Sigma(x) (\nabla^2 f(x))^j \nabla^2 u(x) (\nabla^2 f(x))^k\right\}, \quad (39)$$

for some absolute constants $\tilde{a}_{i,j,k}$ with $i+j+k=p-1$. The reason why we have this form is because of our induction assumption and Lemma 13. The reason why $i+j+k=p-1$ is that to have η^{p+1} , we must have $l_1+l_2+\dots+l_n=p+1-n$. For the first step, we have h_{l_1} . According to the induction assumption, it can offer (l_1-1) -th order of $\nabla^2 f(x)$. For the remaining steps, we have ∇g_{l_s} , which can offer (l_s+1) -th order of $\nabla^2 f(x)$. Therefore, in total we have $\nabla f(x)$ to the power of $l_1-1+l_2+l_3+\dots+l_n+n-1=p+1-n-1+n-1=p-1$. According to the property of the trace operator, Equation (39) can also be written as

$$\frac{1}{2}\eta^{p+1}\tilde{a}_{i,j,k} \text{Tr}\left\{(\nabla^2 f(x))^{k+i} \Sigma(x) (\nabla^2 f(x))^j \nabla^2 u(x)\right\}.$$

Now we try to match the η^{p+1} terms in Equation (13) and Equation (16). Note that in Equation (13), the term associated with η^{p+1} for $p \geq 2$ is 0, therefore we have the following equality for solving h_p :

$$\frac{1}{2}\eta^{p+1} \left(\text{Tr}\{h_p(x)^\top \nabla^2 u(x)\} + \sum_{n=2}^{p+1} \tilde{a}_{i,j,k} \text{Tr}\left\{(\nabla^2 f(x))^{k+i} \Sigma(x) (\nabla^2 f(x))^j \nabla^2 u(x)\right\} \right) = 0,$$

which implies (since this should hold for any u)

$$h_p(x) = - \sum_{n=2}^{p+1} \tilde{a}_{i,j,k} (\nabla^2 f(x))^j \Sigma(x) (\nabla^2 f(x))^{k+i}.$$

So far, by induction, we have proved that h_p has the form of Equation (19) (regardless of the constants). Next we will try to find these constants. We will stick to the notation in Lemma 2, i.e., using $a_{i,j}$ for the rest of the proof, i.e.,

$$h_p(x) = \sum_{k=0}^{p-1} a_{k,p-1-k} \cdot (\nabla^2 f(x))^k \Sigma(x) (\nabla^2 f(x))^{p-1-k}.$$

Similar to the proof of Equation (38), we have

$$\begin{aligned} a_{k,p-1-k} = & - \sum_{n=2}^p \frac{1}{n!} \sum_{l=0}^k \sum_{r=0}^{p-1-k} a_{l,r} \sum_{q=0}^{n-1} \binom{n-1}{q} \rho(q, k-q-l, \{c_k\}_{k=0}^{+\infty}) \\ & \rho(n-1-q, p-k-n+q-r, \{c_k\}_{k=0}^{+\infty}). \end{aligned} \quad (40)$$

The reason is that we have the following selection process:

- (a) Such terms can be found in $\frac{\eta^n}{n!}\mathcal{L}^n u$ for $n=2$ to $p+1$.
- (b) We try to find term with

$$\text{Tr}\left\{(\nabla^2 f(x))^{p-1-k} \Sigma(x) (\nabla^2 f(x))^k \nabla^2 u\right\},$$

which can be found from Sequence

$$\underbrace{(\nabla^2 f(x))^l \Sigma(x) (\nabla^2 f(x))^r}_{h_{l_1}} : (\nabla^2 f(x))^{k-l} \nabla^2 u (\nabla^2 f(x))^{p-1-k-r}.$$

- (c) For $(\nabla^2 f(x))^k$, we can have $(\nabla^2 f(x))^l$ coming from h_{l_1} . Also h_{l_1} can contribute to $(\nabla f(x))^{p-1-k}$ with $(\nabla^2 f(x))^r$. That is why we have summations over l and r with coefficients $a_{l,r}$.
- (d) As mentioned before, we have for the selection at step $2 \leq k \leq n$,

$$\nabla^2 (g_{l_2} \cdot \nabla (g_{l_3} \cdot \nabla (\cdots g_{l_n} \cdot \nabla u))).$$

According to Lemma 13, there are $\binom{n-1}{q}$ combinations such that the number of ∇g resulting in the LHS of $\nabla^2 u$ is q .

- (e) For the LHS of $\Sigma(x)$, we have q of ∇g selected from the last step. The indices should sum up to $k - q - l$, since we will generate additional q of $\nabla^2 f(x)$ and h_{l_1} provides l . Therefore, we have coefficient $\rho(q, k - q - l, \{c_k\}_{k=0}^{+\infty})$ similarly for the RHS.

A.2.4 Proof of Lemma 9 and the Recursive Expressions of $\{c_i\}$ and $\{a_{i,j}\}$

Lemma 10. Recall the recursive definition of $b_{s,m}$ in Equation (38),

$$b_{s,m} = \sum_{n=2}^{s+m+2} \frac{1}{n!} \sum_{i=2}^n \sum_{q=0}^{n-i} \binom{n-i}{q} \rho(q+1, m-q, \{c_k\}_{k=0}^{+\infty}) \rho(n-1-q, s+q-n+2, \{c_k\}_{k=0}^{+\infty}),$$

where $s, m \geq 0$, $s+m \geq 1$, $c_k = -\frac{1}{k+1}$. We have $b_{s,m} + b_{m,s} = 0$.

Proof. Let $c(x) = \sum_{k=0}^{+\infty} c_k x^k$, and we know that $c(x) = \frac{\log(1-x)}{x}$. Define

$$b(x, y) = \sum_{s,m \geq 0}^{+\infty} b_{s,m} x^s y^m.$$

Then we have

$$\begin{aligned} & b(x, y) \\ &= \sum_{s,m \geq 0}^{+\infty} x^s y^m \sum_{n=2}^{s+m+2} \frac{1}{n!} \sum_{i=2}^n \sum_{q=0}^{n-i} \binom{n-i}{q} \rho(q+1, m-q, \{c_k\}_{k=0}^{+\infty}) \rho(n-1-q, s+q-n+2, \{c_k\}_{k=0}^{+\infty}) \\ &= \sum_{n=2}^{+\infty} \frac{1}{n!} \sum_{s+m \geq n-2}^{+\infty} x^s y^m \sum_{i=2}^n \sum_{q=0}^{n-i} \binom{n-i}{q} \rho(q+1, m-q, \{c_k\}_{k=0}^{+\infty}) \rho(n-1-q, s+q-n+2, \{c_k\}_{k=0}^{+\infty}) \\ &= \sum_{n=2}^{+\infty} \frac{1}{n!} \sum_{s+m \geq n-2}^{+\infty} x^s y^m \sum_{q=0}^{n-2} \sum_{i=2}^{n-q} \binom{n-i}{q} \rho(q+1, m-q, \{c_k\}_{k=0}^{+\infty}) \rho(n-1-q, s+q-n+2, \{c_k\}_{k=0}^{+\infty}) \\ &= \sum_{n=2}^{+\infty} \frac{1}{n!} \sum_{s+m \geq n-2}^{+\infty} x^s y^m \sum_{q=0}^{n-2} \binom{n-1}{q+1} \rho(q+1, m-q, \{c_k\}_{k=0}^{+\infty}) \rho(n-1-q, s+q-n+2, \{c_k\}_{k=0}^{+\infty}) \\ &= \sum_{n=2}^{+\infty} \frac{1}{n!} \sum_{s+m \geq n-2}^{+\infty} x^s y^m \sum_{q=1}^{n-2} \binom{n-1}{q} \rho(q, m-q+1, \{c_k\}_{k=0}^{+\infty}) \rho(n-q, s+q-n+1, \{c_k\}_{k=0}^{+\infty}) \\ &= \frac{1}{y} \sum_{n=2}^{+\infty} \frac{1}{n!} \sum_{s+m \geq n-2}^{+\infty} x^s y^{m+1} \sum_{q=1}^{n-2} \binom{n-1}{q} \rho(q, m-q+1, \{c_k\}_{k=0}^{+\infty}) \rho(n-q, s+q-n+1, \{c_k\}_{k=0}^{+\infty}), \end{aligned}$$

where in the forth equality, we used hockey-stick identity [Ross, 1997], and in the fifth equality, we replace q with $q-1$. Note that

$$\sum_{s+m \geq n-2}^{+\infty} x^s y^{m+1} \sum_{q=1}^{n-2} \binom{n-1}{q} \rho(q, m-q+1, \{c_k\}_{k=0}^{+\infty}) \rho(n-q, s+q-n+1, \{c_k\}_{k=0}^{+\infty}) \quad (41)$$

is equivalent to

$$(yc(y) + xc(x))^{n-1} c(x) - (xc(x))^{n-1} c(x). \quad (42)$$

To see why this is the case, let us first look at $(yc(y) + xc(x))^{n-1} c(x)$. To have y^{m+1} , we can select $yc(y)$ from $(yc(y) + xc(x))^{n-1}$ for q times, which results in coefficients $\binom{n-1}{q}$ and $\rho(q, m - q + 1, \{c_k\}_{k=0}^{+\infty})$. For x^s , we select $n - 1 - q$ of $xc(x)$ from $(yc(y) + xc(x))^{n-1}$, and obtain $\rho(n - q, s + q - n + 1, \{c_k\}_{k=0}^{+\infty})$. Note that in Equation (41), the sum of q starts from 1, which means we have not considered the case where $yc(y)$ is never selected in $(yc(y) + xc(x))^{n-1}$. That is why in Equation (42), we subtract $(xc(x))^{n-1} c(x)$.

Next, we proceed with

$$\begin{aligned} b(x, y) &= \frac{1}{y} \sum_{n=2}^{+\infty} \frac{1}{n!} \left((yc(y) + xc(x))^{n-1} c(x) - (xc(x))^{n-1} c(x) \right) \\ &= \frac{1}{y} \sum_{n=2}^{+\infty} \frac{1}{n!} (yc(y) + xc(x))^{n-1} c(x) - \frac{1}{y} \sum_{n=2}^{+\infty} \frac{1}{n!} (xc(x))^{n-1} c(x). \end{aligned} \quad (43)$$

For the first part, we have

$$\begin{aligned} \frac{1}{y} \sum_{n=2}^{+\infty} \frac{1}{n!} (yc(y) + xc(x))^{n-1} c(x) &= \frac{c(x)}{y(yc(y) + xc(x))} \sum_{n=2}^{+\infty} \frac{1}{n!} (yc(y) + xc(x))^n \\ &= \frac{c(x)}{y(yc(y) + xc(x))} \left(e^{yc(y) + xc(x)} - 1 - (yc(y) + xc(x)) \right), \end{aligned}$$

where in the last equality we used Taylor expansion $e^x = \sum_{n=0}^{+\infty} \frac{1}{n!} x^n$. Plugging in the definition of $c(x)$, we have

$$\begin{aligned} &\frac{c(x)}{y(yc(y) + xc(x))} \left(e^{yc(y) + xc(x)} - 1 - (yc(y) + xc(x)) \right) \\ &= \frac{\log(1-x)}{xy \log((1-x)(1-y))} ((1-x)(1-y) - 1 - \log((1-x)(1-y))) \\ &= \frac{\log(1-x)}{xy \log((1-x)(1-y))} (xy - x - y - \log((1-x)(1-y))). \end{aligned}$$

For the second part of Equation (43),

$$\begin{aligned} \frac{1}{y} \sum_{n=2}^{+\infty} \frac{1}{n!} (xc(x))^{n-1} c(x) &= \frac{1}{xy} \sum_{n=2}^{+\infty} \frac{1}{n!} (xc(x))^n = \frac{1}{xy} \left(e^{xc(x)} - 1 - xc(x) \right) \\ &= \frac{1}{xy} (1 - x - 1 - \log(1-x)) = \frac{1}{xy} (-x - \log(1-x)). \end{aligned}$$

Combining the two parts, we get

$$\begin{aligned} b(x, y) &= \frac{\log(1-x)}{xy \log((1-x)(1-y))} (xy - x - y - \log((1-x)(1-y))) + \frac{1}{xy} (x + \log(1-x)) \\ &= \frac{\log(1-x)}{xy \log((1-x)(1-y))} (xy - x - y) + \frac{1}{y}. \end{aligned}$$

Now to prove the required result, we consider the generator function

$$b(x, y) + b(y, x)$$

$$\begin{aligned}
&= \frac{\log(1-x)}{xy \log((1-x)(1-y))} (xy - x - y) + \frac{1}{y} + \frac{\log(1-y)}{xy \log((1-x)(1-y))} (xy - x - y) + \frac{1}{x} \\
&= \frac{1}{xy} (xy - x - y) + \frac{1}{x} + \frac{1}{y} = 1.
\end{aligned}$$

Note that the coefficients of $b(x, y) + b(y, x)$ for $x^s y^m$ with $s + m \geq 1$ is $b_{s,m} + b_{m,s}$, which means $b_{s,m} + b_{m,s} = 0$. \square

Lemma 11. Define $a_{0,0} = 1$ and for $s, m \geq 0$ and $s + m \geq 1$, recall the recursive definition in Equation (40),

$$\begin{aligned}
a_{s,m} = & - \sum_{n=2}^{s+m+1} \frac{1}{n!} \sum_{l=0}^s \sum_{r=0}^m a_{l,r} \sum_{q=0}^{n-1} \binom{n-1}{q} \rho(q, s - q - l, \{c_k\}_{k=0}^{+\infty}) \\
& \rho(n - 1 - q, m + 1 - n + q - r, \{c_k\}_{k=0}^{+\infty}),
\end{aligned}$$

where $c_k = -\frac{1}{1+k}$. Then we have $a(x, y) = \sum_{s,m \geq 0}^{+\infty} a_{s,m} x^s y^m = \frac{\log((1-x)(1-y))}{xy - x - y}$.

Proof. We begin with

$$\begin{aligned}
a(x, y) &= \sum_{s,m \geq 0}^{+\infty} a_{s,m} x^s y^m \\
&= 1 - \sum_{s,m \geq 1}^{+\infty} x^s y^m \sum_{n=2}^{s+m+1} \frac{1}{n!} \sum_{l=0}^s \sum_{r=0}^m a_{l,r} \sum_{q=0}^{n-1} \binom{n-1}{q} \rho(q, s - q - l, \{c_k\}_{k=0}^{+\infty}) \\
&\quad \cdot \rho(n - 1 - q, m + 1 - n + q - r, \{c_k\}_{k=0}^{+\infty}) \\
&= 1 - \sum_{n=2}^{+\infty} \frac{1}{n!} \sum_{s+m \geq n-1}^{+\infty} x^s y^m \sum_{l=0}^s \sum_{r=0}^m a_{l,r} \sum_{q=0}^{n-1} \binom{n-1}{q} \rho(q, s - q - l, \{c_k\}_{k=0}^{+\infty}) \\
&\quad \cdot \rho(n - 1 - q, m + 1 - n + q - r, \{c_k\}_{k=0}^{+\infty})
\end{aligned}$$

Similar to the proof technique used in Lemma 10, we note that

$$\sum_{s+m \geq n-1}^{+\infty} x^s y^m \sum_{l=0}^s \sum_{r=0}^m a_{l,r} \sum_{q=0}^{n-1} \binom{n-1}{q} \rho(q, s - q - l, \{c_k\}_{k=0}^{+\infty}) \rho(n - 1 - q, m + 1 - n + q - r, \{c_k\}_{k=0}^{+\infty})$$

is equivalent to $a(x, y) (xc(x) + yc(y))^{n-1}$, where $c(x) = \sum_{k=0}^{+\infty} c_k x^k = \frac{\log(1-x)}{x}$. To constitute $x^s y^m$, we first select $a_{l,r} x^l y^r$ from $a(x, y)$, and then select q times $xc(x)$ from $(xc(x) + yc(y))^{n-1}$.

Then we have

$$\begin{aligned}
a(x, y) &= 1 - \sum_{n=2}^{+\infty} \frac{1}{n!} a(x, y) (xc(x) + yc(y))^{n-1} \\
&= 1 - \frac{a(x, y)}{xc(x) + yc(y)} \sum_{n=2}^{+\infty} \frac{1}{n!} (xc(x) + yc(y))^n \\
&= 1 - \frac{a(x, y)}{xc(x) + yc(y)} \left(e^{xc(x) + yc(y)} - 1 - (xc(x) + yc(y)) \right).
\end{aligned}$$

Plugging in the definition of $c(x)$, we obtain

$$a(x, y) = 1 - \frac{a(x, y)}{\log((1-x)(1-y))} ((1-x)(1-y) - 1 - \log((1-x)(1-y)))$$

$$= 1 - \frac{a(x, y)}{\log((1-x)(1-y))} (xy - x - y - \log((1-x)(1-y))).$$

Solving this equation for $a(x, y)$ gives us the desired result. \square

A.3 Proof of Theorem 1

Next, we need to show that $b(x)$ and $\mathcal{D}(x)$ is convergent. Solving for $b(x)$ is similar to the proof of Rosca et al. [2022, Theorem A.2]. Here, we present the derivation of the diffusion term. We have

$$\mathcal{D}(x) = \sum_{p=0}^{+\infty} \eta^p h_p(x) = \sum_{p=0}^{+\infty} \eta^p \sum_{k=0}^{p-1} a_{k,p-1-k} \cdot (\nabla^2 f(x))^k \Sigma(x) (\nabla^2 f(x))^{p-1-k},$$

where $a_{k,p-1-k}$ is determined in Lemma 2. The above equation implies

$$\begin{aligned} U^\top \mathcal{D}U &= U^\top \left(\sum_{p=0}^{+\infty} \eta^p \sum_{k=0}^{p-1} a_{k,p-1-k} \cdot (\nabla^2 f(x))^k \Sigma(x) (\nabla^2 f(x))^{p-1-k} \right) U \\ &= \sum_{p=0}^{+\infty} \eta^p \sum_{k=0}^{p-1} a_{k,p-1-k} \cdot \Lambda^k U^\top \Sigma(x) U \Lambda^{p-1-k}. \end{aligned}$$

Since Λ is a diagonal matrix, we have

$$\begin{aligned} [U^\top \mathcal{D}U]_{i,j} &= \sum_{p=0}^{+\infty} \eta^p \sum_{k=0}^{p-1} a_{k,p-1-k} \cdot \lambda_i^k [U^\top \Sigma(x) U]_{i,j} \lambda_j^{p-1-k} \\ &= \eta \sum_{p=0}^{+\infty} \sum_{k=0}^{p-1} a_{k,p-1-k} \cdot (\eta \lambda_i)^k [U^\top \Sigma(x) U]_{i,j} (\eta \lambda_j)^{p-1-k} \\ &= \eta \sum_{k=0}^{+\infty} \sum_{p=k+1}^{+\infty} a_{k,p-1-k} \cdot (\eta \lambda_i)^k [U^\top \Sigma(x) U]_{i,j} (\eta \lambda_j)^{p-1-k} \\ &= \eta [U^\top \Sigma(x) U]_{i,j} \sum_{k=0}^{+\infty} \sum_{q=0}^{+\infty} a_{k,q} \cdot (\eta \lambda_i)^k (\eta \lambda_j)^q, \end{aligned}$$

where in the last equality we let $q = p - 1 - k$. Then according to Lemma 2, we have

$$[U^\top \mathcal{D}U]_{i,j} = \eta [U^\top \Sigma(x) U]_{i,j} a(\eta \lambda_i, \eta \lambda_j),$$

where $a(x, y) = \frac{\log(1-x)(1-y)}{xy - (x+y)}$.

A.4 Proof of Lemma 3

In the first condition, the matrix $U^\top \Sigma U$ becomes diagonal. We can check that the diagonal elements are always positive definite, and by taking square root of the eigenvalues, we obtain

$$D = U \sqrt{\tilde{\Lambda} \eta \frac{\log(1-\eta\Lambda)^2}{(1-\eta\Lambda)^2 - 1}} U^\top, \quad (44)$$

where $\Sigma = U \tilde{\Lambda} U^\top$ and $\nabla^2 f(x) = U \Lambda U^\top$.

For the second condition, we consider small stepsize regime. We will proceed to show that the RHS matrix of Equation (23), denoted as M is positive semi-definite, so that such a square root always exists. Consider matrix K , whose (i, j) -th element is defined as

$$K_{i,j} = \frac{\log(1 - \eta\lambda_i) + \log(1 - \eta\lambda_j)}{(1 - \eta\lambda_i)(1 - \eta\lambda_j) - 1}.$$

We consider small η , i.e., $\eta < \frac{1 - \sqrt{2}}{\|\nabla^2 f(x)\|}$, therefore, K is real. The matrix M can then be written as

$$M = \eta U^\top \Sigma U \odot K = \eta U^\top \Sigma U \odot (\mathbf{1} + K - \mathbf{1}) = \eta (U^\top \Sigma U + U^\top \Sigma U \odot (K - \mathbf{1})),$$

where $\mathbf{1}$ is a all-one matrix. Now since $\eta > 0$, to determine the positive semi-definiteness of M , it is sufficient to determine positive semi-definiteness of $U^\top \Sigma U + U^\top \Sigma U \odot (K - \mathbf{1})$.

Note that for matrix $U^\top \Sigma U$, since U is orthogonal, it only changes the eigenspace of Σ , but does not change the eigenvalues. To see why this is the case, assume λ is a eigenvalue of Σ with v being the corresponding eigenvector. Then we have $\Sigma v = \lambda v$. Then $U^{-1}v$ is a eigenvector for $U^\top \Sigma U$ with eigenvalue λ , since

$$U^\top \Sigma U U^{-1}v = U^\top \Sigma v = U^\top \lambda v = \lambda U^{-1}v.$$

Going back to our problem, since $U^\top \Sigma U$ is positive definite, a sufficient condition for matrix $U^\top \Sigma U + U^\top \Sigma U \odot (K - \mathbf{1})$ to be PSD is that

$$\lambda_{\min}(U^\top \Sigma U) = \lambda_{\min}(\Sigma) \geq \|U^\top \Sigma U \odot (K - \mathbf{1})\|. \quad (45)$$

Let us look at $\|U^\top \Sigma U \odot (K - \mathbf{1})\|$, we know that

$$\begin{aligned} \|U^\top \Sigma U \odot (K - \mathbf{1})\| &\leq \sqrt{d} \|U^\top \Sigma U\| \sup_{i,j} |[K - \mathbf{1}]_{i,j}| \\ &= \sqrt{d} \|U^\top \Sigma U\| \sup_{i,j} \left| \frac{\log((1 - \eta\lambda_i)(1 - \eta\lambda_j))}{(1 - \eta\lambda_i)(1 - \eta\lambda_j) - 1} - 1 \right| \\ &= \sqrt{d} \lambda_{\max}(\Sigma) \sup_{i,j} \left| \frac{\log((1 - \eta\lambda_i)(1 - \eta\lambda_j))}{(1 - \eta\lambda_i)(1 - \eta\lambda_j) - 1} - 1 \right|, \end{aligned}$$

where we used Lemma 14 for the inequality.

According to Lemma 12,

$$\sup_{i,j} \left| \frac{\log((1 - \eta\lambda_i)(1 - \eta\lambda_j))}{(1 - \eta\lambda_i)(1 - \eta\lambda_j) - 1} - 1 \right| \leq \sup_{i,j} 1 - (1 - \max\{|\eta\lambda_i|, |\eta\lambda_j|\})^2 \leq 1 - (1 - \eta \|\nabla^2 f(x)\|)^2$$

Plugging in back to Equation (45), a sufficient condition for M to be PSD is

$$\lambda_{\min}(\Sigma) \geq \sqrt{d} \lambda_{\max}(\Sigma) \left(1 - (1 - \eta \|\nabla^2 f(x)\|)^2 \right).$$

Rearranging the terms gives us the condition in the theorem.

A.5 Proof of Theorem 2

To show the result, it is sufficient to show that the eigenvalues of D are lower bounded away from 0. For the first condition, we have an explicit form of D in Equation (44). Note that when the abstract value of all entries of $\eta\Lambda$ are smaller than 1, entries of $\log(1 - \eta\Lambda)^2 / ((1 - \eta\Lambda)^2 - 1)$ are lower bounded away from 0. Therefore, as long as eigenvalues of Σ are lower bounded, i.e., Σ is positive definite, the eigenvalues of D are lower bounded from 0. For the second condition, Similar to the proof for Lemma 3, we know that as long as the stepsize satisfies the condition, the eigenvalues of the diffusion coefficient are positive and lower bounded.

Now, we show that why lower boundedness of eigenvalues of D is sufficient to prove the result. We need to show that the drift term b and diffusion term D are Lipschitz. According to Lemma 15, the drift term is Lipschitz, and according to Lemma 16, we know that DD^\top is Lipschitz. Therefore, $\partial[DD^\top]_{i,j}/\partial x_k$ is upper bounded. Then according to Lin and Maji [2017, Equation (7)], we have

$$\text{vec} \left(\frac{\partial D_{i,j}}{\partial DD^\top} \right) = (D \otimes I + I \otimes D)^{-1} \text{vec} (\tilde{\mathbf{1}}_{i,j}),$$

where vec is the vectorization of matrices and \otimes denotes the Kronecker product. $\tilde{\mathbf{1}}_{i,j}$ is a matrix whose (i,j) -th element is 1 and all other elements are 0. Next, we get

$$\begin{aligned} \frac{\partial D_{i,j}}{\partial x_k} &= \sum_{p,q} \frac{\partial D_{i,j}}{\partial [DD^\top]_{p,q}} \frac{\partial [DD^\top]_{p,q}}{\partial x_k} \\ &= \sum_{p,q} [(D \otimes I + I \otimes D)^{-1} \text{vec} (\tilde{\mathbf{1}}_{i,j})]_{qd+p} \frac{\partial [DD^\top]_{p,q}}{\partial x_k} \\ &\leq \sum_{p,q} \left\| (D \otimes I + I \otimes D)^{-1} \text{vec} (\tilde{\mathbf{1}}_{i,j}) \right\| \left| \frac{\partial [DD^\top]_{p,q}}{\partial x_k} \right| \\ &\leq \sum_{p,q} \left\| (D \otimes I + I \otimes D)^{-1} \right\| \left| \frac{\partial [DD^\top]_{p,q}}{\partial x_k} \right|. \end{aligned}$$

It remains to show that the eigenvalues of $(D \otimes I + I \otimes D)^{-1}$ is bounded. According to Steeb and Hardy [2011, Theorem 2.15], the eigenvalues of $D \otimes I + I \otimes D$ are $\{a + b \mid a, b \in \{\lambda_i\}_{i=1}^d\}$, where λ_i are the eigenvalues of D . Therefore, the eigenvalues of $D \otimes I + I \otimes D$ are lower bounded since we have the eigenvalues of D being lower bounded by a positive constant. This implies that eigenvalues of $(D \otimes I + I \otimes D)^{-1}$ are upper bounded, which concludes the proof.

A.6 Helper Lemmas

Lemma 12. For any $x, y \in \mathbb{R}$ and $\frac{\sqrt{2}}{2} - 1 \leq x, y \leq 1 - \frac{\sqrt{2}}{2}$, it holds that

$$\left| \frac{\log((1-x)(1-y))}{(1-x)(1-y)-1} - 1 \right| \leq 1 - (1 - \max\{|x|, |y|\})^2.$$

Proof. Let $z = (1-x)(1-y)$, then the LHS becomes $\left| \frac{\log z}{z-1} - 1 \right|$. We first study the function

$$f(z) = \frac{\log z}{z-1} - 1,$$

whose gradient is given by

$$f'(z) = \frac{\frac{z-1}{z} - \log z}{(z-1)^2} = \frac{1 - \frac{1}{z} - \log z}{(z-1)^2} \leq 0,$$

where the last inequality comes from the fact $\log z \geq 1 - \frac{1}{z}$ for $z > 0$. Also note that $f(1) = 0$, therefore, we know that

$$|f(z)| = \begin{cases} \frac{\log z}{z-1} - 1, & z \leq 1 \\ 1 - \frac{\log z}{z-1}, & z > 1. \end{cases}$$

According to previous analysis, the maximum of $\left| \frac{\log z}{z-1} - 1 \right|$ would be at the minimum or maximum possible value of z . Denoting $m := \max\{|x|, |y|\}$ with $0 \leq m \leq 1 - \frac{\sqrt{2}}{2}$, then we know that

$$\left| \frac{\log((1-x)(1-y))}{(1-x)(1-y)-1} - 1 \right| \leq \max \left\{ \frac{\log(1-m)^2}{(1-m)^2-1} - 1, 1 - \frac{\log(1+m)^2}{(1+m)^2-1} \right\}$$

Next, we will show that for $0 \leq m \leq 1$,

$$\frac{\log(1-m)^2}{(1-m)^2-1} - 1 \geq 1 - \frac{\log(1+m)^2}{(1+m)^2-1}.$$

We start with

$$\begin{aligned} & \frac{\log(1-m)^2}{(1-m)^2-1} - 1 - \left(1 - \frac{\log(1+m)^2}{(1+m)^2-1} \right) \\ &= \frac{2(m+2)\log(1-m) + 2(m-2)\log(1+m) - 2m(m+2)(m-2)}{m(m+2)(m-2)}. \end{aligned}$$

Since $m(m+2)(m-2) < 0$, it suffice to show that the numerator is less or equal than 0. We let

$$g(m) = 2(m+2)\log(1-m) + 2(m-2)\log(1+m) - 2m(m+2)(m-2),$$

whose gradient is

$$\begin{aligned} g'(m) &= \frac{m+2}{m-1} + \log(1-m) + \frac{m-2}{1+m} + \log(1+m) - 3m^2 + 4 \\ &\leq \frac{m+2}{m-1} + \frac{m-2}{1+m} - 4m^2 + 4 = \frac{3m^2(m^2-3)}{(1-m)(m+1)} \leq 0, \end{aligned}$$

where the inequality holds because $\log z \leq z-1$ for $z > 0$. Therefore, for $0 \leq m \leq 1$, we have $g(m) \leq g(0) = 0$. So far, we have proved that

$$\left| \frac{\log((1-x)(1-y))}{(1-x)(1-y)-1} - 1 \right| \leq \frac{\log(1-m)^2}{(1-m)^2-1} - 1.$$

Next, we will prove that an upper bound is as follows

$$\frac{\log(1-m)^2}{(1-m)^2-1} - 1 \leq 1 - (1-m)^2,$$

for $0 \leq m \leq 1 - \frac{\sqrt{2}}{2}$. With a change of variable for $z = (1-m)^2$, to prove the above inequality is the same as showing the following for $\frac{1}{2} \leq z \leq 1$,

$$\frac{\log z}{z-1} - 1 - (1-z) = \frac{\log z}{z-1} + z - 2 = \frac{\log z + z^2 - 3z + 2}{z-1} \leq 0.$$

Then it is sufficient to show

$$h(z) := \log z + z^2 - 3z + 2 \geq 0.$$

We have

$$h'(z) = \frac{1}{z} + 2z - 3 = \frac{(z-1)(2z-1)}{z} \leq 0.$$

Therefore $h(z) \geq h(1) = 0$ for $\frac{1}{2} \leq z \leq 1$. The whole proof is finished. \square

Lemma 13. Let $u : \mathbb{R}^d \rightarrow \mathbb{R}$ and $\{v_i(x)\}_{i=1}^n$ be vector fields, i.e., $v_i : \mathbb{R}^d \rightarrow \mathbb{R}^d$. The terms in the result of

$$\nabla^2 (v_1 \cdot \nabla (v_2 \cdot \nabla (v_3 \cdot \nabla (\cdots v_n \cdot \nabla u)))) ,$$

that contain only $\nabla^2 u$ and ∇v_i for $i \in [1, n]$ are

$$\sum_{S \subseteq [1, n]} \left(\prod_{i \in \tilde{S}} \nabla v_i \right) \nabla^2 u \left(\prod_{i \in [1, n] \setminus S} \nabla v_i \right),$$

where \cdot is the inner product between vectors, \tilde{S} is the ascending ordered set containing all elements from S , \hat{S} is the corresponding descending ordered set, and \setminus is the set difference operator.

Proof. We will prove this by induction. First, let us consider the case of $n = 1$, then clearly, we have

$$\nabla^2 (v_1 \cdot \nabla u) = \nabla v_1 \nabla^2 u + \nabla^2 u \nabla v_1 + \mathcal{C},$$

where \mathcal{C} contains irrelevant terms, i.e., terms with higher order gradients of v_i and u . Now assume the conclusion holds true for $n = 1, \dots, m-1$, then when $n = m$, we have

$$\begin{aligned} & \nabla^2 (v_1 \cdot \nabla (v_2 \cdot \nabla (v_3 \cdot \nabla (\cdots v_m \cdot \nabla u)))) \\ &= \nabla v_1 \nabla^2 (v_2 \cdot \nabla (v_3 \cdot \nabla (\cdots v_m \cdot \nabla u))) + \nabla^2 (v_2 \cdot \nabla (v_3 \cdot \nabla (\cdots v_m \cdot \nabla u))) \nabla v_1 + \mathcal{C} \\ &= \nabla v_1 \sum_{S \subseteq [2, m]} \left(\prod_{i \in \tilde{S}} \nabla v_i \right) \nabla^2 u \left(\prod_{i \in [2, m] \setminus S} \nabla v_i \right) + \sum_{S \subseteq [2, m]} \left(\prod_{i \in \tilde{S}} \nabla v_i \right) \nabla^2 u \left(\prod_{i \in [2, m] \setminus S} \nabla v_i \right) \nabla v_1 + \mathcal{C} \\ &= \sum_{S \subseteq [1, m]} \left(\prod_{i \in \tilde{S}} \nabla v_i \right) \nabla^2 u \left(\prod_{i \in [1, m] \setminus S} \nabla v_i \right) + \mathcal{C}, \end{aligned}$$

which concludes the proof. \square

Lemma 14. We have for any $A, B \in \mathbb{R}^{d \times d}$,

$$\|A \odot B\| \leq \sqrt{d} \sup_{i,j} A_{i,j} \|B\|.$$

Proof. Let e_1, e_2, \dots, e_d be the standard basis of \mathbb{R}^d . Then we have for any $1 \leq k \leq d$,

$$\|(A \odot B)e_k\| \leq \sup_{i,j} A_{i,j} \|Be_k\| \leq \sup_{i,j} A_{i,j} \|B\|.$$

Then for any vector $v \in \mathbb{R}^d$, which can be written as $v = v_1 e_1 + v_2 e_2 + \cdots$, we have

$$\|(A \odot B)v\| \leq \sum_{k=1}^d |v_k| \|(A \odot B)e_k\| \leq \sup_{i,j} A_{i,j} \|B\| \sum_{k=1}^d |v_k| \leq \sup_{i,j} A_{i,j} \|B\| \sqrt{d} \|v\|,$$

where the last inequality we used Cauchy-Schwartz inequality. \square

B Approximation Error Analysis

B.1 Proofs for Section 5

Proof for Theorem 3. The proof follows the idea of Theorem 2.2 of Feng et al. [2017], however our proof is more difficult since we need to deal with more complicated HA-SME. The assumption of $\|F(x; \xi)\|_{c^7} < \infty$

implies $\|f(x)\|_{C^7} < \infty$ and $\|\Sigma(x)\|_{C^6} < \infty$. According to Lemma 15, we have boundedness of $\|b(x)\|_{C^5}$, where $b(x)$ is the drift term of HA-SME. According to Lemma 15, we have boundedness of the diffusion term of HA-SME, i.e., $\frac{\|U(x)L(x)U(x)^\top\|_{C^5}}{\eta}$ is upper bounded. Let $u^n(x)$ defined the same as in Feng et al. [2017], i.e., $u^n(x_0) = \mathbb{E}[u(x_n)]$. According to Theorem 2.1 of Feng et al. [2017], for small enough η , we have boundedness of $\|u^n\|_{C^6}$.

Starting both from $u^n(x)$, we first measure the error between the discrete-time SGD and continuous-time iterates after one-step. For the discrete-time SGD, by Taylor expansion, and boundedness of $\nabla f(x; \xi)$ and $\|u^n(x)\|_{C^6}$, we have

$$\begin{aligned} & \left| u^{n+1}(x) - u^n(x) + \eta \langle \nabla f(x), \nabla u^n(x) \rangle - \frac{1}{2} \eta^2 \mathbb{E} [\nabla f(x; \xi) \nabla f(x; \xi)^\top] : \nabla^2 u^n(x) \right| \\ &= \left| u^{n+1}(x) - u^n(x) + \eta \langle \nabla f(x), \nabla u^n(x) \rangle - \frac{1}{2} \eta^2 (\nabla f(x) \nabla f(x)^\top + \Sigma(x)) : \nabla^2 u^n(x) \right| \\ &\leq \mathcal{O}(\eta^3). \end{aligned} \quad (46)$$

In continuous time, after time η , according to Lemma 17, we have

$$\left| e^{\eta \mathcal{L}} u^n(x) - u^n(x) - \eta \mathcal{L} u^n(x) - \frac{\eta^2}{2} \mathcal{L}^2 u^n(x) \right| \leq \mathcal{O}(\eta^3). \quad (47)$$

Note that different from previous SDEs (Equations (3) and (6)), now $\eta \mathcal{L} u^n(x)$ and $\frac{\eta^2}{2} \mathcal{L}^2 u^n(x)$ contains infinite many terms and we need to consider their errors. We know that

$$\eta \mathcal{L} u^n(x) = \eta b(x) \cdot \nabla u^n(x) + \frac{\eta}{2} D(x) D(x)^\top : \nabla^2 u^n(x),$$

where $b(x)$ is the drift term of HA-SME. By Taylor expansion of $\mathcal{L} u^n$ w.r.t. η and Lemma 18, we have

$$\begin{aligned} & \left| \eta b(x) \cdot \nabla u^n(x) + \eta \nabla f(x) \cdot \nabla u^n(x) + \frac{\eta^2}{2} \nabla^2 f(x) \nabla f(x) \cdot \nabla u^n(x) \right. \\ & \quad \left. + \frac{\eta}{2} U(x) L(x) U(x)^\top : \nabla^2 u^n(x) - \frac{1}{2} \eta^2 \Sigma(x) : \nabla^2 u^n(x) \right| \leq \mathcal{O}(\eta^3). \end{aligned}$$

Then we have

$$\left| \eta \mathcal{L} u^n(x) + \eta \nabla f(x) \cdot \nabla u^n(x) + \frac{\eta^2}{2} \nabla^2 f(x) \nabla f(x) \cdot \nabla u^n(x) - \frac{1}{2} \eta^2 \Sigma(x) : \nabla^2 u^n(x) \right| \leq \mathcal{O}(\eta^3). \quad (48)$$

Next, we look at the errors in $\frac{\eta^2}{2} \mathcal{L}^2 u^n(x)$. By Taylor expansion of $\mathcal{L}^2 u^n$ w.r.t. η and Lemma 18, we have

$$\left| \frac{\eta^2}{2} \mathcal{L}^2 u^n(x) - \frac{\eta^2}{2} \nabla^2 f(x) \nabla f(x) \cdot \nabla u^n(x) - \frac{\eta^2}{2} \nabla f(x) \nabla f(x)^\top : \nabla^2 u^n(x) \right| \leq \mathcal{O}(\eta^3). \quad (49)$$

Combining Equations (47) to (49), we get

$$\left| e^{\eta \mathcal{L}} u^n(x) - u^n(x) + \eta \nabla f(x) \cdot \nabla u^n(x) - \frac{\eta^2}{2} \Sigma(x) : \nabla^2 u^n(x) - \frac{\eta^2}{2} \nabla f(x) \nabla f(x)^\top : \nabla^2 u^n(x) \right| \leq \mathcal{O}(\eta^3).$$

Combining the above equation and Equation (46), we have

$$|e^{\eta \mathcal{L}} u^n(x) - u^{n+1}(x)| \leq \mathcal{O}(\eta^3).$$

Denote

$$E^n = \|u^n(x) - u(x, n\eta)\|_{L^\infty}.$$

We obtain

$$\begin{aligned}
E^{n+1} &= \|u^{n+1}(x) - u(x, (n+1)\eta) + e^{\eta\mathcal{L}}u^n(x) - e^{\eta\mathcal{L}}u^n(x)\|_{L^\infty} \\
&\leq \|e^{\eta\mathcal{L}}(u^n(x) - u(x, n\eta))\|_{L^\infty} + \|u^{n+1}(x) - e^{\eta\mathcal{L}}u^n(x)\|_{L^\infty} \\
&= \|e^{\eta\mathcal{L}}(u^n(x) - u(x, n\eta))\|_{L^\infty} + \mathcal{O}(\eta^3) \\
&\leq \|u^n(x) - u(x, n\eta)\|_{L^\infty} + \mathcal{O}(\eta^3) = E^n + \mathcal{O}(\eta^3),
\end{aligned}$$

where the last inequality comes from the L^∞ contraction of $e^{t\mathcal{L}}$ (see Lemma 2.1 of [Feng et al. \[2017\]](#)). Then we know that

$$E^n \leq n\mathcal{O}(\eta^3) = \frac{T}{\eta}\mathcal{O}(\eta^3) \leq \mathcal{O}(\eta^2).$$

□

Proof of Lemma 4. The lemma follows by Lemmas 15 and 16

□

Proof for Theorem 4. The assumption of $\|F(x; \xi)\|_{c^8} < \infty$ implies $\|f(x)\|_{c^8} < \infty$. According to Lemma 15, we have boundedness of $\|b(x)\|_{C^6}$, where $b(x)$ is the drift term of HA-SME. According to Lemma 15, we have boundedness of the diffusion term of HA-SME, i.e., $\frac{\|U(x)L(x)U(x)^\top\|_{C^6}}{\eta}$ is upper bounded. Denote $M_p^n := \sum_{1 \leq |J| \leq p} |D^J u^n(x)|$.

Similar to the proof for Theorem 3, we first have

$$\left\| u^{n+1} - u^n + \eta \nabla f \cdot \nabla u - \frac{1}{2} \eta^2 \Sigma : \nabla^2 u^n \right\|_{L^\infty} \leq \mathcal{O}(\eta^3 s^3 M_3^n).$$

First, we expand $e^{\eta\mathcal{L}}u^n$ using Taylor's expansion and Lemma 17,

$$\left\| e^{\eta\mathcal{L}}u^n - u^n - \eta \mathcal{L}u^n - \frac{1}{2} \eta^2 \mathcal{L}^2 u^n - \frac{1}{3!} \eta^3 \mathcal{L}^3 u^n \right\|_{L^\infty} \leq \mathcal{O}(\eta^4 \lambda^3 s^4 M_8^n).$$

Then using Lemma 18, we find the expansion of $\mathcal{L}u^n$, $\mathcal{L}^2 u^n$ and $\mathcal{L}^3 u^n$, respectively.

$$\begin{aligned}
\mathcal{L}u^n &= -\nabla f \cdot \nabla u^n + \eta \left(-\frac{1}{2} \nabla^2 f \nabla f \cdot \nabla u^n + \frac{1}{2} \Sigma : \nabla^2 u^n \right) \\
&\quad + \frac{\eta^2}{2} \left(-\frac{2}{3} (\nabla^2 f)^2 \nabla f \cdot \nabla u^n + \frac{1}{2} (\Sigma \nabla^2 f + \nabla^2 f \Sigma) : \nabla^2 u^n \right) + \mathcal{O}(\eta^3 \lambda^3 s M_2^n). \tag{50}
\end{aligned}$$

For $\mathcal{L}^2 u^n$, we have

$$\begin{aligned}
\mathcal{L}^2 u^n &= \nabla f(x)^\top \nabla^2 f \nabla u^n + \nabla f^\top \nabla^2 u^n \nabla f \\
&\quad + \eta \left(\nabla f^\top (\nabla^2 f)^2 \nabla u^n + \nabla f^\top \nabla^2 f \nabla^2 u^n \nabla f - \frac{1}{2} \Sigma : (\nabla^2 u^n \nabla^2 f + \nabla^2 f \nabla^2 u^n) + \mathcal{O}(M_3^n) \right) \\
&\quad + \mathcal{O}(\eta^2 \lambda^3 s^2 M_4^n).
\end{aligned}$$

For $\mathcal{L}^3 u^n$, we have

$$\mathcal{L}^3 u^n = -\nabla f^\top (\nabla^2 f)^2 \nabla u^n - 3 \nabla f^\top \nabla^2 f (\nabla u^n)^2 + \mathcal{O}(M_3^n) + \mathcal{O}(\eta \lambda^3 s^3 M_6^n).$$

Summarizing the above, we obtain

$$\|e^{\eta\mathcal{L}}u^n - u^{n+1}\|_{L^\infty} \leq \mathcal{O}(\eta^3 s^3 M_3^n + \eta^4 \lambda^3 s^4 M_8^n).$$

Following the last few steps in the proof of Theorem 3, we obtain

$$E^n \leq \sum_{k=0}^{n-1} \mathcal{O}(\eta^3 s^3 M_3^k + \eta^4 \lambda^3 s^4 M_8^k)$$

finish the proof. \square

Proof for Theorem 5. The proof follows similarly to the proof of Theorem 4. For SME-2, in the expansion of $\mathcal{L}u^n$, i.e., Equation (50), the term

$$\frac{\eta^2}{2} \left(-\frac{2}{3} (\nabla^2 f)^2 \nabla f \cdot \nabla u^n + \frac{1}{2} (\Sigma \nabla^2 f + \nabla^2 f \Sigma) : \nabla^2 u^n \right)$$

is missing. Therefore, after cancellation of terms, there will be error terms of $\lambda^2 s \|\nabla u^n\|$ and $\lambda \|\nabla^2 u^n\|$. For SPF, in Equation (50), the term

$$\frac{\eta^2}{2} \left(\frac{1}{2} (\Sigma \nabla^2 f + \nabla^2 f \Sigma) : \nabla^2 u^n \right)$$

is missing. Therefore, it results in additional error of $\lambda \|\nabla^2 u^n\|$. \square

Proof of Lemma 5. We will show the results for both the convex and strongly-convex (corresponding to our Remark 10) settings. According to Feng et al. [2017], for any $n \geq 0$, $u^{n+1}(x)$ can be written as

$$u^{n+1}(x) = \mathbb{E} [u^n(x - \eta \nabla F(x; \xi))].$$

Let us check the first-order derivatives of u^{n+1} . Denoting $y = x - \eta \nabla F(x; \xi)$, we obtain

$$\nabla u^{n+1}(x) = \mathbb{E} [(I - \eta \nabla^2 F(x; \xi)) \nabla u^n(y)].$$

1. If $f(\cdot)$ is strongly-convex, we obtain

$$\sup_x \|\nabla u^{n+1}(x)\| \leq (1 - \eta \mu) \sup_x \|\nabla u^n(x)\|.$$

With small η , we have $\eta \sup_{x, \xi} \|\nabla^2 F(x; \xi)\| < 1$, and the recursion form is a contraction:

$$\sup_x \|\nabla u^n(x)\| \leq (1 - \mu \eta)^n \sup_x \|\nabla u(x)\| \leq e^{-\mu \eta n} \sup_x \|\nabla u(x)\| \leq \mathcal{O}(e^{-\mu \eta n} \|u\|_{C^1}).$$

2. If $f(\cdot)$ is convex, we have

$$\sup_x \|\nabla u^{n+1}(x)\| \leq \sup_x \|\nabla u^n(x)\| \leq \mathcal{O}(\|u\|_{C^1}).$$

The notation $\mathcal{O}(\cdot)$ does not depend on n , η or upper bounds for derivatives of F in $\mathcal{O}(\cdot)$ with orders higher than the second order.

Next, we consider the second-order gradients:

$$\nabla^2 u^{n+1}(x) = \mathbb{E} [(I - \eta \nabla^2 F(x; \xi)) \nabla^2 u^n(y) (I - \eta \nabla^2 F(x; \xi)) - \eta \nabla u^n(y)^\top \nabla^3 f(x)].$$

Then we also obtain a recursion for the 2-norm of its vector form:

$$\underbrace{\sup_x \|\text{vec}(\nabla^2 u^{n+1}(x))\|_2}_{a_{n+1}} \tag{51}$$

$$\begin{aligned}
&= \sup_x \|\nabla^2 u^{n+1}(x)\|_F \\
&\leq \sup_x \|(I - \eta \nabla^2 F(x; \xi)) \nabla^2 u^n(y) (I - \eta \nabla^2 F(x; \xi))\|_F + \eta \sup_x \|\nabla u^n(y)^\top \nabla^3 f(x)\|_F \\
&= \sup_x \|\text{vec}((I - \eta \nabla^2 F(x; \xi)) \nabla^2 u^n(y) (I - \eta \nabla^2 F(x; \xi)))\|_2 + \eta \sup_x \|\nabla u^n(y)^\top \nabla^3 f(x)\|_F \\
&= \sup_x \|(I - \eta \nabla^2 F(x; \xi))^{\otimes 2} \text{vec}(\nabla^2 u^n(y))\|_2 + \eta \sup_x \|\nabla u^n(y)^\top \nabla^3 f(x)\|_F \\
&\leq \sup_x \|(I - \eta \nabla^2 F(x; \xi))^{\otimes 2}\|_2 \|\text{vec}(\nabla^2 u^n(y))\|_2 + \eta \sup_x \|\nabla u^n(y)^\top \nabla^3 f(x)\|_F \\
&\leq \sup_x \|I - \eta \nabla^2 F(x; \xi)\|_2^2 \|\text{vec}(\nabla^2 u^n(y))\|_2 + \eta \sup_x \|\nabla u^n(y)^\top \nabla^3 f(x)\|_F,
\end{aligned} \tag{52}$$

where \otimes is the Kronecker product, and we used that $\|A \otimes B\|_2 \leq \|A\|_2 \|B\|_2$ for matrices A and B .

1. If $f(\cdot)$ is strongly-convex, the recursion becomes

$$\underbrace{\sup_x \|\text{vec}(\nabla^2 u^{n+1}(x))\|_2}_{a_{n+1}} \leq \underbrace{(1 - \eta\mu)^2}_{c} \underbrace{\sup_x \|\text{vec}(\nabla^2 u^n(x))\|_2}_{a_n} + \underbrace{\eta \sup_x \|\nabla u^n(y)^\top \nabla^3 f(x)\|_F}_{b_n}. \tag{53}$$

According to our assumption and previous results, $b_n \leq \mathcal{O}(\eta e^{-\mu\eta n} \|u\|_{C^1})$. Also we choose small η such that $1 - \eta\mu > 0$. It holds for the recursion that

$$a_{n+1} \leq c^{n+1} a_0 + \sum_{s=0}^n c^{n-s} b_s.$$

In our case, it becomes

$$\begin{aligned}
\sup_x \|\text{vec}(\nabla^2 u^n(x))\|_2 &\leq (1 - \eta\mu)^{2n} \sup_x \|\text{vec}(\nabla^2 u(x))\|_2 + \sum_{s=0}^n (1 - \eta\mu)^{2(n-s)} \mathcal{O}(\eta e^{-\mu\eta s} \|u\|_{C^1}) \\
&\leq (1 - \eta\mu)^n \sup_x \|\text{vec}(\nabla^2 u(x))\|_2 + \sum_{s=0}^n e^{-\mu\eta 2(n-s)} \mathcal{O}(\eta e^{-\mu\eta s} \|u\|_{C^1}) \\
&\leq e^{-\mu\eta n} \sup_x \|\text{vec}(\nabla^2 u(x))\|_2 + \sum_{s=0}^n e^{\mu\eta s} \mathcal{O}(\eta e^{-2\mu\eta n} \|u\|_{C^1}) \\
&= e^{-\mu\eta n} \sup_x \|\text{vec}(\nabla^2 u(x))\|_2 + \frac{e^{\eta\mu(n+1)} - 1}{e^{\eta\mu} - 1} \mathcal{O}(\eta e^{-2\mu\eta n} \|u\|_{C^1}) \\
&\leq e^{-\mu\eta n} \sup_x \|\text{vec}(\nabla^2 u(x))\|_2 + \frac{e^{\eta\mu(n+1)}}{e^{\eta\mu} - 1} \mathcal{O}(\eta e^{-2\mu\eta n} \|u\|_{C^1}) \\
&\leq e^{-\mu\eta n} \sup_x \|\text{vec}(\nabla^2 u(x))\|_2 + \frac{e^{\eta\mu n}}{e^{\eta\mu} - 1} \mathcal{O}(\eta e^{-2\mu\eta n} \|u\|_{C^1}) \\
&= e^{-\mu\eta n} \sup_x \|\text{vec}(\nabla^2 u(x))\|_2 + \frac{1}{e^{\eta\mu} - 1} \mathcal{O}(\eta e^{-\mu\eta n} \|u\|_{C^1}) \\
&\leq e^{-\mu\eta n} \sup_x \|\text{vec}(\nabla^2 u(x))\|_2 + \frac{1}{\eta\mu} \mathcal{O}(\eta e^{-\mu\eta n} \|u\|_{C^1}) \\
&= e^{-\mu\eta n} \sup_x \|\text{vec}(\nabla^2 u(x))\|_2 + \mathcal{O}(e^{-\mu\eta n} \|u\|_{C^1}) \\
&\leq \mathcal{O}(e^{-\mu\eta n} \|u\|_{C^2}),
\end{aligned} \tag{54}$$

where we used that $e^x \geq x + 1$.

2. If $f(\cdot)$ is convex, we have

$$\sup_x \|\text{vec}(\nabla^2 u^{n+1}(x))\|_2 \leq \sup_x \|\text{vec}(\nabla^2 u^n(x))\|_2 + \mathcal{O}(\eta).$$

Therefore, we obtain

$$\sup_x \|\text{vec}(\nabla^2 u^n(x))\|_2 \leq \mathcal{O}(T\|u\|_{C^2}).$$

Next, we proceed with induction.

1. If $f(\cdot)$ is strongly-convex, assume it holds that for any $0 < s \leq p$, we have $\sup_x \|\text{vec}(\nabla^s u^n(x))\|_F \leq \mathcal{O}(e^{-\mu\eta n}\|u\|_{C^s})$. Then, we study the $p+1$ -th order gradient of u^{n+1} :

$$\|\text{vec}(\nabla^{p+1} u^{n+1}(x))\|_2 = \left\| (I - \eta \nabla^2 F(x; \xi))^{\otimes p+1} \text{vec}(\nabla^{p+1} u^n(y)) \right\|_2 + \eta \mathcal{O}(e^{-\mu\eta n}\|u\|_{C^p}).$$

The first term is the result by applying the ∇ operator $p+1$ times on u . For other terms, at least one ∇ is applied on $(I - \eta \nabla^2 F(x; \xi))$, which results in a η and gradients of F higher than the second-order (which is hidden in $\mathcal{O}(\cdot)$). Also, the gradients of u are at most the p -th order, which by induction are already upper bounded. Therefore, similarly to Equation (53), we obtain

$$\begin{aligned} & \sup_x \|\text{vec}(\nabla^{p+1} u^{n+1}(x))\|_2 \\ & \leq \sup_x \left\| (I - \eta \nabla^2 F(x; \xi))^{\otimes p+1} \text{vec}(\nabla^{p+1} u^n(y)) \right\|_2 + \eta \mathcal{O}(e^{-\mu\eta n}\|u\|_{C^p}) \\ & \leq \sup_x \left\| (I - \eta \nabla^2 F(x; \xi)) \right\|_2^{p+1} \sup_x \|\text{vec}(\nabla^{p+1} u^n(x))\|_2 + \eta \mathcal{O}(e^{-\mu\eta n}\|u\|_{C^p}) \\ & \leq (1 - \eta\mu)^{p+1} \sup_x \|\text{vec}(\nabla^{p+1} u^n(x))\|_2 + \eta \mathcal{O}(e^{-\mu\eta n}\|u\|_{C^p}), \end{aligned}$$

which can be then recursively bounded similarly to Equation (54), i.e.,

$$\begin{aligned} & \sup_x \|\text{vec}(\nabla^{p+1} u^n(x))\|_2 \\ & \leq e^{-\mu\eta n} \sup_x \|\text{vec}(\nabla^{p+1} u(x))\|_2 + \mathcal{O}(e^{-\mu\eta n}\|u\|_{C^p}) \\ & \leq \mathcal{O}(e^{-\mu\eta n}\|u\|_{C^{p+1}}). \end{aligned}$$

Now we know that

$$\sum_{1 \leq |J| \leq p} |D^J u^n(x)| \leq \mathcal{O}(e^{-\mu\eta n}\|u\|_{C^p}).$$

It follows

$$\begin{aligned} & \eta \sum_{k=0}^{\lfloor T/\eta \rfloor - 1} \sum_{1 \leq |J| \leq p} |D^J u^k(x)| \leq \eta \sum_{k=0}^{\lfloor T/\eta \rfloor - 1} \mathcal{O}(e^{-\mu\eta k}\|u\|_{C^p}) \\ & \leq \eta \frac{1 - e^{-\eta\mu \lfloor T/\eta \rfloor}}{1 - e^{-\mu\eta}} \mathcal{O}(\|u\|_{C^p}) \leq \frac{\eta}{1 - e^{-\mu\eta}} \mathcal{O}(\|u\|_{C^p}) \leq \mathcal{O}(\|u\|_{C^p}). \end{aligned}$$

2. If $f(\cdot)$ is convex, we assume for any $0 < s \leq p$, $\sup_x \|\text{vec}(\nabla^s u^n(x))\|_F \leq \mathcal{O}(T^{s-1}\|u\|_{C^s})$. Similarly to the strongly-convex case, we obtain

$$\|\text{vec}(\nabla^{p+1} u^{n+1}(x))\|_2 = \left\| (I - \eta \nabla^2 F(x; \xi))^{\otimes p+1} \text{vec}(\nabla^{p+1} u^n(y)) \right\|_2 + \eta \mathcal{O}(T^{p-1}\|u\|_{C^p}),$$

which implies

$$\sup_x \|\text{vec}(\nabla^{p+1} u^n(x))\|_2 \leq \mathcal{O}(T^p \|u\|_{C^{p+1}}).$$

Further it holds that

$$\eta \sum_{k=0}^{\lfloor T/\eta \rfloor - 1} \sum_{1 \leq |J| \leq p} |D^J u^k(x)| \leq \mathcal{O}(T^{p+1} \|u\|_{C^p}).$$

□

Proof for Theorem 6. The proof is simply to combine the results from Theorem 4 and Lemma 5. □

B.2 Helper Lemmas

Lemma 15. For $n \geq 0$, assume $f \in C_b^{n+2}(\mathbb{R}^d)$ and denote $\lambda := \sup_{x \in \mathbb{R}^d} \|\nabla^2 f(x)\|$ and $s := \sup_{x \in \mathbb{R}^d} \|\nabla f(x)\|$. There exist constants η_0 and $C > 0$, both independent of λ and s , such that for any η satisfying $\eta < \eta_0$ and $\eta\lambda < C$, the drift term of HA-SME, defined in in Equation (22), satisfies

$$\max_{0 \leq i \leq d} |[b(x)]_i| < \mathcal{O}(s) \text{ and } \max_{0 \leq i \leq d} \|[b(x)]_i\|_{C^n} < \mathcal{O}(s + \lambda),$$

where $[b(x)]_i$ is the i -th entry of $b(x)$, and $\mathcal{O}(\cdot)$ hides the dependence on the upper bounds for the derivatives of f higher than the second-order derivatives.

Proof. Recall the definition of the drifting term of HA-SME in Equation (22)

$$b(x) = U(x) \frac{\log(I - \eta \Lambda(x))}{\eta \Lambda(x)} U(x)^\top \nabla f(x).$$

We first note that $b(x)$ can be written as

$$b(x) = - \sum_{p=0}^{\infty} \frac{1}{p+1} \eta^p (\nabla^2 f(x))^p \nabla f(x).$$

The (i, j) -th element of A^p for matrix $A \in \mathbb{R}^{d \times d}$ can be represented as

$$[A^p]_{i,j} = \sum_{s_1=1}^d [A]_{i,s_1} \sum_{s_2=1}^d [A]_{s_1,s_2} \sum_{s_3=1}^d [A]_{s_2,s_3} \cdots \sum_{s_{p-1}=1}^d [A]_{s_{p-2},s_{p-1}} [A]_{s_{p-1},j}.$$

Therefore, for any i , the i -th element of $b(x)$ can be written as

$$\begin{aligned} [b(x)]_i &= - \sum_{p=0}^{\infty} \frac{1}{p+1} \eta^p \left[(\nabla^2 f(x))^p \nabla f(x) \right]_i \\ &= - \sum_{p=0}^{\infty} \frac{1}{p+1} \eta^p \sum_{s_1=1}^d [\nabla^2 f(x)]_{i,s_1} \sum_{s_2=1}^d [\nabla^2 f(x)]_{s_1,s_2} \cdots \sum_{s_p=1}^d [\nabla^2 f(x)]_{s_{p-1},s_p} [\nabla f(x)]_{s_p} \\ &= - \sum_{p=0}^{\infty} \frac{1}{p+1} \eta^p \underbrace{\sum_{s_1=1}^d \partial_i \partial_{s_1} f(x) \sum_{s_2=1}^d \partial_{s_1} \partial_{s_2} f(x) \cdots \sum_{s_p=1}^d \partial_{s_{p-1}} \partial_{s_p} f(x) \partial_{s_p} f(x)}_{(A)}. \end{aligned}$$

Notice that Term (A) can be expanded as a summation of d^p terms, each of which contains $p + 1$ factors. Note that the first-order and second-order partial derivatives are upper bounded by s and λ respectively, i.e., $|D^\alpha f| \leq s$ for $|a| = 1$ and $|D^\alpha f| \leq \lambda$ for $|a| = 2$, and we have

$$|[b(x)]_i| \leq \sum_{p=0}^{\infty} \frac{1}{p+1} \eta^p d^p \lambda^p s = s \sum_{p=0}^{\infty} \frac{1}{p+1} (\eta d \lambda)^p.$$

We get a power series in the above equation, and according to Cauchy–Hadamard theorem [Cauchy, 1821], the convergence radius for $g(x) = \sum_{p=0}^{\infty} \frac{1}{p+1} x^p$ is

$$\frac{1}{\limsup_{p \rightarrow \infty} \left| \frac{1}{p+1} \right|^{\frac{1}{p}}} = \frac{1}{1} = 1.$$

Then we know that $[b(x)]_i$ is upper bounded by $\mathcal{O}(s)$ as long as

$$\eta d \lambda < 1 \implies \eta \lambda < \frac{1}{d}.$$

Next, we consider the first-order derivative of $b(x)$. We denote the upper bound for higher order partial derivatives as B , i.e., $\max_{2 < |a| \leq n+2} |D^\alpha f| \leq B$. Recall that in $b(x)$, Term (A) contains d^p terms and each term has p factors of second-order derivatives of $f(x)$ and one factor of the first-order derivative of $f(x)$. If we take gradient of Term (A) w.r.t. x , each term, according to the product rule of gradients and by taking derivatives w.r.t. each factor, will result in: (1) p terms, each consisting of one factors of $\partial^3 f$, $p - 1$ factor of $\partial^2 f$, and one factor of ∂f ; (2) 1 term consisting of $p + 1$ factors of $\partial^2 f$. Therefore, we can bound

$$\begin{aligned} |\partial_j [b(x)]_i| &\leq \sum_{p=0}^{\infty} \frac{1}{p+1} \eta^p d^p (p B s \lambda^{p-1} + \lambda^{p+1}) \\ &= s \sum_{p=0}^{\infty} \frac{p}{p+1} d^p \eta B (\eta \lambda)^{p-1} + \lambda \sum_{p=0}^{\infty} \frac{1}{p+1} (d \eta \lambda)^p \end{aligned}$$

For the second summation, the convergence radius of the power series is the same as the upper bound for $[b(x)]_i$, and it is bounded by $\mathcal{O}(\lambda)$ for sufficiently small η and $\eta \lambda$. For the first summation, comparing to the upper bound of $[b(x)]_i$, the coefficients of the power series are multiplied by p . However, this will not change the convergence radius. It is known that for sequences a_p and b_p , if $\limsup_{p \rightarrow \infty} a_p = A$ and $\lim_{p \rightarrow \infty} b_p = B$, then $\limsup_{p \rightarrow \infty} (a_p b_p) = AB$. Note that

$$\lim_{p \rightarrow \infty} |p|^{\frac{1}{p}} = 1.$$

Therefore, by applying Cauchy–Hadamard theorem, multiplying the coefficients with p would not change the radius of convergence. Therefore, if we have $\eta \lambda$ and ηB smaller than the convergence radius of $\sum_p \frac{1}{1+p} x^p$, that is 1, the first summation in the upper bound of $|\partial_j [b(x)]_i|$ can be upper bounded by some constants. As a result, we can conclude that

$$|\partial_j [b(x)]_i| \leq \mathcal{O}(s + \lambda).$$

Following the same idea, we identify that after applying twice partial derivatives on $b(x)$, i.e., $\partial_j \partial_k [b(x)]_i$, each term in Term (A) becomes:

$$p \partial^4 f (\partial^2 f)^{p-1} \partial f + p(p-1) (\partial^3 f)^2 (\partial^2 f)^{p-2} \partial f + (2p+1) \partial^3 f (\partial^2 f)^p$$

Thus, we have

$$\begin{aligned} |\partial_j \partial_k [b(x)]_i| &\leq \sum_{p=0}^{\infty} \frac{1}{p+1} \eta^p d^p (p(p-1)B^2 s \lambda^{p-2} + pBs \lambda^{p-1} + (2p+1)B\lambda^p) \\ &= s \sum_{p=0}^{\infty} \frac{p(p-1)}{p+1} d^p (B\eta)^2 (\lambda\eta)^{p-2} + s \sum_{p=0}^{\infty} \frac{p}{p+1} d^p B\eta (\lambda\eta)^{p-1} + B \sum_{p=0}^{\infty} \frac{2p+1}{p+1} d^p (\lambda\eta)^p. \end{aligned}$$

By the same reason as what we did for the $\partial_j [b(x)]_i$, the three summations converge, and are upper bounded by some constants not relying on λ .

For derivatives higher than the second ones, we can follow the same logic to show that as long as ηB and $\eta\lambda$ is small enough, the derivatives are upper bounded and such bound does not rely on λ . Specifically, for the k -th order derivative of $b(x)$ with $k \geq 2$, we will have terms of the following form derived from each term in Term (A):

$$\mathcal{O}(p^k) \left(\prod_{j=1}^m \partial^{q_j} f \right) (\partial^2 f)^s (\partial f)^r,$$

with $m + s + r = p + 1$ and $q_j \geq 3$, $s \leq p$ and $r \leq 1$. As we only consider derivatives of $b(x)$ up to some finite order. We have finite such terms and they can be bounded using the idea presented previously. \square

Lemma 16. For $n \geq 0$, assume $f \in C_b^{n+2}(\mathbb{R}^d)$ and $[\Sigma]_{i,j} \in C_b^n(\mathbb{R}^d)$ for all $1 \leq i, j \leq d$ where $[A]_{i,j}$ is the (i, j) -th entry of matrix A , then there exists $\eta_0, C > 0$, such that for any $\eta < \eta_0$ and $\eta\lambda < C$, where $\lambda := \sup_{x \in \mathbb{R}^d} \|\nabla^2 f(x)\|$ and C, η_0 does not depend on λ , we have that the diffusion term $D(x)$ of stochastic principal flow satisfy

$$\max_{0 \leq i, j \leq d} \frac{\| [D(x)D(x)^\top]_{i,j} \|_{C^n}}{\eta} < \mathcal{O}(1),$$

where $\mathcal{O}(\cdot)$ hides the dependence on the upper bounds for the derivatives of f higher than the second-order derivatives and $\max_{0 \leq i, j \leq d} \|[\Sigma]_{i,j}\|_{C^n}$.

Proof. The proof idea is similar to the proof of Lemma 15, however, in this case, we do not have an explicit form for the coefficients of the power series. The diffusion term can be represented as

$$D(x)D(x)^\top = \sum_{p=1}^{\infty} \eta^p \sum_{k=0}^{p-1} a_{k,p-1-k} \cdot (\nabla^2 f(x))^k \Sigma(x) (\nabla^2 f(x))^{p-1-k},$$

where $a_{k,p-1-k}$ are absolute constants such that by Taylor expansion at $(0, 0)$,

$$g(x, y) := \frac{\log(1-x)(1-y)}{xy - (x+y)} = \sum_{s,m \geq 0}^{+\infty} a_{s,m} x^s y^m.$$

For the power series above, we know that its convergence radius is greater or equal than 1 for both x and y , meaning that $x < 1$ and $y < 1$ is a sufficient condition for it to converge. Also, according to the Cauchy–Hadamard theorem for multiple variables [Shabat, 1992], the signs of the coefficients do affect the convergence radius, therefore the convergence radius of

$$\tilde{g}(x, y) := \sum_{s,m \geq 0}^{+\infty} |a_{s,m}| x^s y^m$$

is also greater or equal than 1. Now we look back into $D(x)D(x)^\top$. We note that the (i, j) -th element of $A^p B A^k$ for $A, B \in \mathbb{R}^{d \times d}$ can be written as

$$\begin{aligned} [A^p B A^k]_{i,j} &= \sum_{s_1=1}^d [A]_{i,s_1} \sum_{s_2=1}^d [A]_{s_1,s_2} \cdots \sum_{s_p=1}^d [A]_{s_{p-1},s_p} \sum_{m=1}^d [S]_{s_p,m} \sum_{q_1=1}^d [A]_{m,q_1} \sum_{q_2=1}^d [A]_{q_1,q_2} \cdots \\ &\quad \sum_{q_{k-1}=1}^d [A]_{q_{k-2},q_{k-1}} [A]_{q_{k-1},j}. \end{aligned}$$

Therefore, we can derive that

$$\begin{aligned} &[D(x)D(x)^\top]_{i,j} \\ &= \sum_{p=1}^{\infty} \eta^p \sum_{k=0}^{p-1} a_{k,p-1-k} \sum_{s_1=1}^d [\nabla^2 f(x)]_{i,s_1} \sum_{s_2=1}^d [\nabla^2 f(x)]_{s_1,s_2} \cdots \sum_{s_k=1}^d [\nabla^2 f(x)]_{s_{k-1},s_k} \sum_{m=1}^d [\Sigma(x)]_{s_k,m} \\ &\quad \sum_{q_1=1}^d [\nabla^2 f(x)]_{m,q_1} \sum_{q_2=1}^d [\nabla^2 f(x)]_{q_1,q_2} \cdots \sum_{q_{p-k-2}=1}^d [\nabla^2 f(x)]_{q_{p-k-3},q_{p-k-2}} [\nabla^2 f(x)]_{q_{p-k-2},j} \\ &= \sum_{p=1}^{\infty} \eta^p \sum_{k=0}^{p-1} a_{k,p-1-k} \sum_{s_1=1}^d \partial_i \partial_{s_1} f(x) \sum_{s_2=1}^d \partial_{s_1} \partial_{s_2} f(x) \cdots \sum_{s_k=1}^d \partial_{s_{k-1}} \partial_{s_k} f(x) \sum_{m=1}^d [\Sigma(x)]_{s_k,m} \\ &\quad \sum_{q_1=1}^d \partial_m \partial_{q_1} f(x) \sum_{q_2=1}^d \partial_{q_1} \partial_{q_2} f(x) \cdots \sum_{q_{p-k-2}=1}^d \partial_{q_{p-k-3}} \partial_{q_{p-k-2}} f(x) \partial_{q_{p-k-2}} \partial_j f(x). \end{aligned}$$

Let us look at the term associated with $a_{k,p-1-k}$, i.e., everything after $a_{k,p-1-k}$ in the above equation. It contains $p-1$ summations, thus resulting in d^{p-1} terms. Each term has p factors consisting of one element of $\Sigma(x)$ and others being second-order derivatives of $f(x)$. Denoting $S := \max_{i,j} \|\Sigma(x)\|_{C^6}$, we can derive

$$\begin{aligned} \left| [D(x)D(x)^\top]_{i,j} \right| &\leq \sum_{p=1}^{\infty} \eta^p \sum_{k=0}^{p-1} |a_{k,p-1-k}| d^{p-1} S \lambda^{p-1} \\ &= \eta S \sum_{p=1}^{\infty} \sum_{k=0}^{p-1} |a_{k,p-1-k}| (\eta d \lambda)^{p-1} \\ &= \eta S \sum_{p=1}^{\infty} \sum_{k=0}^{p-1} |a_{k,p-1-k}| (\eta d \lambda)^k (\eta d \lambda)^{p-1-k} \\ &= \eta S \sum_{s,m \geq 0} |a_{s,m}| (\eta d \lambda)^s (\eta d \lambda)^m. \end{aligned}$$

According to our previous reasoning, the power series is convergent if

$$\eta d \lambda < 1 \quad \implies \quad \eta \lambda < \frac{1}{d},$$

and we have

$$\max_{i,j} \frac{\left\| [D(x)D(x)^\top]_{i,j} \right\|_{C^0}}{\eta} < \infty.$$

Next, we consider the first-order derivative of $D(x)D(x)^\top$. Similar to the reasoning in the proof of Lemma 15, after taking derivatives there are pd^{p-1} terms associated with coefficients $a_{k,p-1-k}$, and each term

has p factors consisting of one factor being derivatives of $\Sigma(x)$ or $\Sigma(x)$ and others being up to third-order derivatives of $f(x)$. Specifically, we have the following terms associated with $a_{k,p-1-k}$:

$$(p-1)\partial^3 f (\partial^2 f)^{p-2} \Sigma + (\partial^2 f)^{p-1} \partial \Sigma.$$

Let B be the constant such that $\max_{2 < |a| \leq n+2 \text{ and } |a| \neq 2} |D^a f| \leq B$, and let $m := \max\{B\eta, \lambda\eta\}$. We have

$$\left| \partial_k [D(x)D(x)^\top]_{i,j} \right| \leq \eta S \sum_{p=1}^{\infty} \sum_{k=0}^{p-1} |a_{k,p-1-k}| (p-1) d^{p-1} B\eta (\lambda\eta)^{p-2} + \eta S \sum_{p=1}^{\infty} \sum_{k=0}^{p-1} |a_{k,p-1-k}| (d\lambda\eta)^{p-1}.$$

The second summation can be bounded the same way as before. For the first summation, it is upper bounded by

$$\eta S \sum_{p=1}^{\infty} \sum_{k=0}^{p-1} |a_{k,p-1-k}| (p-1) (dm)^k (dm)^{p-1-k} = \eta S \sum_{s,m \geq 0} (s+m) |a_{s,m}| (dm)^s (dm)^m.$$

Now we have a power series with coefficients multiplied by $(s+m)$ compared to the previous one. However this would not change the convergence radius. Denote the convergence radius of $\tilde{g}(x, y)$ as r_1 and r_2 . According to Cauchy–Hadamard theorem for multiple variables,

$$\limsup_{s+m \rightarrow \infty} |a_{s,m} r_1^s r_2^m|^{\frac{1}{s+m}} = 1.$$

We note that r_1 and r_2 are also convergence radius for our new power series, since

$$\begin{aligned} \limsup_{s+m \rightarrow \infty} |(s+m) a_{s,m} r_1^s r_2^m|^{\frac{1}{s+m}} &= \limsup_{s+m \rightarrow \infty} |a_{s,m} r_1^s r_2^m|^{\frac{1}{s+m}} \underbrace{\lim_{s+m \rightarrow \infty} |s+m|^{\frac{1}{s+m}}}_{=1} \\ &= \limsup_{s+m \rightarrow \infty} |a_{s,m} r_1^s r_2^m|^{\frac{1}{s+m}} = 1. \end{aligned}$$

Therefore a sufficient condition for the convergence of the power series is

$$\max\{\eta\lambda, \eta B\} < \frac{1}{d}.$$

The proof is similar for higher-order derivatives. Every time we take derivative, the coefficients would be multiplied by a factor of order $s+m$, however, that would not change the radius of convergence. Specifically, for the k -th derivative of $D(x)D(x)^\top$ with $k \geq 2$, terms associated with $a_{k,p-1-k}$ have the following form:

$$\mathcal{O}(p^k) \left(\prod_{j=1}^m \partial^{q_j} f \right) (\partial^2 f)^s \partial^r \Sigma,$$

with $m+s=p-1$, $q_j \geq 3$, $s \leq p-1$ and $r \leq k$. These terms can be bounded using similar idea of the previous proof. □

Lemma 17. *Let \mathcal{L} be the infinitesimal generator for an SDE defined as*

$$dX_t = b(X_t)dt + D(X_t)dW_t,$$

where $b: \mathbb{R}^d \rightarrow \mathbb{R}^d$ and $D: \mathbb{R}^d \rightarrow \mathbb{R}^{d \times d}$. We have for any $n \geq 1$ and $t > 0$, it holds

$$\left\| e^{t\mathcal{L}} u - \sum_{p=0}^{n-1} \frac{t^p}{p!} \mathcal{L}^p u \right\|_{L^\infty} \leq \mathcal{O} \left(t^n \max_i \|b\|_{C^0} \|b\|_{C^{2(n-1)}}^{n-1} \|DD^\top\|_{C^{2(n-1)}}^n \|u\|_{C^{2n}} \right),$$

where $\|b\|_{C^m} := \max_{0 \leq i \leq d} \|[b]_i\|_{C^m}$ and $\|DD^\top\|_{C^m} := \max_{0 \leq i \leq d} \|[DD^\top]_{i,j}\|_{C^m}$.

Proof. According to the Taylor expansion of $e^{t\mathcal{L}}$ on t , we obtain for any x

$$\left| e^{t\mathcal{L}}u(x) - \sum_{p=0}^{n-1} \frac{t^p}{p!} \mathcal{L}^p u(x) \right| = \left| \frac{t^n}{n!} \frac{\partial^n e^{t\mathcal{L}}u(x)}{(\partial t)^n} \right|_{t=s},$$

for some $0 \leq s \leq t$. According to Feng et al. [2017, Lemma 2.1], $e^{t\mathcal{L}}$ is a contraction, therefore, we have

$$\begin{aligned} \left\| e^{t\mathcal{L}}u(x) - \sum_{p=0}^{n-1} \frac{t^p}{p!} \mathcal{L}^p u(x) \right\|_{L^\infty} &= \left\| \frac{t^n}{n!} \frac{\partial^n e^{t\mathcal{L}}u(x)}{(\partial t)^n} \right\|_{t=s} \Big\|_{L^\infty} \\ &\leq \frac{t^n}{n!} \|\mathcal{L}^n u\|_{L^\infty}. \end{aligned}$$

Note that \mathcal{L} is linear operator and it will apply ∇^2 operator. Therefore, we obtain gradients of b and DD^\top up to the $2(n-1)$ -th order and gradients of u up to the $2n$ -th order. Note that we bound the first b using $\|b\|_{C^0}$ and the following $n-1$ occurrences of b using $\|b\|_{C^{2(n-1)}}$, since they have different dependence on λ for HA-SME according to Lemma 15. It would be more convenient for fine-grained analysis later. \square

Lemma 18. For $n \geq 0$, assume $f \in C_b^{2n}(\mathbb{R}^d)$ and $[\Sigma(x)]_{i,j} \in C_b^{2n-2}(\mathbb{R}^d)$ for any $0 \leq i, j \leq d$. Let \mathcal{L} be the infinitesimal generator for HA-SME, which depends on η . We have for any function $u : \mathbb{R}^d \rightarrow \mathbb{R}$, and integer $n, p > 0$,

$$\left\| \frac{\partial^p \mathcal{L}^n u}{(\partial \eta)^p} \right\|_{L^\infty} \leq \mathcal{O}(\lambda^{n+p-1} s^n \|u\|_{C^{2n}}),$$

where $\lambda := \sup_{x \in \mathbb{R}^d} \|\nabla^2 f(x)\|$, $s := \sup_{x \in \mathbb{R}^d} \|\nabla f(x)\|$ and $\mathcal{O}(\cdot)$ hides the dependence on the upper bounds for the derivatives of f other than the second-order derivatives and $\max_{0 \leq i, j \leq d} \|[\Sigma]_{i,j}\|_{C^n}$.

Proof. We note that when taking partial gradient of b w.r.t. η , the dependence on λ on the upper bounds for the derivatives, i.e., $\left\| \left[\frac{\partial b}{\partial \eta} \right]_i \right\|_{C^m}$, would increase its order by 1. That is to say, if $\left\| \left[\frac{\partial^k b}{(\partial \eta)^k} \right]_i \right\|_{C^m} \leq \mathcal{O}(\lambda^q)$, then $\left\| \left[\frac{\partial^{k+1} b}{(\partial \eta)^{k+1}} \right]_i \right\|_{C^m} \leq \mathcal{O}(\lambda^{q+1})$. The reason is that gradients w.r.t. x of b can be written as power series of η and $\eta\lambda$ (see the proof of Lemma 15). Whenever we taking partial derivative w.r.t. η , the order of η compared to λ in each term is decreased by 1. Then we can take a λ factor out and the remaining series still converges (the same reasoning as in the proof of Lemma 15). The same logic applies to DD^\top . In $\mathcal{L}^n u$, we will have at most $n-1$ occurrences of gradients of b . Therefore, before taking derivatives w.r.t. η , the upper bounds would be at most λ^{n-1} . After taking the derivative p times, the order of λ is at most $n+p-1$. Similar logic applies to DD^\top and corresponding Lemma 16. \square

C Exact Match of SGD on Quadratics

Before diving into the proof, we will introduce some basics about complex normal distribution and complex OU process.

C.1 Complex Normal Distribution

Since our proposed SDE may operate in complex space, similar to PF, we provide here some basics about the complex distribution, specifically the complex normal distribution. A complex random vector is defined by two real random variables:

$$z = x + iy,$$

where x and y are two real random vectors, which may be correlated. The random vector z is called a complex normal vector if $\begin{bmatrix} x \\ y \end{bmatrix}$ is a normal vector. In contrast to real-valued random vector, there are three parameters that define a complex normal variable $\mathcal{CN}(\mu, \Gamma, C)$,

$$\mu := \mathbb{E}[z] \quad (\text{Expectation})$$

$$\Gamma := \mathbb{E}[(z - \mathbb{E}[z])(z - \mathbb{E}[z])^H] \quad (\text{Covariance})$$

$$C := \mathbb{E}[(z - \mathbb{E}[z])(z - \mathbb{E}[z])^\top] \quad (\text{Pseudo-Covariance})$$

Similar to the real case, for $z \sim \mathcal{CN}(\mu, \Gamma, C)$, the following property holds

$$Az + b \sim \mathcal{CN}(A\mu + b, A\Gamma A^H, ACA^\top).$$

If we look at the real and imaginary part separately, we have

$$\begin{aligned} \Gamma &= \text{Cov}[x, x] + \text{Cov}[y, y] + i(\text{Cov}[y, x] - \text{Cov}[x, y]), \\ C &= \text{Cov}[x, x] - \text{Cov}[y, y] + i(\text{Cov}[y, x] + \text{Cov}[x, y]). \end{aligned} \quad (55)$$

For the covariance of x and y , we have

$$\text{Cov}[x, x] = \frac{1}{2} \text{Re}(\Gamma + C), \quad \text{Cov}[y, y] = \frac{1}{2} \text{Re}(\Gamma - C). \quad (56)$$

C.2 Proofs for Section 6

Proof for Proposition 1. Solution for SGD Let us consider more general covariance matrix Σ instead of $\sigma^2 I$. The iterates of SGD can be written as

$$\begin{aligned} x_k &= x_{k-1} - \eta(Ax_{k-1} + \xi_{k-1}) \\ &= (I - \eta A)x_{k-1} - \eta \xi_{k-1} \\ &= (I - \eta A)^2 x_{k-2} - \eta(I - \eta A)\xi_{k-2} - \eta \xi_{k-1} \\ &\dots \\ &= (I - \eta A)^k x_0 - \eta \sum_{m=0}^{k-1} (I - \eta A)^m \xi_{k-1-m}. \end{aligned}$$

Clearly, it is a linear combination of independent Gaussian variables, therefore x_{k+1} is also has a Gaussian distribution. Moreover,

$$\begin{aligned} \mathbb{E}[x_k] &= (I - \eta A)^k x_0 = U(I - \eta \Lambda)^k U^\top x_0 \\ \text{Cov}[x_k, x_k] &= \eta^2 \sum_{m=0}^{k-1} (I - \eta A)^m \Sigma (I - \eta A)^m = \eta^2 \sum_{m=0}^{k-1} U(I - \eta \Lambda)^m U^\top \Sigma U(I - \eta \Lambda)^m U^\top. \end{aligned}$$

Plugging in $\Sigma = \sigma^2 I$ gives us the desired result.

The three SDEs considered applied on quadratics with Assumption 2 are OU processes. According to [Särkkä and Solin \[2019, Section 6.2\]](#), for a linear time-invariant SDE

$$dX_t = F X_t dt + L dW_t,$$

the solution would be a Gaussian variable and its mean and covariance satisfy

$$\mathbb{E}[X(x_0, t)] = \exp(Ft) x_0$$

$$\text{Cov} [X(x_0, t), X(x_0, t)] = \int_0^t \exp (F(t-\tau)) L L^\top \exp (F(t-\tau))^\top d\tau.$$

In our case, since we assume isotropic noise, i.e., the noise covariance is $\sigma^2 I$, the diffusion coefficients of the three SDEs we consider is also isotropic, i.e., $\sqrt{\eta}\sigma I$. Under this condition, F and L commute, and the covariance has closed form solution.

Solution for SME-1 The SDE SME-1 applied on the problem we consider is

$$dX_t = -AX_t dt + \sqrt{\eta}\sigma I dW_t.$$

Then the mean is

$$\mathbb{E} [X(x_0, t)] = \exp (-At) x_0,$$

and the covariance is

$$\begin{aligned} \text{Cov} [X(x_0, t), X(x_0, t)] &= \int_0^t \exp (A(\tau-t)) \eta \sigma^2 \exp (A(\tau-t)) d\tau \\ &= \eta \sigma^2 \int_0^t U \exp (\Lambda(\tau-t)) U^\top U \exp (\Lambda(\tau-t)) U^\top d\tau \\ &= \eta \sigma^2 U \int_0^t \exp (\Lambda(\tau-t)) \exp (\Lambda(\tau-t)) d\tau U^\top \\ &= \eta \sigma^2 U \int_0^t \exp (2\Lambda(\tau-t)) d\tau U^\top \\ &= \eta \sigma^2 U \frac{I - \exp(-2\Lambda t)}{2\Lambda} U^\top. \end{aligned}$$

Solution for SME-2 The SDE SME-2 applied on the problem we consider is

$$dX_t = -(A + \frac{\eta}{2} A^2) X_t dt + \sqrt{\eta}\sigma I dW_t.$$

Then the mean is

$$\mathbb{E} [X(x_0, t)] = \exp \left(- \left(A + \frac{\eta}{2} A^2 \right) t \right) x_0,$$

and the covariance is

$$\begin{aligned} \text{Cov} [X(x_0, t), X(x_0, t)] &= \int_0^t \exp \left(\left(A + \frac{\eta}{2} A^2 \right) (\tau-t) \right) \eta \sigma^2 \exp \left(\left(A + \frac{\eta}{2} A^2 \right) (\tau-t) \right) d\tau \\ &= \eta \sigma^2 \int_0^t U \exp \left(\left(\Lambda + \frac{\eta}{2} \Lambda^2 \right) (\tau-t) \right) U^\top U \exp \left(\left(\Lambda + \frac{\eta}{2} \Lambda^2 \right) (\tau-t) \right) U^\top d\tau \\ &= \eta \sigma^2 U \int_0^t \exp \left(\left(\Lambda + \frac{\eta}{2} \Lambda^2 \right) (\tau-t) \right) \exp \left(\left(\Lambda + \frac{\eta}{2} \Lambda^2 \right) (\tau-t) \right) d\tau U^\top \\ &= \eta \sigma^2 U \int_0^t \exp \left(2 \left(\Lambda + \frac{\eta}{2} \Lambda^2 \right) (\tau-t) \right) d\tau U^\top \\ &= \eta \sigma^2 U \frac{I - \exp(-2 \left(\Lambda + \frac{\eta}{2} \Lambda^2 \right) t)}{2 \left(\Lambda + \frac{\eta}{2} \Lambda^2 \right)} U^\top. \end{aligned}$$

Solution for SPF The SDE SPF applied on the problem we consider is

$$dX_t = U \frac{\log(1 - \eta\Lambda)}{\eta} U^\top X_t dt + \sqrt{\eta}\sigma I dW_t.$$

Then the mean is

$$\begin{aligned}\mathbb{E}[X(x_0, t)] &= \exp\left(U \frac{\log(1 - \eta\Lambda)}{\eta} U^\top t\right) x_0 \\ &= U \exp\left(\log(1 - \eta\Lambda)^{t/\eta}\right) U^\top x_0 \\ &= U (1 - \eta\Lambda)^{t/\eta} U^\top x_0,\end{aligned}$$

and the covariance is

$$\begin{aligned}\text{Cov}[X(x_0, t), X(x_0, t)] &= \int_0^t \exp\left(U \frac{\log(1 - \eta\Lambda)}{\eta} U^\top(\tau - t)\right) \eta \sigma^2 \exp\left(U \frac{\log(1 - \eta\Lambda)}{\eta} U^\top(\tau - t)\right) d\tau \\ &= \eta \sigma^2 U \int_0^t \exp\left(2 \frac{\log(1 - \eta\Lambda)}{\eta}(\tau - t)\right) d\tau U^\top \\ &= \eta \sigma^2 U \left(\frac{\eta}{-2 \log(1 - \eta\Lambda)} \left(1 - \exp\left(\frac{2 \log(1 - \eta\Lambda)}{\eta} t\right)\right) \right) U^\top \\ &= \eta^2 \sigma^2 U \left(\frac{1}{-2 \log(1 - \eta\Lambda)} \left(1 - (1 - \eta\Lambda)^{2t/\eta}\right) \right) U^\top.\end{aligned}$$

□

Proof for Desideratum 1. If the distribution of complex variable matches the real variable, then by the definition of matching, we have

$$\begin{aligned}\mathbb{E}[\text{Re}(z)] &= \mathbb{E}[\tilde{z}] & \mathbb{E}[\text{Im}(z)] &= 0 \\ \text{Cov}[\text{Re}(z), \text{Re}(z)] &= \text{Cov}[\tilde{z}, \tilde{z}] & \text{Cov}[\text{Im}(z), \text{Im}(z)] &= 0.\end{aligned}$$

Then according to Equation (55), we get

$$\begin{aligned}\Gamma(z) &= \text{Cov}[\text{Re}(z), \text{Re}(z)] + \text{Cov}[\text{Im}(z), \text{Im}(z)] + i(\text{Cov}[\text{Im}(z), \text{Re}(z)] - \text{Cov}[\text{Re}(z), \text{Im}(z)]) \\ &= \text{Cov}[\text{Re}(z), \text{Re}(z)] = \text{Cov}[\tilde{z}, \tilde{z}] \\ \Gamma(z) &= \text{Cov}[\text{Re}(z), \text{Re}(z)] - \text{Cov}[\text{Im}(z), \text{Im}(z)] + i(\text{Cov}[\text{Im}(z), \text{Re}(z)] + \text{Cov}[\text{Re}(z), \text{Im}(z)]) \\ &= \text{Cov}[\text{Re}(z), \text{Re}(z)] = \text{Cov}[\tilde{z}, \tilde{z}],\end{aligned}$$

as $\text{Im}(z) = 0$ deterministically. Next, we consider the opposite direction. The means match trivially. According to Equation (56), we have

$$\begin{aligned}\text{Cov}[\text{Re}(z), \text{Re}(z)] &= \frac{1}{2}(\Gamma(z) + C(z)) = \text{Cov}[\tilde{z}, \tilde{z}] \\ \text{Cov}[\text{Im}(z), \text{Im}(z)] &= \frac{1}{2}(\Gamma(z) - C(z)) = 0,\end{aligned}$$

which completes the proof. □

Proof for Proposition 2. Consider function

$$f(x) = \frac{1}{2} x^\top \begin{bmatrix} 1 & 0 \\ 0 & -1 \end{bmatrix} x,$$

and

$$\Sigma = \begin{bmatrix} \Sigma_{11} & \Sigma_{12} \\ \Sigma_{12} & \Sigma_{22} \end{bmatrix} \quad \text{with} \quad \Sigma_{11}, \Sigma_{12}, \Sigma_{22} > 0 \quad \text{and} \quad \Sigma_{11}\Sigma_{22} - \Sigma_{12}^2 = 0.$$

Note that the last condition implies that Σ is positive semi-definite and not positive definite. It is easy to come up with such a Σ , e.g., $\begin{bmatrix} 1 & 2 \\ 2 & 4 \end{bmatrix}$.

According to Lemma 6, a necessary condition for matching the discrete-time iterates is that the RHS of Equation (28) is positive semi-definite, otherwise it cannot be decomposed to $(U^\top D)(U^\top D)^H$. Therefore, as long as we can show that the determinant of Σ is negative, i.e., it contains a negative eigenvalue, then we can claim that there is no such a decomposition, i.e., no linear SDE can match the discrete-time iterates.

The RHS matrix of Equation (28) in our case is

$$\begin{bmatrix} \frac{2\Sigma_{11} \operatorname{Re}(\log(1-\eta))}{\eta-2} & \frac{\Sigma_{12}(\log(1-\eta)+\log(1+\eta))}{-\eta} \\ \frac{\Sigma_{12}(\log(1+\eta)+\log(1-\eta))}{-\eta} & \frac{2\Sigma_{22} \log(1+\eta)}{\eta+2} \end{bmatrix},$$

where we used $x + \bar{x} = 2 \operatorname{Re}(x)$ to simplify the result. Then, our goal is to show

$$\frac{4\Sigma_{11}\Sigma_{22} \operatorname{Re}(\log(1-\eta)) \log(1+\eta)}{(\eta-2)(\eta+2)} - \frac{\Sigma_{12}^2 (\log(1-\eta) + \log(1+\eta)) (\overline{\log(1-\eta)} + \log(1+\eta))}{\eta^2} < 0.$$

It is then sufficient to show the following:

$$\frac{(\log(1-\eta) + \log(1+\eta)) (\overline{\log(1-\eta)} + \log(1+\eta)) (\eta-2)(\eta+2)}{4\eta^2 \operatorname{Re}(\log(1-\eta)) \log(1+\eta)} > \frac{\Sigma_{11}\Sigma_{22}}{\Sigma_{12}^2} = 1. \quad (57)$$

To see why this is the case, notice that for all $\eta > 0$, it holds that

$$\frac{\operatorname{Re}(\log(1-\eta))}{\eta-2} > 0.$$

Next, we will discuss in three different cases, i.e., $0 < \eta < 1$, $1 < \eta < 2$ and $\eta > 2$, to prove the above inequality. For the boundary case, one can check that the inequality holds when $\eta \rightarrow 2$.

When $0 < \eta < 1$ In this case, we have $\operatorname{Re}(\log(1-\eta)) < 0$, therefore, Equation (57) is equivalent to

$$\begin{aligned} & 4\eta^2 \operatorname{Re}(\log(1-\eta)) \log(1+\eta) > (\log(1-\eta) + \log(1+\eta)) (\overline{\log(1-\eta)} + \log(1+\eta)) (\eta-2)(\eta+2) \\ \iff & 4(\log(1-\eta) + \log(1+\eta))(\overline{\log(1-\eta)} + \log(1+\eta)) > \eta^2(\log(1-\eta) - \log(1+\eta))(\overline{\log(1-\eta)} - \log(1+\eta)). \end{aligned} \quad (58)$$

When $0 < \eta < 1$, we have $\overline{\log(1-\eta)} = \log(1-\eta)$, which implies the following equivalence of Equation (58):

$$\begin{aligned} & 4(\log(1-\eta) + \log(1+\eta))^2 > \eta^2(\log(1-\eta) - \log(1+\eta))^2 \\ \iff & 4(\log(1-\eta^2))^2 > \eta^2(\log(1-\eta) - \log(1+\eta))^2 \\ \iff & -2\log(1-\eta^2) > \eta(\log(1+\eta) - \log(1-\eta)) \\ \iff & \underbrace{\eta \log(1+\eta) - \eta \log(1-\eta) + 2\log(1-\eta^2)}_{g(\eta)} < 0. \end{aligned}$$

Now we analyze the function $g(\eta)$.

$$\begin{aligned} g'(\eta) &= \log(1+\eta) + \frac{\eta}{1+\eta} - \log(1-\eta) + \frac{\eta}{1-\eta} - \frac{4\eta}{1-\eta^2} \\ &= \log\left(\frac{1+\eta}{1-\eta}\right) - \frac{2\eta}{1-\eta^2} \end{aligned}$$

$$\begin{aligned}
&= \log\left(1 + \frac{2\eta}{1-\eta}\right) - \frac{2\eta}{1-\eta^2} \\
&\leq \frac{\frac{2\eta}{1-\eta}\left(6 + \frac{2\eta}{1-\eta}\right)}{6 + \frac{8\eta}{1-\eta}} - \frac{2\eta}{1-\eta^2} \\
&= \frac{12\eta - 8\eta^2}{(1-\eta)(6+2\eta)} - \frac{2\eta}{1-\eta^2} \\
&= -\frac{8\eta^3}{(1-\eta)(1+\eta)(6+2\eta)} < 0,
\end{aligned}$$

where the first inequality is according to Lemma 19. Now we know that $g(\eta)$ is strictly decreasing over $0 < \eta < 1$, therefore $\sup_{0 < \eta < 1} g(\eta) < g(0) = 0$.

When $1 < \eta < 2$ In this case, we also obtain Equation (58). In addition, since $\log(1-\eta) = \pi i + \log(\eta-1)$, we have

$$\log(1-\eta)\overline{\log(1-\eta)} = \log^2(1-\eta) + \pi^2.$$

Therefore, Equation (58) is equivalent to

$$\begin{aligned}
&4(\log^2(\eta-1) + \pi^2 + 2\log(\eta-1)\log(1+\eta) + \log^2(1+\eta)) \\
&\quad > \eta^2(\log^2(\eta-1) + \pi^2 - 2\log(\eta-1)\log(1+\eta) + \log^2(1+\eta)) \\
\iff &4(\log(\eta-1) + \log(1+\eta))^2 - \eta^2(\log(\eta-1) - \log(1+\eta))^2 + \pi^2(4 - \eta^2) > 0 \\
\iff &(4 - \eta^2)(\log^2(\eta-1) + \log^2(\eta+1) + \pi^2) + (8 + 2\eta^2)\log(\eta-1)\log(1+\eta) > 0.
\end{aligned} \tag{59}$$

To prove the above inequality, it is sufficient to prove a lower bound of LHS is greater than 0.

$$\begin{aligned}
&(4 - \eta^2)(\log^2(\eta-1) + \log^2(\eta+1) + \pi^2) + (8 + 2\eta^2)\log(\eta-1)\log(1+\eta) \\
&> (4 - \eta^2)(\log^2(\eta-1) + \log^2(\eta+1) + \pi^2) + (8 + 2\eta^2)\log(\eta-1)\eta \\
&\geq (4 - \eta^2)(\log^2(\eta-1) + \log^2(\eta+1) + \pi^2) + (22\eta - 12)\log(\eta-1) \\
&\geq (6 - 3\eta)\log^2(\eta-1) + (4 - \eta^2)(\log^2(1+\eta) + \pi^2) + (22\eta - 12)\log(\eta-1) \\
&\geq \underbrace{(6 - 3\eta)\log^2(\eta-1) + (4 - \eta^2)((\eta\log(3/2) + \log(4/3))^2 + \pi^2) + (22\eta - 12)\log(\eta-1)}_{h(\eta)},
\end{aligned}$$

where the first inequality is because $\log(1+\eta) < \eta$ for $1 < \eta < 2$, and the second inequality holds as $2\eta^3 + 2\eta \leq 22\eta - 12$. This can be seen by noticing that $2\eta^3 + 2\eta$ is convex on this interval and $22\eta - 12$ is the linear interpolation of the endpoints. Similarly, $4 - \eta^2$ is concave, and lower bounded by linear interpolation $6 - 3\eta$, which gives us the third inequality. The final inequality comes from the linear interpolation of endpoints of concave function $\log(1+\eta)$.

Next, we study the lower bound of $h(\eta)$. By taking its derivative, we obtain

$$\begin{aligned}
h'(\eta) &= \frac{1}{\eta-1}(3(1-\eta)\log^2(\eta-1) + (16\eta-10)\log(\eta-1) - 4\eta^4\log^2(3/2)) \\
&\quad + \eta^3(4\log^2(3/2) - 6\log(3/2)\log(4/3)) + \eta^2(6\log(3/2)\log(4/3) - 2\log^2(4/3) - 2\pi^2 + 8\log^2(3/2)) \\
&\quad + \eta(2\log^2(4/3) + 2\pi^2 - 8\log^2(3/2) + 8\log(4/3)\log(3/2) + 22) - 8\log(4/3)\log(3/2) - 12 \\
&\leq \frac{1}{\eta-1}((16\eta-10)\log(\eta-1) - 4\eta^4\log^2(3/2) + \eta^3(4\log^2(3/2) - 6\log(3/2)\log(4/3)) \\
&\quad + \eta^2(6\log(3/2)\log(4/3) - 2\log^2(4/3) - 2\pi^2 + 8\log^2(3/2)))
\end{aligned}$$

$$\begin{aligned}
& + \eta(2\log^2(4/3) + 2\pi^2 - 8\log^2(3/2) + 8\log(4/3)\log(3/2) + 22) - 8\log(4/3)\log(3/2) - 12) \\
& \leq \frac{1}{\eta-1}(16\eta - 32 - 4\eta^4\log^2(3/2) + \eta^3(4\log^2(3/2) - 6\log(3/2)\log(4/3)) \\
& \quad + \eta^2(6\log(3/2)\log(4/3) - 2\log^2(4/3) - 2\pi^2 + 8\log^2(3/2)) \\
& \quad + \eta(2\log^2(4/3) + 2\pi^2 - 8\log^2(3/2) + 8\log(4/3)\log(3/2) + 22) - 8\log(4/3)\log(3/2) - 12) \\
& \leq \frac{1}{\eta-1}(16\eta - 32 + 2.5 - 3\eta + \eta^3(4\log^2(3/2) - 6\log(3/2)\log(4/3)) \\
& \quad + \eta^2(6\log(3/2)\log(4/3) - 2\log^2(4/3) - 2\pi^2 + 8\log^2(3/2)) \\
& \quad + \eta(2\log^2(4/3) + 2\pi^2 - 8\log^2(3/2) + 8\log(4/3)\log(3/2) + 22) - 8\log(4/3)\log(3/2) - 12) \\
& \leq \frac{1}{\eta-1}(16\eta - 32 + 2.5 - 3\eta + 0.09 - 0.1\eta \\
& \quad + \eta^2(6\log(3/2)\log(4/3) - 2\log^2(4/3) - 2\pi^2 + 8\log^2(3/2)) \\
& \quad + \eta(2\log^2(4/3) + 2\pi^2 - 8\log^2(3/2) + 8\log(4/3)\log(3/2) + 22) - 8\log(4/3)\log(3/2) - 12).
\end{aligned}$$

where the second, third and forth inequalities are according to Lemmas 20 to 22 respectively. The remaining numerator is a quadratic function of η , and one can easily verify that it is less than 0. Therefore, we conclude that $h'(\eta) < 0$. Hence $h(x) \geq h(2) = 0$.

When $\eta > 2$ In this case, our target becomes to prove Equation (59), however with the opposite sign of the inequality.

$$\begin{aligned}
& 4(\log(\eta-1) + \log(1+\eta))^2 - \eta^2(\log(\eta-1) - \log(1+\eta))^2 + \pi^2(4 - \eta^2) \\
& \leq 4(\log(\eta-1) + \log(1+\eta))^2 - 4(\log(\eta-1) - \log(1+\eta))^2 + \pi^2(4 - \eta^2) \\
& = 16\log(\eta-1)\log(1+\eta) + \pi^2(4 - \eta^2) \\
& < 16(\eta-2)\log(1+\eta) + \pi^2(4 - \eta^2) \\
& \leq 16(\eta-2)\frac{\eta(6+\eta)}{6+4\eta} + \pi^2(4 - \eta^2) \\
& = \frac{(8-2\pi^2)\eta^3 + (32-3\pi^2)\eta^2 + (8\pi^2-96)\eta + 12\pi^2}{3+2\eta} \\
& = \frac{-(x-2)((2\pi^2-8)x^2 + (7\pi^2-48)x + 6\pi^2)}{3+2\eta},
\end{aligned}$$

where the second inequality holds as $\log(x) < x-1$ for $x > 1$ and the third inequality is according to Lemma 19. In addition, $(2\pi^2-8)x^2 + (7\pi^2-48)x + 6\pi^2 \geq 0$, therefore, we have

$$4(\log(\eta-1) + \log(1+\eta))^2 - \eta^2(\log(\eta-1) - \log(1+\eta))^2 + \pi^2(4 - \eta^2) < 0,$$

which concludes the proof. □

Proof for Lemma 6. To match the expectation, the argument is similar to the proof in Rosca et al. [2022, Section A.6]. Here, we proceed to match the covariance and pseudo-covariance. Let us first look at the continuous-time process. We denote the covairance of X as $\Gamma(X)$. According to Lemma 23, we have

$$\begin{aligned}
& [U^\top \Gamma(t)U]_{i,j} \\
& = \frac{[U^\top \Sigma U]_{i,j} \left(\log(1 - \eta\lambda_i) + \overline{\log(1 - \eta\lambda_i)} \right)}{\eta\lambda_i\lambda_j - (\lambda_i + \lambda_j)} \int_0^t \exp\left(\tau \frac{\log(1 - \eta\lambda_i)}{\eta}\right) \exp\left(\tau \frac{\overline{\log(1 - \eta\lambda_j)}}{\eta}\right) d\tau
\end{aligned}$$

$$\begin{aligned}
&= \frac{\eta [U^\top \Sigma U]_{i,j} \left(\log(1 - \eta \lambda_i) + \overline{\log(1 - \eta \lambda_i)} \right)}{(1 - \eta \lambda_i)(1 - \eta \lambda_j) - 1} \int_0^t \exp \left(\frac{\tau}{\eta} \left(\log(1 - \eta \lambda_i) + \overline{\log(1 - \eta \lambda_j)} \right) \right) d\tau \\
&= \frac{\eta [U^\top \Sigma U]_{i,j} \left(\log(1 - \eta \lambda_i) + \overline{\log(1 - \eta \lambda_i)} \right)}{(1 - \eta \lambda_i)(1 - \eta \lambda_j) - 1} \frac{\eta}{\log(1 - \eta \lambda_i) + \overline{\log(1 - \eta \lambda_i)}} \left(\exp \left(\frac{t}{\eta} \left(\log(1 - \eta \lambda_i) + \overline{\log(1 - \eta \lambda_j)} \right) \right) - 1 \right) \\
&= \frac{\eta^2 [U^\top \Sigma U]_{i,j}}{(1 - \eta \lambda_i)(1 - \eta \lambda_j) - 1} \left(\exp \left(\frac{t}{\eta} \left(\log(1 - \eta \lambda_i) + \overline{\log(1 - \eta \lambda_j)} \right) \right) - 1 \right) \\
&= \frac{\eta^2 [U^\top \Sigma U]_{i,j}}{(1 - \eta \lambda_i)(1 - \eta \lambda_j) - 1} \left(((1 - \eta \lambda_i)(1 - \eta \lambda_j))^{\frac{t}{\eta}} - 1 \right),
\end{aligned}$$

where we used the fact that for complex-valued variable z , it holds that $\exp(\bar{z}) = \overline{\exp(z)}$. Now we consider time stamp $t = k\eta$ for $k = 1, 2, \dots$, where we have

$$\begin{aligned}
[U^\top \Gamma(k\eta) U]_{i,j} &= \frac{\eta^2 [U^\top \Sigma U]_{i,j}}{(1 - \eta \lambda_i)(1 - \eta \lambda_j) - 1} \left(((1 - \eta \lambda_i)(1 - \eta \lambda_j))^k - 1 \right) \\
&= \eta^2 [U^\top \Sigma U]_{i,j} \sum_{m=0}^{k-1} ((1 - \eta \lambda_i)(1 - \eta \lambda_j))^m.
\end{aligned}$$

Then we have

$$U^\top \Gamma(k\eta) U = \eta^2 \sum_{m=0}^{k-1} (I - \eta \Lambda)^m U^\top \Sigma U (I - \eta \Lambda)^m,$$

which implies

$$\begin{aligned}
\Gamma(k\eta) &= \eta^2 \sum_{m=0}^{k-1} U (I - \eta \Lambda)^m U^\top \Sigma U (I - \eta \Lambda)^m U^\top \\
&= \eta^2 \sum_{m=0}^{k-1} (I - \eta A)^m \Sigma (I - \eta A)^m,
\end{aligned}$$

which matches the covariance of discrete-time variable. The proof for matching pseudo-covariance is almost the same. \square

Proof of Theorem 7. This is a direct result from Lemma 6. \square

C.3 Helper Lemmas

Lemma 19 (Topsøe [2007, Equation (22)]). *For $x \in \mathbb{R}$ and $x \geq 0$, it holds that*

$$\log(1 + x) \leq \frac{x(6 + x)}{6 + 4x}.$$

Lemma 20. *For $x \in \mathbb{R}$ and $1 \leq x \leq 2$, it holds that*

$$(5 - 8x) \log(x - 1) \geq 16 - 8x.$$

Proof. Denote $f(x) = (5 - 8x) \log(x - 1) - 16 + 8x$, and we have

$$f'(x) = \frac{-8(x - 1) \log(x - 1) - 3}{x - 1}.$$

Let $g(x) = (x - 1) \log(x - 1)$, then we get

$$g'(x) = 1 + \log(x - 1).$$

We know that the minimum of $g(x)$ is obtained at $x = 1/e + 1$, i.e., $g(x) \geq -1/e$. Therefore,

$$f'(x) \leq \frac{8/e - 3}{x - 1} \leq 0.$$

Hence $f(x)$ is decreasing, and $f(x) \geq f(2) \geq 0$, which concludes the proof. \square

Lemma 21. For $x \in \mathbb{R}$ and $1 \leq x \leq 2$, it holds that

$$-4x^4 \log^2(3/2) \leq 5/2 - 3x.$$

Proof. Denote $f(x) = -4x^4 \log^2(3/2) - 2.5 + 3x$. We have

$$f'(x) = -16x^3 \log^2(3/2) + 3, \quad \text{and} \quad f''(x) = -48x^2 \log^2(3/2) < 0.$$

Therefore, $f'(x)$ is decreasing and is 0 when $x = \sqrt[3]{\frac{3}{16 \log^2(3/2)}}$. Hence, $f(x)$ obtains its maximum at this point and $f\left(\sqrt[3]{\frac{3}{16 \log^2(3/2)}}\right) < 0$, which completes the proof. \square

Lemma 22. For $x \in \mathbb{R}$ and $1 \leq x \leq 2$, it holds that

$$x^3 (4 \log^2(3/2) - 6 \log(3/2) \log(4/3)) \leq 0.09 - 0.1x.$$

Proof. Denote $f(x) = x^3 (4 \log^2(3/2) - 6 \log(3/2) \log(4/3)) - 0.09 + 0.1x$. We have

$$f'(x) = 3x^2 (4 \log^2(3/2) - 6 \log(3/2) \log(4/3)) + 0.1 \leq f'(1) \leq 0,$$

since $4 \log^2(3/2) - 6 \log(3/2) \log(4/3) < 0$. Therefore, $f(x)$ is non-increasing and $f(x) \leq f(1) \leq 0$. \square

Lemma 23. Consider complex-valued OU process

$$dz = Azdt + DdW_t,$$

where $z \in \mathbb{C}^d$, $A \in \mathbb{C}^{d \times d}$ is diagonalizable with orthogonal basis, i.e., $A = USU^\top$ with diagonal matrix S and orthogonal matrix U , $D \in \mathbb{C}^{d \times m}$, and $W_t \in \mathbb{C}^m$ is a standard real Brownian motion. The covariance and pseudo-covariance at time t are

$$\begin{aligned} \Gamma(t) &= U \int_0^t \exp(\tau S) U^\top D D^H U \exp(\tau \bar{S}) d\tau U^\top \\ C(t) &= U \int_0^t \exp(\tau S) U^\top D D^\top U \exp(\tau S) d\tau U^\top. \end{aligned}$$

Proof. Recall that the covariance and pseudo-covariance are closely related to 4 matrices, $\text{Cov}[\text{Re}(z), \text{Re}(z)]$, $\text{Cov}[\text{Im}(z), \text{Im}(z)]$, $\text{Cov}[\text{Re}(z), \text{Im}(z)]$, $\text{Cov}[\text{Im}(z), \text{Re}(z)]$. Therefore, we study the dynamics of these matrices.

We first notice that complex-valued OU process can be re-written as a real-valued SDE.

$$d \begin{bmatrix} \text{Re}(z) \\ \text{Im}(z) \end{bmatrix} = \begin{bmatrix} \text{Re}(A) & -\text{Im}(A) \\ \text{Im}(A) & \text{Re}(A) \end{bmatrix} \begin{bmatrix} \text{Re}(z) \\ \text{Im}(z) \end{bmatrix} dt + \begin{bmatrix} \text{Re}(D) \\ \text{Im}(D) \end{bmatrix} dW_t.$$

We assume $z(0)$ is a deterministic variable, i.e., its covariance is 0, then according to Equation (6.20) of [Särkkä and Solin \[2019\]](#),

$$\begin{aligned} \mathbb{E} \begin{bmatrix} \text{Re}(z(t)) - \mathbb{E}[\text{Re}(z(t))] \\ \text{Im}(z(t)) - \mathbb{E}[\text{Im}(z(t))] \end{bmatrix} \begin{bmatrix} \text{Re}(z(t)) - \mathbb{E}[\text{Re}(z(t))] \\ \text{Im}(z(t)) - \mathbb{E}[\text{Im}(z(t))] \end{bmatrix}^\top &= \begin{bmatrix} \text{Cov}[\text{Re}(z), \text{Re}(z)] & \text{Cov}[\text{Re}(z), \text{Im}(z)] \\ \text{Cov}[\text{Im}(z), \text{Re}(z)] & \text{Cov}[\text{Im}(z), \text{Im}(z)] \end{bmatrix} \\ = \int_0^t \exp \left(\tau \begin{bmatrix} \text{Re}(A) & -\text{Im}(A) \\ \text{Im}(A) & \text{Re}(A) \end{bmatrix} \right) \begin{bmatrix} \text{Re}(D) \\ \text{Im}(D) \end{bmatrix} \left(\exp \left(\tau \begin{bmatrix} \text{Re}(A) & -\text{Im}(A) \\ \text{Im}(A) & \text{Re}(A) \end{bmatrix} \right) \begin{bmatrix} \text{Re}(D) \\ \text{Im}(D) \end{bmatrix} \right)^\top d\tau, \end{aligned} \quad (60)$$

where the exponential operator is matrix exponential.

Next, let us look at the matrix $\exp \left(\tau \begin{bmatrix} \text{Re}(A) & -\text{Im}(A) \\ \text{Im}(A) & \text{Re}(A) \end{bmatrix} \right)$, which has some special properties. Note that we have

$$\text{Re}(A) = U \text{Re}(S) U^\top, \quad \text{and} \quad \text{Im}(A) = U \text{Im}(S) U^\top.$$

Therefore, we have

$$\begin{bmatrix} \text{Re}(A) & -\text{Im}(A) \\ \text{Im}(A) & \text{Re}(A) \end{bmatrix} = \begin{bmatrix} U \text{Re}(S) U^\top & -U \text{Im}(S) U^\top \\ U \text{Im}(S) U^\top & U \text{Re}(S) U^\top \end{bmatrix} = \begin{bmatrix} U & \\ & U \end{bmatrix} \begin{bmatrix} \text{Re}(S) & -\text{Im}(S) \\ \text{Im}(S) & \text{Re}(S) \end{bmatrix} \begin{bmatrix} U^\top & \\ & U^\top \end{bmatrix}.$$

Note that the matrix $\begin{bmatrix} U & \\ & U \end{bmatrix}$ is orthogonal, so by the definition of matrix exponential,

$$\begin{aligned} \exp \left(\tau \begin{bmatrix} \text{Re}(A) & -\text{Im}(A) \\ \text{Im}(A) & \text{Re}(A) \end{bmatrix} \right) &= \sum_{p=0}^{\infty} \frac{\tau^p}{p!} \begin{bmatrix} \text{Re}(A) & -\text{Im}(A) \\ \text{Im}(A) & \text{Re}(A) \end{bmatrix}^p \\ &= \begin{bmatrix} U & \\ & U \end{bmatrix} \sum_{p=0}^{\infty} \frac{\tau^p}{p!} \begin{bmatrix} \text{Re}(S) & -\text{Im}(S) \\ \text{Im}(S) & \text{Re}(S) \end{bmatrix}^p \begin{bmatrix} U^\top & \\ & U^\top \end{bmatrix} \\ &= \begin{bmatrix} U & \\ & U \end{bmatrix} \exp \left(\tau \begin{bmatrix} \text{Re}(S) & -\text{Im}(S) \\ \text{Im}(S) & \text{Re}(S) \end{bmatrix} \right) \begin{bmatrix} U^\top & \\ & U^\top \end{bmatrix}. \end{aligned}$$

By the property of matrix exponential, if for matrices X and Y , we have $XY = YX$, then $\exp(X + Y) = \exp(X) \exp(Y)$. We verify that this property holds for our case:

$$\begin{bmatrix} \text{Re}(S) & -\text{Im}(S) \\ \text{Im}(S) & \text{Re}(S) \end{bmatrix} = \begin{bmatrix} \text{Re}(S) & \\ & \text{Re}(S) \end{bmatrix} + \begin{bmatrix} & -\text{Im}(S) \\ \text{Im}(S) & \end{bmatrix},$$

and

$$\begin{bmatrix} \text{Re}(S) & \\ & \text{Re}(S) \end{bmatrix} \begin{bmatrix} & -\text{Im}(S) \\ \text{Im}(S) & \end{bmatrix} = \begin{bmatrix} \text{Re}(S) \text{Im}(S) & -\text{Re}(S) \text{Im}(S) \\ & \end{bmatrix} = \begin{bmatrix} & -\text{Im}(S) \\ \text{Im}(S) & \end{bmatrix} \begin{bmatrix} \text{Re}(S) & \\ & \text{Re}(S) \end{bmatrix}.$$

Therefore, we have

$$\begin{aligned} \exp \left(\tau \begin{bmatrix} \text{Re}(S) & -\text{Im}(S) \\ \text{Im}(S) & \text{Re}(S) \end{bmatrix} \right) &= \exp \left(\tau \begin{bmatrix} \text{Re}(S) & \\ & \text{Re}(S) \end{bmatrix} \right) \exp \left(\tau \begin{bmatrix} & -\text{Im}(S) \\ \text{Im}(S) & \end{bmatrix} \right) \\ &= \begin{bmatrix} \exp(\tau \text{Re}(S)) & \\ & \exp(\tau \text{Re}(S)) \end{bmatrix} \exp \left(\tau \begin{bmatrix} & -\text{Im}(S) \\ \text{Im}(S) & \end{bmatrix} \right), \end{aligned}$$

Where the last equality holds because $\text{Re}(S)$ is diagonal. Next, we will show that

$$\exp \left(\tau \begin{bmatrix} & -\text{Im}(S) \\ \text{Im}(S) & \end{bmatrix} \right) = \begin{bmatrix} \cos(\tau \text{Im}(S)) & -\sin(\tau \text{Im}(S)) \\ \sin(\tau \text{Im}(S)) & \cos(\tau \text{Im}(S)) \end{bmatrix},$$

where the sin and cos operators are applied element-wise. To see this, let us write down the expansion of the matrix exponential.

$$\begin{aligned} \exp\left(\tau \begin{bmatrix} \text{Im}(S) & -\text{Im}(S) \\ \text{Im}(S) & -\text{Im}(S) \end{bmatrix}\right) &= I + \begin{bmatrix} \tau \text{Im}(S) & -\tau \text{Im}(S) \\ \tau \text{Im}(S) & -\tau \text{Im}(S) \end{bmatrix} + \frac{1}{2} \begin{bmatrix} -\tau^2 \text{Im}(S)^2 & -\tau^2 \text{Im}(S)^2 \\ -\tau^2 \text{Im}(S)^2 & -\tau^2 \text{Im}(S)^2 \end{bmatrix} \\ &\quad + \frac{1}{3!} \begin{bmatrix} -\tau^3 \text{Im}(S)^3 & \tau^3 \text{Im}(S)^3 \\ -\tau^3 \text{Im}(S)^3 & \tau^3 \text{Im}(S)^3 \end{bmatrix} + \frac{1}{4!} \begin{bmatrix} \tau^4 \text{Im}(S)^4 & \tau^4 \text{Im}(S)^4 \\ \tau^4 \text{Im}(S)^4 & \tau^4 \text{Im}(S)^4 \end{bmatrix} + \dots \\ &= \begin{bmatrix} \cos(\tau \text{Im}(S)) & -\sin(\tau \text{Im}(S)) \\ \sin(\tau \text{Im}(S)) & \cos(\tau \text{Im}(S)) \end{bmatrix}. \end{aligned}$$

Now going back to Equation (60), we have

$$\begin{aligned} &\begin{bmatrix} \text{Cov}[\text{Re}(z), \text{Re}(z)] & \text{Cov}[\text{Re}(z), \text{Im}(z)] \\ \text{Cov}[\text{Im}(z), \text{Re}(z)] & \text{Cov}[\text{Im}(z), \text{Im}(z)] \end{bmatrix} \\ &= \begin{bmatrix} U & \\ & U \end{bmatrix} \int_0^t \begin{bmatrix} \exp(\tau \text{Re}(S)) \cos(\tau \text{Im}(S)) & -\exp(\tau \text{Re}(S)) \sin(\tau \text{Im}(S)) \\ \exp(\tau \text{Re}(S)) \sin(\tau \text{Im}(S)) & \exp(\tau \text{Re}(S)) \cos(\tau \text{Im}(S)) \end{bmatrix} \begin{bmatrix} U^\top \text{Re}(D) \\ U^\top \text{Im}(D) \end{bmatrix} \\ &\quad \left(\begin{bmatrix} \exp(\tau \text{Re}(S)) \cos(\tau \text{Im}(S)) & -\exp(\tau \text{Re}(S)) \sin(\tau \text{Im}(S)) \\ \exp(\tau \text{Re}(S)) \sin(\tau \text{Im}(S)) & \exp(\tau \text{Re}(S)) \cos(\tau \text{Im}(S)) \end{bmatrix} \begin{bmatrix} U^\top \text{Re}(D) \\ U^\top \text{Im}(D) \end{bmatrix} \right)^\top d\tau \begin{bmatrix} U^\top & \\ & U^\top \end{bmatrix} \\ &= \begin{bmatrix} U & \\ & U \end{bmatrix} \int_0^t \begin{bmatrix} P(\tau) & Q(\tau) \\ M(\tau) & N(\tau) \end{bmatrix} d\tau \begin{bmatrix} U^\top & \\ & U^\top \end{bmatrix}, \end{aligned}$$

where

$$\begin{aligned} P(\tau) &= \exp(\tau \text{Re}(S)) \cos(\tau \text{Im}(S)) U^\top \text{Re}(D) \text{Re}(D)^\top U \exp(\tau \text{Re}(S)) \cos(\tau \text{Im}(S)) \\ &\quad - \exp(\tau \text{Re}(S)) \cos(\tau \text{Im}(S)) U^\top \text{Re}(D) \text{Im}(D)^\top U \exp(\tau \text{Re}(S)) \sin(\tau \text{Im}(S)) \\ &\quad - \exp(\tau \text{Re}(S)) \sin(\tau \text{Im}(S)) U^\top \text{Im}(D) \text{Re}(D)^\top U \exp(\tau \text{Re}(S)) \cos(\tau \text{Im}(S)) \\ &\quad + \exp(\tau \text{Re}(S)) \sin(\tau \text{Im}(S)) U^\top \text{Im}(D) \text{Im}(D)^\top U \exp(\tau \text{Re}(S)) \sin(\tau \text{Im}(S)), \\ Q(\tau) &= \exp(\tau \text{Re}(S)) \cos(\tau \text{Im}(S)) U^\top \text{Re}(D) \text{Re}(D)^\top U \exp(\tau \text{Re}(S)) \sin(\tau \text{Im}(S)) \\ &\quad + \exp(\tau \text{Re}(S)) \cos(\tau \text{Im}(S)) U^\top \text{Re}(D) \text{Im}(D)^\top U \exp(\tau \text{Re}(S)) \cos(\tau \text{Im}(S)) \\ &\quad - \exp(\tau \text{Re}(S)) \sin(\tau \text{Im}(S)) U^\top \text{Im}(D) \text{Re}(D)^\top U \exp(\tau \text{Re}(S)) \sin(\tau \text{Im}(S)) \\ &\quad - \exp(\tau \text{Re}(S)) \sin(\tau \text{Im}(S)) U^\top \text{Im}(D) \text{Im}(D)^\top U \exp(\tau \text{Re}(S)) \cos(\tau \text{Im}(S)), \\ M(\tau) &= \exp(\tau \text{Re}(S)) \sin(\tau \text{Im}(S)) U^\top \text{Re}(D) \text{Re}(D)^\top U \exp(\tau \text{Re}(S)) \cos(\tau \text{Im}(S)) \\ &\quad - \exp(\tau \text{Re}(S)) \sin(\tau \text{Im}(S)) U^\top \text{Re}(D) \text{Im}(D)^\top U \exp(\tau \text{Re}(S)) \sin(\tau \text{Im}(S)) \\ &\quad + \exp(\tau \text{Re}(S)) \cos(\tau \text{Im}(S)) U^\top \text{Im}(D) \text{Re}(D)^\top U \exp(\tau \text{Re}(S)) \cos(\tau \text{Im}(S)) \\ &\quad - \exp(\tau \text{Re}(S)) \cos(\tau \text{Im}(S)) U^\top \text{Im}(D) \text{Im}(D)^\top U \exp(\tau \text{Re}(S)) \sin(\tau \text{Im}(S)), \\ N(\tau) &= \exp(\tau \text{Re}(S)) \sin(\tau \text{Im}(S)) U^\top \text{Re}(D) \text{Re}(D)^\top U \exp(\tau \text{Re}(S)) \sin(\tau \text{Im}(S)) \\ &\quad + \exp(\tau \text{Re}(S)) \sin(\tau \text{Im}(S)) U^\top \text{Re}(D) \text{Im}(D)^\top U \exp(\tau \text{Re}(S)) \cos(\tau \text{Im}(S)) \\ &\quad + \exp(\tau \text{Re}(S)) \cos(\tau \text{Im}(S)) U^\top \text{Im}(D) \text{Re}(D)^\top U \exp(\tau \text{Re}(S)) \sin(\tau \text{Im}(S)) \\ &\quad + \exp(\tau \text{Re}(S)) \cos(\tau \text{Im}(S)) U^\top \text{Im}(D) \text{Im}(D)^\top U \exp(\tau \text{Re}(S)) \cos(\tau \text{Im}(S)). \end{aligned}$$

Now we have

$$\begin{bmatrix} U^\top \text{Cov}[\text{Re}(z), \text{Re}(z)] U & U^\top \text{Cov}[\text{Re}(z), \text{Im}(z)] U \\ U^\top \text{Cov}[\text{Im}(z), \text{Re}(z)] U & U^\top \text{Cov}[\text{Im}(z), \text{Im}(z)] U \end{bmatrix} = \begin{bmatrix} \int_0^t P(\tau) d\tau & \int_0^t Q(\tau) d\tau \\ \int_0^t M(\tau) d\tau & \int_0^t N(\tau) d\tau \end{bmatrix}.$$

Denote the covariance of $z(t)$ as $\Gamma(t)$. According to the definition of covariance for complex random variables, we have

$$U^\top \Gamma(t) U = \int_0^t P(\tau) d\tau + \int_0^t N(\tau) d\tau + i \left(\int_0^t M(\tau) d\tau - \int_0^t Q(\tau) d\tau \right).$$

Let us denote the i -th eigenvalue of A as a_i , i.e., the i -th diagonal element of S . Since $\exp(\tau \operatorname{Re}(S)) \cos(\tau \operatorname{Im}(S))$ and $\exp(\tau \operatorname{Re}(S)) \sin(\tau \operatorname{Im}(S))$ are both diagonal, we have the (i, j) -th element of $U^\top \Gamma(t) U$ satisfies

$$\begin{aligned}
& [U^\top \Gamma(t) U]_{i,j} \\
&= \int_0^t \exp(\tau \operatorname{Re}(a_i) + \operatorname{Re}(a_j)) \cos(\tau \operatorname{Im}(a_i)) \cos(\tau \operatorname{Im}(a_j)) [U^\top \operatorname{Re}(D) \operatorname{Re}(D)^\top U]_{i,j} d\tau \\
&\quad + \int_0^t \exp(\tau \operatorname{Re}(a_i) + \operatorname{Re}(a_j)) \sin(\tau \operatorname{Im}(a_i)) \sin(\tau \operatorname{Im}(a_j)) [U^\top \operatorname{Re}(D) \operatorname{Re}(D)^\top U]_{i,j} d\tau \\
&\quad + i \int_0^t \exp(\tau \operatorname{Re}(a_i) + \operatorname{Re}(a_j)) \sin(\tau \operatorname{Im}(a_i)) \cos(\tau \operatorname{Im}(a_j)) [U^\top \operatorname{Re}(D) \operatorname{Re}(D)^\top U]_{i,j} d\tau \\
&\quad - i \int_0^t \exp(\tau \operatorname{Re}(a_i) + \operatorname{Re}(a_j)) \cos(\tau \operatorname{Im}(a_i)) \sin(\tau \operatorname{Im}(a_j)) [U^\top \operatorname{Re}(D) \operatorname{Re}(D)^\top U]_{i,j} d\tau \\
&\quad - \int_0^t \exp(\tau \operatorname{Re}(a_i) + \operatorname{Re}(a_j)) \cos(\tau \operatorname{Im}(a_i)) \sin(\tau \operatorname{Im}(a_j)) [U^\top \operatorname{Re}(D) \operatorname{Im}(D)^\top U]_{i,j} d\tau \\
&\quad + \int_0^t \exp(\tau \operatorname{Re}(a_i) + \operatorname{Re}(a_j)) \sin(\tau \operatorname{Im}(a_i)) \cos(\tau \operatorname{Im}(a_j)) [U^\top \operatorname{Re}(D) \operatorname{Im}(D)^\top U]_{i,j} d\tau \\
&\quad - i \int_0^t \exp(\tau \operatorname{Re}(a_i) + \operatorname{Re}(a_j)) \sin(\tau \operatorname{Im}(a_i)) \sin(\tau \operatorname{Im}(a_j)) [U^\top \operatorname{Re}(D) \operatorname{Im}(D)^\top U]_{i,j} d\tau \\
&\quad - i \int_0^t \exp(\tau \operatorname{Re}(a_i) + \operatorname{Re}(a_j)) \cos(\tau \operatorname{Im}(a_i)) \cos(\tau \operatorname{Im}(a_j)) [U^\top \operatorname{Re}(D) \operatorname{Im}(D)^\top U]_{i,j} d\tau \\
&\quad - \int_0^t \exp(\tau \operatorname{Re}(a_i) + \operatorname{Re}(a_j)) \sin(\tau \operatorname{Im}(a_i)) \cos(\tau \operatorname{Im}(a_j)) [U^\top \operatorname{Im}(D) \operatorname{Re}(D)^\top U]_{i,j} d\tau \\
&\quad + \int_0^t \exp(\tau \operatorname{Re}(a_i) + \operatorname{Re}(a_j)) \cos(\tau \operatorname{Im}(a_i)) \sin(\tau \operatorname{Im}(a_j)) [U^\top \operatorname{Im}(D) \operatorname{Re}(D)^\top U]_{i,j} d\tau \\
&\quad + i \int_0^t \exp(\tau \operatorname{Re}(a_i) + \operatorname{Re}(a_j)) \cos(\tau \operatorname{Im}(a_i)) \cos(\tau \operatorname{Im}(a_j)) [U^\top \operatorname{Im}(D) \operatorname{Re}(D)^\top U]_{i,j} d\tau \\
&\quad + i \int_0^t \exp(\tau \operatorname{Re}(a_i) + \operatorname{Re}(a_j)) \sin(\tau \operatorname{Im}(a_i)) \sin(\tau \operatorname{Im}(a_j)) [U^\top \operatorname{Im}(D) \operatorname{Re}(D)^\top U]_{i,j} d\tau \\
&\quad + \int_0^t \exp(\tau \operatorname{Re}(a_i) + \operatorname{Re}(a_j)) \sin(\tau \operatorname{Im}(a_i)) \sin(\tau \operatorname{Im}(a_j)) [U^\top \operatorname{Im}(D) \operatorname{Im}(D)^\top U]_{i,j} d\tau \\
&\quad + \int_0^t \exp(\tau \operatorname{Re}(a_i) + \operatorname{Re}(a_j)) \cos(\tau \operatorname{Im}(a_i)) \cos(\tau \operatorname{Im}(a_j)) [U^\top \operatorname{Im}(D) \operatorname{Im}(D)^\top U]_{i,j} d\tau \\
&\quad - i \int_0^t \exp(\tau \operatorname{Re}(a_i) + \operatorname{Re}(a_j)) \cos(\tau \operatorname{Im}(a_i)) \sin(\tau \operatorname{Im}(a_j)) [U^\top \operatorname{Im}(D) \operatorname{Im}(D)^\top U]_{i,j} d\tau \\
&\quad + i \int_0^t \exp(\tau \operatorname{Re}(a_i) + \operatorname{Re}(a_j)) \sin(\tau \operatorname{Im}(a_i)) \cos(\tau \operatorname{Im}(a_j)) [U^\top \operatorname{Im}(D) \operatorname{Im}(D)^\top U]_{i,j} d\tau.
\end{aligned}$$

Let us look at the terms associated with $[U^\top \operatorname{Re}(D) \operatorname{Re}(D)^\top U]_{i,j}$. According to properties of trigonometric functions, we have

$$\begin{aligned}
\cos(x) \cos(y) + \sin(x) \sin(y) &= \cos(x - y) \\
\sin(x) \cos(y) - \cos(x) \sin(y) &= \sin(x - y),
\end{aligned}$$

which implies the factor associated with $[U^\top \text{Re}(D) \text{Re}(D)^\top U]_{i,j}$ is

$$\begin{aligned} & \int_0^t \exp(\tau \text{Re}(a_i) + \text{Re}(a_j)) \cos(\tau \text{Im}(a_i) - \tau \text{Im}(a_j)) d\tau \\ & + \int_0^t i \exp(\tau \text{Re}(a_i) + \text{Re}(a_j)) \sin(\tau \text{Im}(a_i) - \tau \text{Im}(a_j)) d\tau. \end{aligned} \quad (61)$$

Note that for complex variable z , $\text{Re}(\exp(z)) = \exp(\text{Re}(z)) \cos(\text{Im}(z))$ and $\text{Im}(\exp(z)) = \exp(\text{Re}(z)) \sin(\text{Im}(z))$. To see why this is the case, by Euler's formula,

$$\exp(z) = \exp(\text{Re}(z) + i \text{Im}(z)) = \exp(\text{Re}(z)) \exp(i \text{Im}(z)) = \exp(\text{Re}(z)) (\cos(\text{Im}(z)) + i \sin(\text{Im}(z))).$$

Therefore, going back to Equation (61), this factor is equal to

$$\begin{aligned} & \int_0^t \text{Re}(\exp(\tau(\text{Re}(a_i) + \text{Re}(a_j) + i(\text{Im}(a_i) - \text{Im}(a_j)))) d\tau \\ & + \int_0^t i \text{Im}(\exp(\tau(\text{Re}(a_i) + \text{Re}(a_j) + i(\text{Im}(a_i) - \text{Im}(a_j)))) d\tau \\ & = \int_0^t \exp(\tau(\text{Re}(a_i) + \text{Re}(a_j) + i(\text{Im}(a_i) - \text{Im}(a_j)))) d\tau \\ & = \int_0^t \exp(\tau(a_i + \bar{a}_j)) d\tau, \end{aligned}$$

where \bar{x} is the complex conjugate of x .

Similarly, we can calculate the factors associated with $[U^\top \text{Im}(D) \text{Re}(D)^\top U]_{i,j}$, $[U^\top \text{Re}(D) \text{Im}(D)^\top U]_{i,j}$, and $[U^\top \text{Im}(D) \text{Im}(D)^\top U]_{i,j}$.

$$\begin{aligned} & [U^\top \Gamma(t) U]_{i,j} \\ & = [U^\top \text{Re}(D) \text{Re}(D)^\top U]_{i,j} \int_0^t \exp(\tau(a_i + \bar{a}_j)) d\tau - i [U^\top \text{Re}(D) \text{Im}(D)^\top U]_{i,j} \int_0^t \exp(\tau(a_i + \bar{a}_j)) d\tau \\ & \quad + i [U^\top \text{Im}(D) \text{Re}(D)^\top U]_{i,j} \int_0^t \exp(\tau(a_i + \bar{a}_j)) d\tau + [U^\top \text{Im}(D) \text{Im}(D)^\top U]_{i,j} \int_0^t \exp(\tau(a_i + \bar{a}_j)) d\tau \\ & = [U^\top \text{Re}(D) \text{Re}(D)^\top U + U^\top \text{Im}(D) \text{Im}(D)^\top U + i U^\top \text{Im}(D) \text{Re}(D)^\top U - i U^\top \text{Re}(D) \text{Im}(D)^\top U]_{i,j} \int_0^t \exp(\tau(a_i + \bar{a}_j)) d\tau \\ & = [U^\top D D^H U]_{i,j} \int_0^t \exp(\tau(a_i + \bar{a}_j)) d\tau. \end{aligned}$$

Therefore, we can obtain that

$$\Gamma(t) = U \int_0^t \exp(\tau S) U^\top D D^H U \exp(\tau \bar{S}) d\tau U^\top.$$

Similarly, for pseudo-covariance C , we have

$$C(t) = U \int_0^t \exp(\tau S) U^\top D D^\top U \exp(\tau S) d\tau U^\top.$$

□

D Escape Analysis

Proof of Theorem 8. Let us w.l.o.g. assume that $x_0 = 0$ and $f(0) = 0$. Let $S_1 = [-b, b]$ for $b > 0$. We can find a small enough b independent of η , such that $f''(x) \leq -\hat{c}_1$ for some $\hat{c}_1 > 0$. Therefore, $f''(x)$ is $-\Theta(1)$, and $f'(x) < 0$ in $(0, b]$. It is known that the hitting time $\mathbb{E}[\tau]$ for the one-dimensional SDE

$$dX_t = b(X_t)dt + \sqrt{\mathcal{D}(X_t)}dW_t$$

can be analytically formulated as [Pavliotis, 2014]:

$$\mathbb{E}[\tau] = 2 \int_0^b \frac{\exp(-\psi(z))}{\mathcal{D}(z)} dz \int_z^b \exp(\psi(y)) dy, \quad (62)$$

where $\psi'(x) = -2b(x)/\mathcal{D}(x)$. Since we assume the function to be symmetric, we can focus on the right half of S_1 .

In this problem HA-SME is

$$dx = \frac{\log(1 - \eta f''(x))}{\eta f''(x)} f'(x) dt + \sqrt{\sigma(x) \frac{2 \log(1 - \eta f''(x))}{\eta f''(x)^2 - 2f''(x)}} dW_t.$$

Then $\psi'(x)$ in Equation (62) becomes such that:

$$\psi'(x) = \frac{1}{\sigma(x)} \left(\frac{2}{\eta} - f''(x) \right) f'(x).$$

Since we assume that $-f''(x)$ and $\sigma(x)$ is $\Theta(1)$ as the domain is compact, we have

$$f'(x) = - \int_0^x f''(y) dy = -\Theta(x), \quad \text{and} \quad \psi'(x) = -\Theta\left(\frac{x}{\eta}\right).$$

For \mathcal{D} , if we do a Taylor expansion around η , we will obtain

$$\mathcal{D} = \sigma(x) (\eta + O(\eta^2)) = \Theta(\eta).$$

We first start with the upper bound. For small enough η , we can split the integral into two parts, let $m_1 = \sqrt{\eta}$, we have

$$\mathbb{E}[\tau] = \int_0^{m_1} \frac{\exp(-\psi(x))}{\mathcal{D}(x)} dx \int_x^b \exp(\psi(y)) dy + \int_{m_1}^b \frac{\exp(-\psi(x))}{\mathcal{D}(x)} dx \int_x^b \exp(\psi(y)) dy. \quad (63)$$

For the first part, we have

$$\int_0^{m_1} \frac{\exp(-\psi(x))}{\mathcal{D}(x)} dx \int_x^b \exp(\psi(y)) dy.$$

For the inner integral, we let $m_2 = \hat{c}_2 \sqrt{\eta \log \frac{1}{\eta}}$, where $\hat{c}_2 > 0$ does not depend on η and we will determine later. Then, we have

$$\begin{aligned} \int_x^b \exp(\psi(y)) dy &= \int_x^{x+m_2} \exp(\psi(y)) dy + \int_{x+m_2}^b \exp(\psi(y)) dy \\ &\leq \int_x^{x+m_2} \exp(\psi(0)) dy + \int_{x+m_2}^b \exp(\psi(x+m_2)) dy. \end{aligned}$$

Note that

$$\begin{aligned}
\psi(x + m_2) - \psi(x) &= \int_x^{x+m_2} \psi'(y) dy \\
&= -\Theta\left(\frac{1}{\eta}\right) \int_x^{x+m_2} y dy \\
&= -\Theta\left(\frac{1}{\eta}\right) [(x + m_2)^2 - x^2] \\
&\leq -\Theta\left(\frac{m_2^2}{\eta}\right).
\end{aligned}$$

Next, we have

$$\begin{aligned}
&\int_x^{x+m_2} \exp(\psi(0)) dy + \int_{x+m_2}^b \exp(\psi(x + m_2)) dy \\
&\leq m_2 \exp(\psi(0)) + b \exp(\psi(x + m_2)) \\
&= m_2 \exp(\psi(0)) + b \exp(\psi(x) + \psi(x + m_2) - \psi(x)) \\
&\leq m_2 \exp(\psi(0)) + b \exp(\psi(x)) \exp\left(-\Theta\left(\frac{m_2^2}{\eta}\right)\right) \\
&\leq \exp(\psi(0)) \left(m_2 + b \exp\left(-\Theta\left(\frac{m_2^2}{\eta}\right)\right)\right) \\
&\leq \exp(\psi(0))(m_2 + b\eta) \\
&\leq O\left(\sqrt{\eta \log \frac{1}{\eta}}\right) \exp(\psi(0)),
\end{aligned}$$

where we choose \hat{c}_2 such that $-\Omega\left(\frac{m_2^2}{\eta}\right) = -\Omega(\hat{c}_2^2 \log \frac{1}{\eta})$ in the third to last line less or equal to $\log \eta$.

Next, we estimate the whole first part of (63). We have that for $|x - 0| \leq m_1$, there exists $\epsilon > 0$, such that $\psi(x) \geq \psi(0) + (\psi''(0) - \epsilon)x^2$. The integral can be upper bounded by

$$\begin{aligned}
&O\left(\sqrt{\eta \log \frac{1}{\eta}}\right) \exp(\psi(0)) \int_0^{m_1} \frac{\exp\left(-(\psi(0) + \frac{1}{2}(\psi''(0) - \epsilon)x^2)\right)}{\mathcal{D}(x)} dx \\
&= O\left(\sqrt{\eta \log \frac{1}{\eta}}\right) \int_0^{m_1} \frac{\exp\left(-\frac{1}{2}(\psi''(0) - \epsilon)x^2\right)}{\mathcal{D}(x)} dx \\
&\leq O\left(\sqrt{\eta \log \frac{1}{\eta}}\right) m_1 \exp\left(\frac{1}{2}|\psi''(0) - \epsilon|m_1^2\right) \\
&\leq O\left(\sqrt{\eta^{-1} \log \frac{1}{\eta}}\right) m_1 \exp\left(O\left(\frac{m_1^2}{\eta}\right)\right),
\end{aligned}$$

since $\psi''(0) = \frac{1}{\sigma(0)}\left(\frac{2}{\eta} - f''(0)\right)f''(0) = -\Theta\left(\frac{1}{\eta}\right)$, $\mathcal{D}(x) = \Theta(\eta)$. In addition, we note that as η gets smaller, m_1 becomes smaller, and thus ϵ gets smaller, while $|\psi''(0)|$ gets larger, therefore, ϵ is negligible compared to $\psi''(0)$. Then we have the upper bound being $O\left(\sqrt{\log \frac{1}{\eta}}\right)$.

Before we move to the second part of (63), we first show that we can choose b independent of η , such that $\psi''(x) \leq 0$ in $[0, b]$. We have

$$\psi''(x) = \frac{1}{\sigma(x)} \left(\underbrace{-f'''(x)f'(x)}_{\leq O(x)} + \underbrace{\left(\frac{2}{\eta} - f''(x)\right)f''(x)}_{\leq -\frac{1}{\eta}} \right) \underbrace{-\frac{1}{\sigma(x)^2} \left(\frac{2}{\eta} - f''(x)\right)f'(x)\sigma'(x)}_{\leq O(x/\eta)},$$

and there exists constants $k_1, k_2 > 0$ such that

$$\psi''(x) \leq \frac{k_1}{\eta}x - \frac{k_2}{\eta},$$

since according to our assumption $f'''(x) \leq O(1)$, $f''(x) = -\Theta(1)$, $-f'(x) = -\int_0^x f''(y)dy = \Theta(x)$, $\sigma(x) = \Theta(1)$ and $|\sigma'(x)| \leq O(1)$. Therefore we can choose b between $[0, \frac{k_2}{k_1}]$ independent of η .

For the second part of (63), we have that the maximum of inner integrand is at x . Further, we have for $y > x$ and $y \leq b$,

$$\psi(y) \leq \psi(x) + \psi'(x)(y - x),$$

since $\psi''(z) \leq 0$ for $z \in [0, b]$. Therefore, for the inner integral,

$$\begin{aligned} \int_x^b \exp(\psi(y))dy &\leq \int_x^b \exp(\psi(x) + \psi'(x)(y - x))dy \\ &= \exp(\psi(x)) \frac{1}{-\psi'(x)} (1 - \exp(\psi'(x)(b - x))) \\ &\leq \exp(\psi(x)) \frac{1}{-\psi'(x)}, \end{aligned}$$

where $\psi'(x) < 0$.

Incorporating with the outer integral, we have

$$\begin{aligned} \int_{m_1}^b \frac{\exp(-\psi(x))}{\mathcal{D}(x)} \exp(\psi(x)) \frac{1}{-\psi'(x)} dx &= \int_{m_1}^b \frac{1}{\mathcal{D}(x)} \frac{1}{-\psi'(x)} dx \\ &= \Theta\left(\frac{1}{\eta}\right) \int_{m_1}^b \frac{1}{-\psi'(x)} dx. \end{aligned}$$

Note that we have $\psi'(x) = -\Theta\left(\frac{1}{\eta}\right)x$. Therefore the above can be upper bounded by

$$\begin{aligned} \Theta\left(\frac{1}{\eta}\right) \int_{m_1}^b \frac{1}{\frac{1}{\eta}x} dx &= \Theta(1) \int_{m_1}^b \frac{1}{x} dx \\ &= \Theta(1)(\log b - \log m_1) \\ &= \Theta(1) \log \frac{1}{m_1} = O\left(\log \frac{1}{\eta}\right), \end{aligned}$$

which completes the proof for the upper bound.

For the lower bound, we can directly start with the second part of (63), which is a lower bound for the whole integral. This time we choose $m_1 = \sqrt{\eta} \log 1/\eta$. For any $\delta > 0$, the inner integral can be lower bounded by

$$\int_x^b \exp(\psi(y))dy \geq \int_x^{x+\delta} \exp(\psi(y))dy.$$

By Taylor's theorem we have for $y \in [x, x + \delta]$,

$$\psi(y) \geq \psi(x) + (\psi'(x) - \epsilon)(y - x),$$

where $\epsilon = \max_{z \in [x, x+\delta]} |\psi''(z)|(y - x)/2$. Then we obtain

$$\int_x^b \exp(\psi(y))dy$$

$$\begin{aligned}
&\geq \int_x^{x+\delta} \exp(\psi(x) + (\psi'(x) - \epsilon)(y - x)) dy \\
&= \exp(\psi(x)) \frac{1}{-(\psi'(x) - \epsilon)} (1 - \exp((\psi'(x) - \epsilon)\delta)) \\
&\geq \Omega\left(\frac{\exp(\psi(x))}{-\psi'(x)}\right),
\end{aligned}$$

where we choose δ to be $\sqrt{\eta}$. The last inequality holds because

$$\psi'(x) = -\Theta\left(\frac{x}{\eta}\right) \leq -\Theta\left(\frac{m_1}{\eta}\right) = O\left(\frac{\log 1/\eta}{\sqrt{\eta}}\right),$$

therefore, $\psi'(x)\delta \rightarrow -\infty$ when $\eta \rightarrow 0$. Note that ϵ is $O(1/\eta \cdot \delta) = O(1/\sqrt{\eta})$, which is negligible compared to $\psi'(x)$.

The outer integral follows the same as the upper bound, where in the proof we only have equality. Therefore, we obtain that the lower bound is

$$\Theta\left(\log \frac{1}{m_1}\right) = \Theta\left(\log \frac{1}{\eta}\right) - \Theta\left(\log \log \frac{1}{\eta}\right) = \Omega\left(\log \frac{1}{\eta}\right).$$

Next, we consider the case when x_0 is a local maximum. For this case, it has been already studied in [Aleksian and Villeneuve \[2025\]](#), where the drift and diffusion terms can depend on η . We have that for small enough η , the drift and diffusion terms of **HA-SME** converge to these of **SME-1**. Therefore, the result can be directly obtained by [Aleksian and Villeneuve \[2025, Corollary 1.9\]](#). \square

Proof of Theorem 9. **SME-2** follows the following dynamics:

$$dX_t = -\frac{1}{\eta} \nabla \left(\underbrace{\hat{f}(X_t) + \frac{1}{4} \|\nabla \hat{f}(X_t)\|^2}_{\tilde{f}(X_t)} \right) dt + \sqrt{\eta \Sigma(X_t)} dW_t, \quad (64)$$

where $\nabla^2 \hat{f}(x) = g(x)$. Let $Y_t = X_{\eta t}$, then we obtain for Y_t :

$$dY_t = -\nabla \tilde{f}(Y_t) dt + \sqrt{\eta^2 \Sigma(Y_t)} dW_t.$$

Note that according to our assumption, x_0 is a local minimum for \tilde{f} as

$$\nabla^2 \tilde{f}(x_0) = \left(I + \frac{1}{2} g(x_0) \right) g(x_0),$$

since $\nabla \tilde{f}(x_0) = 0$. For the negative eigenvalues, we have $\eta \lambda_i$, which equals the corresponding eigenvalues of g , smaller than -2 . Therefore, the corresponding eigenvalues of $\nabla^2 \tilde{f}(x_0)$ are greater than 0. Then we could apply Freidlin and Wentzel's [[Freidlin and Wentzell, 2012](#), [Vent-Tsel' and Freidlin, 1973](#)] estimate for the expected hitting time, where the Jacobian of the drift term has only negative eigenvalues. Let $\tau_{S_1}^Y$ to be the first time that Y_t hits the boundary of S_1 , and we know that $\eta \tau_{S_1}^Y = \tau_{S_1}^X$. According to [Vent-Tsel' and Freidlin \[1973, Lemma 1\]](#), we have

$$\lim_{\eta \rightarrow 0} \eta^2 \log \mathbb{E} [\tau_{S_1}^Y] = \inf_{x \in \partial S_1} V(x),$$

where V is the quasi-potential and is independent of η . Since the boundary of S_1 is also independent of η , $\inf_{x \in \partial S_1} V(x)$ is a constant when considering the asymptotics of η . Then the above implies

$$\lim_{\eta \rightarrow 0} \eta^2 \log \mathbb{E} [\tau_{S_1}^X] = \lim_{\eta \rightarrow 0} \eta^2 \log \eta \mathbb{E} [\tau_{S_1}^Y] = \lim_{\eta \rightarrow 0} \eta^2 \log \mathbb{E} [\tau_{S_1}^Y] = \inf_{x \in \partial S_1} V(x).$$

Therefore, there exists $c_1, \eta_0 > 0$ such that for all $\eta < \eta_0$,

$$\mathbb{E} [\tau_{S_1}^X] \geq \exp \left(\frac{c_1}{\eta^2} \right).$$

For HA-SME, the SDE can also be written as similar to Equation (64), where the drift has factor $1/\eta$ and diffusion has factor $\sqrt{\eta}$. The difference is that now the Jacobian of the drift term contains also positive eigenvalues. To see why this is the case, we compute the Jacobian at x_0

$$\nabla b(x_0) = \frac{1}{\eta} U(x_0) \log \left(I - \hat{\Lambda}(x_0) \right) U(x_0),$$

where $\hat{\Lambda}(x_0)$ is the diagonal matrix of the eigenvalues of $g(x_0)$. Note that we only need to differentiate w.r.t. the $\nabla f(x)$ factor as $\nabla f(x_0) = 0$. According to our assumption, for negative entries of $\hat{\Lambda}(x_0)$, the corresponding eigenvalue of $\nabla b(x_0)$ is positive.

We do the same trick as for the proof of SME-2 to change the time scale and follow Kifer [1981, Theorem 2.2]. The result follows. □